A THERMODYNAMIC DESCRIPTION OF CATION-RNA INTERACTIONS WITH DIFFERING ION ATMOSPHERE COMPOSITION.

by
Robert J. Trachman

A dissertation submitted to The Johns Hopkins University in conformity with the requirements for the degree of Doctor of Philosophy

Baltimore, Maryland
July, 2014

Abstract

The charged nature of nucleic acids imposes a strong relationship between cations and RNA structure. As a result, RNA folding efficiency is highly dependent on the quantity and types of cations in solution. *In vivo*, there are a multitude of cations available to interact with RNA. The principal monovalent cation, K^+, serves to neutralize most of the negative charges derived from nucleic acids. In addition, there are cations of higher valence that perform a number of important functions. Many studies have confirmed the ability of Mg^{2+} to promote native RNA structure. In addition to K^+ and Mg^{2+}, organic cations (polyamines) such as putrescine^{2+}, spermidine^{3+}, and spermine^{4+} are believed to be important for the process of RNA folding. All of these cations, both organic and inorganic, differ dramatically in both structural and physical properties. The purpose of the current work is to i) determine if organic and inorganic divalent cations stabilize the same folded state, ii) determine how different divalent ions interact with RNA to promote folding, and iii) develop an understanding of how the ion atmosphere is organized in the presence of three distinct types of cations (K^+, Mg^{2+} and putrescine^{2+}).

To pursue these goals, a set of RNAs, all characterized at atomic resolution, were selected to represent a range of selectivity for inorganic ions. This structural information, combined with thermodynamic analyses looking at Mg^{2+} excess, thermal stability, ligand binding, and folding efficiency provide a comprehensive look at how ions stabilize the native state of RNA. We find that RNAs with Mg^{2+} chelation sites require either Mg^{2+} or Ca^{2+} to properly fold, while putrescine^{2+} can

stabilize the native state of non-chelators, albeit to a lesser degree than Mg^{2+}. Measurement of Mg^{2+} excess with the native and intermediate states shows that Mg^{2+} is more effective at stabilizing native structure due to a closer approach to the RNA surface. Therefore, organization of the ion atmosphere is dependent on the types of ions in solution as well as the conformation of the RNA.

Advisor: Dr. David E. Draper, Department of Chemistry

Reader: Dr. Doug Barrick, Department of Biophysics

Additional Committee Memebers:

Dr. Sarah Woodson, Department of Biophysics

Dr. Bertrand Garcia-Moreno E., Department of Biophysics

Dr. Gregory Bowman, Department of Biophysics

Acknowledgments

I would first like to thank the faculty of the Johns Hopkins University an JHMI departments of Biophysics and Biophysical Chemistry for accepting me into this great program. These have truly been some of the best years of my life. I would like to especially thank the professors who had first hand experience in teaching me both in the classroom and in my rotations. I know that I am not the easiest student to train given that I am quite opinionated and vocal, even so, your guidance was very much appreciated. My thesis committee members Bertrand, Doug and Sarah were very helpful providing many great ideas for this work. In particular, Sarah Woodson served as a guiding light at the end of my thesis work by allowing me to attend her group meetings and giving me helpful one on one guidance. I would also like to thank Ranice, Jerry, Jess, Chris, Lexi, Nancy and all of the work study students for helping me with my office needs. This also includes all the nonsense chatter and the occasional joke. My sanity may have been jeopardized at times in the lab but you all kept me grounded.

I would like to give a very special thank you to my advisor David. His guidance through out my Ph.D. has been exceptional. After my second year there was an exodus from the lab, which left me as the senior student. Being the inquisitive student that I am, I often found myself peaking my head around his door just to ask a “quick” question or I would get some crazy thought or read a hot new paper and immediately run to his office to chat before thinking things through. Despite my nagging, David was always very welcoming and would entertain my ideas no matter how off base they were. When I look back at my time at Hopkins I

realize what a unique and fantastic experience my graduate education was. I owe most of that to David for first taking me into his lab and then teaching me as much as I was willing to learn. I will always take pride in being a member of the Draper lab.

My time in the Draper lab would not have been nearly as rewarding if it weren't for the guidance and support from previous lab members. Desirae Leipply and Dominic Lambert were both fantastic scientists to look up to in my early years in the lab. Isaac Newton once said "If I have seen further it is by standing on the shoulders of giants." Given the stature of these two relative to my own I think this quote is rather fitting. Their guidance and support throughout my Ph.D. has helped in so many ways. I still look to their work as inspiration and hope to one day achieve the same success that they have both attained.

After Desirae and Dominic left the lab they were quickly replaced by Nan Wang and Ryan Hulscher. I thoroughly enjoyed working with both of them. Nan was always one to share her awesome Asian treats, which I dearly miss. Ryan was always willing to tell a joke. Together these two people created a great work environment. I appreciate everything I have learned from them.

I am very grateful to the labs that helped with technical support of the data collected in this thesis. The Townsend lab was very helpful in the preparation of some of the compounds used in this thesis. In particular Eric Hill, Chad Johnson and Victor Outlaw gave critical advice for synthesizing the diamines mentioned in this work. They were also an excellent resource for nomenclature and other bioorganic questions. The pKa measurements of diamines would not have been possible if it weren't for the ultra precise pH probes and meter of the Garcia-Moreno lab. I am

very thankful to the Wang lab at NCI for sharing some of their beam time at APS for the SAXS experiments and Duncan Kilburn for use of his computer to analyze the resulting data.

My advisors prior to joining the biophysics program were all exceptional mentors. Mike Bruist, Randy Zauhar, Alessandro Senes and Bill DeGrado were all very helpful in the "computational" years of my research career. Tilman Baumstark was the person who introduced me to "the RNA world" and bench work. My time in his lab was short but highly influential.

I have to thank my friends at Hopkins for all of their support over the years. The guys in my class were a very special group of people, always helpful and hard working without being overly competitive. Alfredo Caro and I had many discussions about our research. As a result I think we both learned a tremendous amount about science and life in general. Ammon Posey was a true inspiration. Balancing a graduate students life while taking care of a rather large family is incomprehensible to me. Andrei Levine was always excited to talk about electrostatics. His perspective is unique and his thoughts were always appreciated. Andrew Buller was the biggest proponent and critic of my work. His friendship and encouragement were essential to this work. I will always remember our ground breaking "roof top experiments". Sabin Mulepati is a fantastic scientist and one of the hardest workers I know. I can't wait to go hiking with him in Nepal! It has been so rewarding to see each one of them obtain the successes that they have. I have to thank the "biophysics brewing team" for all of the help and good times over the years. Jackson Buss, Matt

Preimesberger, Hesam Motlagh, Pat Byrne, John Froehlig and Andy Goodrich were a great bunch to grow (yeast) cells and kill (brain) cells with.

Finally, I would like to thank my family for being a constant source of love and support. People always laugh when I say that I am extremely fortunate to be born into a poor loving family. The only reason that statement is funny is because it is true. My mother and father are very hard working honest people who wanted nothing more than for me to be a moral man. I will always be indebted to them for the good life that they have built for me. A big part of that was given to me in the form of my younger brother, Ryan. Life isn't always easy and it was nice to have a partner and friend to share the experiences with. I still laugh thinking about all of the stupid things he did when we were younger and I'm so proud of the man he has become. I also have to thank my brother and his wife Nicole for creating my favorite member of the family, my nephew Nicolas. To my aunts and uncles Mike, Susan, Elaine, Tom, Sandy, Peggy, Mary Anne, Steve, Linda, Dave, Joan, Dave, Cheryl, Matt and Karin; I will always remember the good times we have had and will have in the future. The loving environment you helped create was second to none. I want to give a special thank you to my aunt Sandy who paid for all of my textbooks in college. Without her this thesis would not have been possible. To my cousins Joey, Amanda, Dillon, Marc, David, Sarah, Jennifer, Katie, Allison, Kelsey, Jessica and Nicole; My childhood was a lot more fun due to all of you. Finally I would like to thank my grandparents Bob, Barbra, Joe and Rose. Thank you for bringing this group of people together. I know life was much harder for the four of you than it was for the rest of the family.

Dedication

This thesis is dedicated to my grandparents Rose and Joseph Franco. Thank you for the unconditional love and support, and for teaching me how to love and support others.

Table of Contents

List of Tables

List of Figures

Chapter 1: Introduction

Why study RNA?

All living organisms conduct the same processes of energy transduction and self-replication. These tasks are performed within the fundamental subunit of life, the cell. In 1958 Francis Crick proposed a flow chart that concisely outlined the molecular basis of these universal procedures. This flow chart has since been termed "The central dogma of molecular biology". Since 1958 there have been several additions to the general scheme of the central dogma. Nevertheless, it is still clear that DNA, "the genetic blue print", is transcribed to RNA, which is then translated into protein.

Ever since the dawn of molecular biology most scientists believed that RNA was simply an intermediary molecule that only facilitated the transfer of information. This however is not the case. RNA has been shown to take part in every phase outlined in the central dogma and is critical for the function of living organisms. From the initial task of DNA replication, RNA is required as a primer in lagging strand synthesis and telomere replication. Following the flow of the central dogma, DNA is then read by RNA polymerase in order to produce a messenger RNA (mRNA) capable of transferring the information encoded in the DNA. It is this mRNA product that enters the final stage in the central dogma. The stage of translation occurs when the initiation complex composed of the small ribosomal subunit along with other protein factors bind to mRNA. The result is the initial stage of protein synthesis, which is conducted by the ribosome (~2/3 RNA), mRNA and transfer RNA (tRNA) in addition to many other cofactors.

It is in the translation phase of the central dogma where it becomes evident how diverse RNA is in its function. The mRNA template is rich in information contained in a linear sequence while the globular tRNA and ribosome perform functions dependent on specific three-dimensional shapes. The transfer of information from a linear sequence is an easy concept to understand. Nucleotide bases are arranged so that the order of sequence rather than conformation dictates function. Alternatively, if the RNA is capable of forming a functional three dimensional conformation, then its function is to fold and perform chemistry.

The composition and structure of RNA

RNA like DNA is composed of nucleotide bases attached to sugar-phosphate moieties. Nucleotide bases are planar and capable of hydrogen bonding as well as stacking in solution thus creating favorable interactions between residues. These favorable interactions are countered by the phosphate groups, which bear a negative charge imparting an unfavorable interaction between residues. While DNA is primarily composed of two strands, RNA is typically single stranded. In solution RNA can fold back onto itself transitioning from a linear single stranded molecule (here referred to as the unfolded state or U-state) to a partially folded ensemble containing secondary structure (here referred to as the intermediate state or I-state). The I-state of RNA is not typically well defined. Due to a lack of structural information the I-state is rather enigmatic. Intermediate states are composed of a dynamic ensemble of structures where tertiary interactions (as defined by Tinoco et al.) are transiently formed. (Kwok et al. 2006)

Under the appropriate solution conditions the transient interactions in the I-state become favored in the ensemble, this biases the folding landscape toward the native state (N-state) (Figure 1-1). It is either this folded three dimensional structure or the switching between the N and I-states that gives rise to function of structured RNA. (Winkler et al. 2002; Cate et al. 1997)

Figure 1-1

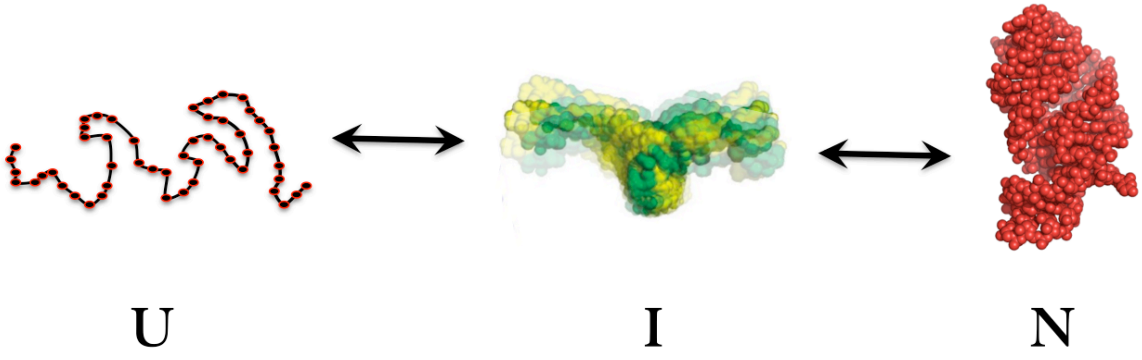

Figure 1-1. General folding pathway of an RNA. The unfolded (U) state composed of covalently linked nucleotides (left) forms secondary structure during folding to the intermediate (I) state (center, image modified from SAXS structure from Leipply et al. Biochemistry 2011). The structurally heterogeneous I-state can then fold to form the native (N) state with stable tertiary interactions (right, PDB ID: 1Y26).

This work will focus on RNA folding, the structural rearrangement from the I to N-state. This has been a productive area of research in recent years with many new insights challenging previous dogma centered on structural characteristics of the N-state. The typical understanding of RNA folding involves the "collapse" of a dynamic structure composed of highly stable secondary structure elements into a compact globule that then "folds" to form stable tertiary interactions. (Moghaddam et al. 2009) Insights contesting the generality of this concept were proposed when a domain of the Tetrahymena group I ribozyme was shown to undergo secondary

structural rearrangements upon folding. (Wu et al. 1998; Zheng et al. 2001) These findings challenged the concept of a "stable" RNA platform upon which tertiary interactions formed and suggested that the energy gained from tertiary interactions may be able to bias RNA secondary structure. From these findings it is clear that properties of both the N and I-state should be of concern to those studying RNA folding today.

The once simple concept of the I-state has continued to become more complex. For instance, rather than possessing only secondary structure, transient tertiary interactions can be found within the I-state ensemble. (Weeks et al. 1996)(Kwok et al. 2006) Folding is facilitated by multiple tertiary interactions forming cooperatively. The coupling of tertiary interactions helps guide the RNA to the appropriate folded structure, the N-state. (Behrouzi et al. 2012) (Leipply et al. 2011) Recent work has even challenged the dynamic properties of the I-state, with a new model suggesting that the "dynamic structure" of the I-state is not nearly as dynamic as once expected. (Roh et al. 2011) Rather, in low salt conditions the I-state more closely resembles a stiff rod as opposed to a flimsy coil while the N-state is more dynamic than previously expected. By increasing the number of populated states through local fluctuations, the N-state can compensate for the entropic cost of folding. Taken together these findings show the importance of understanding the properties of both the I and N-state.

RNA-ion interactions

RNAs with the ability to adopt tertiary structure typically do so *in vivo*. This is due to a multitude of interactions involving cosolvents (e.g. riboswitches) as well as appropriate temperature conditions (e.g. temperature sensors). Many of the factors that determine RNA stability *in vivo* have already been discovered including, cations, structural proteins, crowding, osmolytes and small ligands. (Tang et al. 1989; Kilburn et al. 2010; Lambert et al. 2006; Grohman et al. 2013; Winkler et al. 2002) There is a great deal of evidence in the field suggesting that these factors act upon the I-state of RNA in some fashion. (Adilakshmi et al. 2008; Kilburn et al. 2013; Grilley et al. 2006; Leipply et al. 2010) These studies reinforce the fact that any thorough investigation of RNA folding should account for RNA cosolvent interactions with both the N and I-state of RNA. (Lambert et al. 2012)

As a first step in understanding how salts stabilize RNA tertiary structure, a discussion of how salts interact in solution is necessary. From the perspective of a single anion in a dilute solution of a monovalent salt (e.g. NaCl), the free energy for "pushing" anions away is equal to the free energy of "pulling" cations closer in proximity. This results in an accumulation of cations and an equal depletion of anions from the vicinity of the central anion. This is not the case for polyelectrolytes such as DNA and RNA. Rather than having a large distance between anions in solution, such as in a dilute solution of NaCl, DNA and RNA covalently link nucleotide bases through phosophodiester bonds causing the electrostatic fields of the phosphate groups to overlap. Under moderate salt conditions, the average distance between Na^+ and Cl^- ions will be greater than the distance between

phosphate groups. Under these conditions, the free energy gained by accumulating excess cations in the vicinity of a polynucleotide is much greater than the free energy gained from excluding anions. The result is a large excess of cations and a slight depletion of anions in the vicinity of the polynucleotide, referred to as the polyelectrolyte effect. Previous reports have confirmed the existence of the polyelectrolyte effect. (Strauss et al. 1967) (Bai et al. 2007) Yet, a theory capable of predicting the free energy of ion interactions with a polyelectrolyte has not been universally accepted.

In an attempt to understand and predict the interactions of ions with polynucleotides, three main theories (counterion condensation (CC), ion correlation (IC) and non-linear Piosson-Boltzmann (NLPB)) have been proposed, each possessing strengths and limitations. Historically, the most popular of these theories is CC theory. This theory was derived by Manning in 1969 as a means of calculating the number of ions associated per charge of the polyelectrolyte. (Manning, 1969) One draw back to this theory is the requirement of a uniform spacing between charges of the polyelectrolyte. For DNA in a low concentration of monovalent salt, the approximation of uniform charge separation holds rather well allowing researchers to accurately calculate the number of excess cations and depleted anions. A major draw back of this theory is the inability to capture the electrostatic complexities of RNA. Structured RNAs form pseudoknots which posses highly irregular charge spacing. This makes the application of condensation theory to RNA folding very difficult to capture.

The packing of helices adjacent to one another is a common theme of structured RNAs. A major question in the RNA folding field concerns the driving forces that govern the packing of adjacent helices. Given the large electrostatic potential that is generated by arranging RNA helices in close proximity, electrostatic compensation is undoubtedly a major contributing factor to stability. Exactly how counterions drive folding to the native state is still not well understood. IC theory proposes that the mobile network of ions around nucleic acids undergo correlated fluctuations in solution creating a double layer effect. (Rouzina et al. 1996) Nucleic acid helices in solution pack due to attraction between condensed counterions of one helix interacting with correlated condensed ions on another helix. It has been proposed that upon annealing of helices, docking is stabilized through delocalization of the ion atmosphere. (Murthy et al. 2000) Despite the rigorous derivations, evidence supporting these theories is rather limited. For instance, IC theory is unable to account for why DNA only aggregates under high salt conditions. SAXS conducted on short tethered DNA strands (proposed to mimic the I-state of RNA) provided no evidence of compaction (also known as collapse) in the presence of both mono and divalent cations. (Bai et al. 2005) In addition, mutation of a tertiary interaction involved in a parallel helix packing motif, maintains an extended structure upon titration of Mg^{2+}. (Leipply et al. 2011) These reports show a significant dependence on base pairing in RNA structures rather than relying solely on forces generated by counterions. For these reasons IC theory is not believed to be a major contributing factor in RNA folding.

Of the three theories mentioned for describing ion interactions with polyelectrolytes, NLPB is reasonable at predicting RNA-ion interactions. NLPB calculations attempt to determine the electrostatic potential at a location within a given distance from the polynucleotide. The potential can then be related to the excess and depletion of cations and anions respectively. NLPB was shown to concur with CC theory calculations at low monovalent salt concentrations for a model DNA cylinder. (Anderson et al. 1980) NLPB calculations are also robust, allowing for irregular charge separation of the macromolecule. (Misra et al. 2000) Despite these benefits, NLPB is limited by inherent misrepresentations in the calculations (e.g. implicit solvent, uniform dielectric constant). By treating counterions as a point charges, the calculation is unable to account for the important molecular detail of a hydrated ion of finite volume. Despite these shortcomings, NLPB is capable of predicting the number of excess Mg^{2+} ions for both the N and I-state of an RNA. These calculations have been shown to underestimate excess Mg^{2+} by 30% of the actual value. (Soto et al. 2007) Further algorithm development has imparted an increased amount of molecular detail by providing a distance cutoff from the RNA to the counterion, thus implying the radius of a counterion. (Chu et al. 2007) From NLPB theory also explains the origin of stability imparted to RNA by Mg^{2+} is believed to derive from an increase in entropy, where approximately two monovalent ions are released into the bulk solution upon accumulation of a single excess Mg^{2+} ion. This entropic origin of Mg^{2+} induced stability has been confirmed through single molecule studies. (Fiore et al. 2012) Despite its limitations (Bai et al. 2007), NLPB is

capable of providing qualitative and a semi-quantitative understanding of RNA-ion interactions.

Mg^{2+} is especially proficient at stabilizing the N-state despite significant interactions with the I-state (Schreier et al. 1974; Lynch et al. 1974; Stein et al. 1976) (Grilley et al. 2006) One of the more challenging tasks of understanding RNA folding consists of accounting for the various forms of RNA-Mg^{2+} interactions in each state. Cations can form long-range interactions with RNA while remaining fully hydrated in their primary solvation layer. Cations are also mobile in the vicinity of RNA, therefore they are referred to as "diffuse". (Draper, 2004) Previous theoretical and experimental work has shown that diffuse ions account for most of the RNA stability induced by counterions. (Misra et al. 2000; Leipply et al. 2011) As an ion approaches the surface of an RNA it is possible to shed a single water molecule and initiate direct contact with the RNA surface or contacts can be mediated via water molecules; the term "water-positioned" is given to these two interactions. Currently there are no accounts of experiments resolving the difference in energetics between diffuse and water-positioned ions. A large-scale simulation has shown that water-positioned Mg^{2+} may be coupled to RNA dynamics. (Hayes et al. 2012) More work is required in this field in order to resolve the importance of water positioned ions.

Figure 1-2

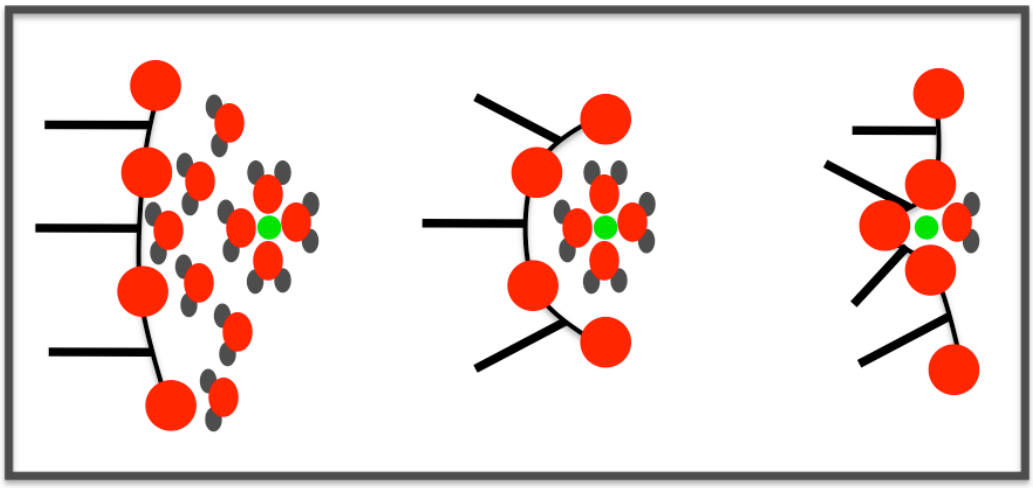

Figure 1-2. Various forms of RNA-cation interactions. (Draper, 2004) Small green spheres represent Mg^{2+} ions, large red spheres with grey spheres attached represent water molecules, and red spheres attached by black lines represent phosphate groups of the RNA. This figure depicts a range of potential ion interactions with RNA. At the far left of the figure, diffuse ions remain fully hydrated and mobile. The center image shows water-positioned ions residing on the surface of RNA. At the far right of the figure an image representing a chelated Mg^{2+} ion is shown.

In addition to cations that reside on the surface of RNA, particular folds crate areas of high negative potential enabling cations to localize within solvent-inaccessible pockets. In some cases these cavities are large and can accommodate specific monovalent ions. (Lambert et al. 2010) In other cases the large negative electrpostatic potential makes it possible replace two inner sphere water molecules of a high charge density counterion (e.g. Mg^{2+}) with two contacts from the RNA. Ions found in these environments are referred to in this thesis as "chelated". (Pyle, 2002; Draper, 2004)

Contrary to popular belief chelated ions are fairly rare in nature. To create a chelation site, RNA must bring phosphate groups into very close proximity resulting

in a negative potential of ~100 kcal/mol. (Misra et al. 2001) Given the energy required to form this site as well as partially dehydrate a Mg^{2+} ion, the total energy gained upon chelating Mg^{2+} is not extraordinarily large. Leipply et al. have shown that for a small rRNA fragment, the free energy gained from chelating a single Mg^{2+} is ~10% of the total $\Delta G_{RNA\text{-}Mg2+}$ under physiologically relevant conditions. (Leipply et al. 2011) Despite the rather small contribution to the stability of the native state, chelated Mg^{2+} ions are important for enabling otherwise conformationally inaccessible folds. In some cases RNA will not fold to a functional structure in the absence of a properly coordinated/occupied chelation site. (Rangan et al. 2003) Such reports have lead to the speculation that Mg^{2+} chelation sites are merely a means of increasing the structural diversity of RNA rather than increasing the stability of a particular fold. (Draper et al. 2008)

Types of ions associated with RNA

The cytoplasm is a highly concentrated electrolyte solution. Negatively charged phosphate groups of DNA and RNA pack together to create a crowded environment. Given this, the cell must compensate for all of the negative charges associated with the phosphate groups of DNA, RNA, and free anions (phosphonucleotides and amino acids). In *E. coli.*, the total phosphate concentration from nucleic acids is approximately 1 molar. (Record et al. 1998) As a result, cations are found in at least equal concentration and may even exceed this value if the concentration of free glutamate rises. Within the cell, K^{+} and Mg^{2+} carry out most of the anionic charge compensation, although nucleic acid binding proteins account for

a significant fraction of charge neutralization as well. The effect of K^+ and Mg^{2+} on RNA stability has been well studied (Shiman et al. 2000; Buchman, 1997; Stein et al. 1976) and has resulted in the elucidation of general principles governing RNA folding. (Draper et al. 2008) Yet the RNA folding problem is far from solved.

In addition to the cations K^+ and Mg^{2+}, polyamines can be found in substantial concentrations *in vivo.* (Tabor et al. 1984) These molecules are organic polyvalent cations that are involved in a number of biological processes. The three most prevalent polyamines in biological systems are spermine^{4+}, spermidine^{3+} and putrescine^{2+}, although the abundance and presence of each of these ions varies depending on the requirement of the organism. For instance, spermine^{4+} is found in very high concentration in sperm cells due to its function in DNA packaging, while *B. subtilis* contains only spermidine^{3+} under some growth conditions. (Woolridge et al. 1997) Generally, eukaryotes have a low concentration of putrescine^{2+} and moderate concentrations of spermidine^{3+} and spermine^{4+} while prokaryotes typically have a higher of concentration putrescine^{2+} than spermidine^{3+} and lack spermine^{4+}.

The biosynthetic pathway for generating polyamines *in vivo* is fairly similar between prokaryotes and eukaryotes. Putrescine^{2+} is required to synthesize both spermidine^{3+} and spermine^{4+}. Putrescine^{2+} can be synthesized through two separate pathways using either ornithine decarboxylase or arginine decarboxylase (the ornithine decarboxylase pathway is much more prevalent in nature). Using putrescine^{2+} as a substrate, spermidine synthase is capable of producing spermidine^{3+} which can then feed into the spermine^{4+} pathway using spermine^{4+} synthase. (Tabor et al. 1984) Knock out mutations in *E. coli* of ornithine

decarboxylase (speC) or arginine decarboxylase (speA) creates a requirement for putrescine^{2+} or spermidine^{3+} to grow at a normal rate or under anaerobic conditions. (Tabor et al. 1976) The viability of these mutant cells grown in the absence of putrescine^{2+} or spermidine^{3+} is due to an alternative biosynthetic pathway for producing spermidine^{3+} via a cadaverine^{2+} intermediate. (Tabor et al. 1976) In eukaryotes, polyamine synthesis is induced by many stimuli. (Tabor et al. 1984) Increases in polyamine concentration have been correlated with increased replication, transcription and translation. Given their cross species-abundance and requirement for vitality, polyamines are a necessity for basic life processes.

For many years researchers have probed the interactions between polyamines and RNA in order to gain insight into the fundamental role of these cations. Early studies mainly focused on tRNA interactions with polyamines and lead to some well established findings. Binding studies of polyamines with tRNA showed that binding affinity followed a trend of valence where spermine^{4+} > spermidine^{3+} > putrescine^{2+}. (Sakai et al. 1975; Heerschap et al. 1985) These initial studies lead researchers to question how these cations interact with RNA. Research began to focus on the structural nature of polyamine interactions with RNA and lead to the crystallization of tRNA in the presence of spermine^{4+}. (Quigley et al. 1978) Other independent studies resolved spermine^{4+} binding to tRNA-phe at atomic resolution as well. (Westhof et al. 1986; Dewan et al. 1985) Although these tRNA structures posses the same fold, spermine^{4+} was found to bind in a different location on tRNA-phe in the Westhof structure (helix adjacent to anticodon loop) than tRNA-

phe from the Dewan structure (helix adjacent to acceptor stem). These findings

Figure 1.3

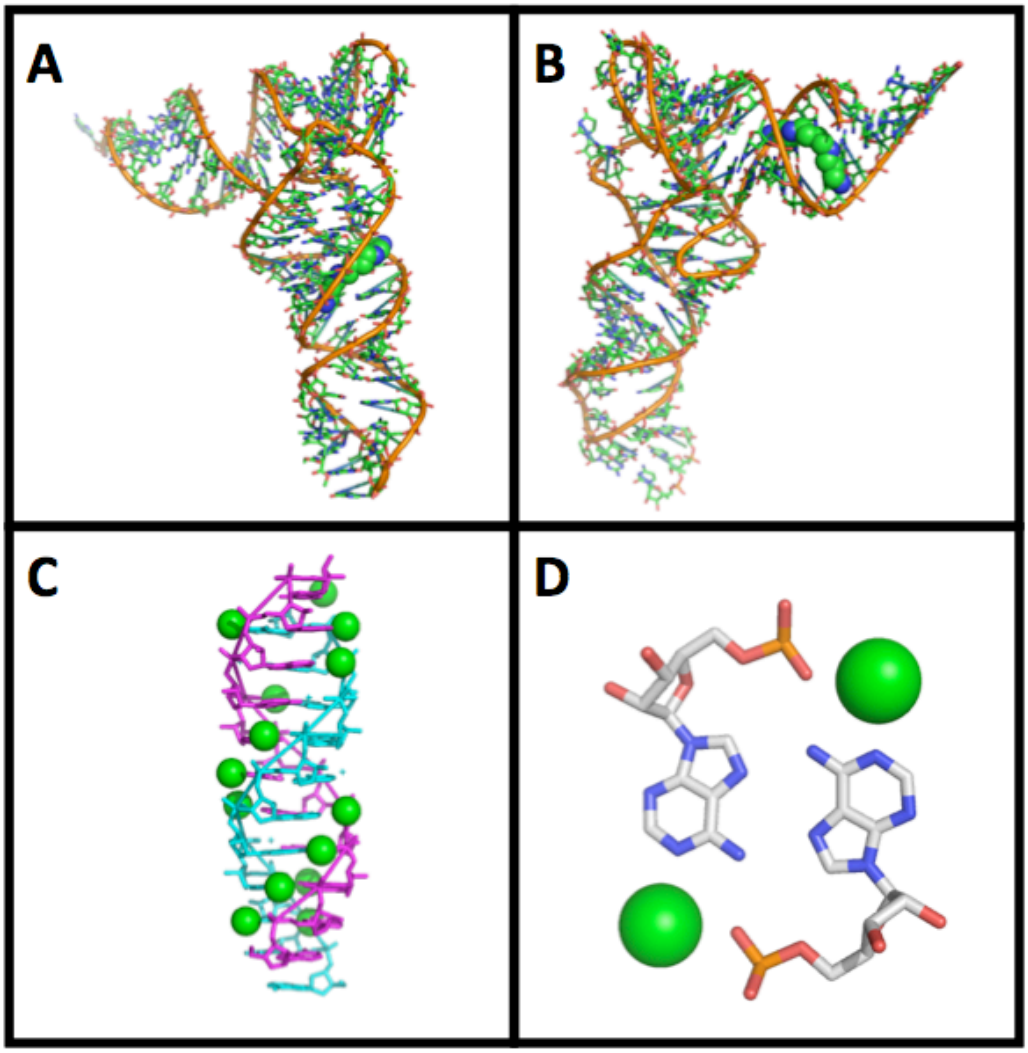

Figure 1-3. Structures of amines interacting with RNA. A) Structure of tRNA-phe (sticks) with spermine^{4+} (space fill) bound within the major groove (PDB ID: 1TN1). B) Structure of tRNA-phe (sticks) with spermine^{4+} (space fill) bound in the major groove adjacent to the acceptor stem (PDB ID: 2TRA). C) Structure of the parallel polyA duplex (magenta and cyan sticks) with bound NH_4^+ (green spheres). D) A single base pair of the parallel polyA duplex with NH_4^+ bound. NH_4^+ ions bridge phosphate and N1 of adenine.

showed that although spermine^{4+} is localized in both structures, binding specificity

is most likely restricted to the major groove with nonspecific hydrophobic

interactions playing a significant role. Solution studies probing spermine^{4+} binding to tRNA-phe found additional binding sites around the TΨC and D-loops. (Frydman et al. 1996) The conclusion from the compilation of these reports is that spermine^{4+} and other polyamines bind nonspecifically to tRNA despite being important to many biological processes.

Although tRNA does not show any specific binding site for spermine^{4+} or other polyamines, it is clear that amines are highly proficient at stabilizing RNA tertiary structure. In the case of monovalent ions, RNA is particularly stable in the presence of NH_4^+ relative to the group I monovalent ions K^+ and Na^+. For instance, the 58mer rRNA fragment, (an RNA known to specifically chelate K^+) has been shown to adopt a native like structure in presence of 1.6M NH_4^+ and absence of divalent ions where the equivalent concentration of K^+ does not induce folding. (Bukhman et al. 1997) A recent report shows that a parallel polyA duplex (first proposed by Rich et al. in 1961) was shown to be stable at neutral pH in the presence of high concentrations of NH_4^+ (the parallel duplex does not form in the presence of Na^+ at neutral pH although it does form at pH 4 in Na^+). (Safaee et al. 2013; Rich et al. 1961) Stabilization of this fold is rationalized by the atomic resolution structure that depicts an ammonium ion bridging the interaction of a phosphate oxygen with N1 in the adenine ring.

All of the data showing a stable structure induced solely by NH_4^+ has been gathered under extreme conditions with NH_4^+ concentrations equal to or exceeding 1.6M. (Bukhman et al. 1997; Koculi et al. 2004; Safaee et al. 2013) Although there are no experiments reporting on the matter, the electrostatics and hydration of RNA

in the presence of NH_4^+ may be altered relative to other monovalent salts at the same concentration. (Draper, 2013)

In mixed electrolyte solutions containing Mg^{2+}, moderate concentrations of NH_4^+ have been shown to stabilize the native state of a 58mer rRNA fragment to relatively the same extent as K^+. (Shiman et al. 2000; Wang et al. 1993) These data suggest that NH_4^+ may interact with a specific binding site, presumably the K^+ chelation site. In addition, the L-box riboswitch has been shown to specifically bind L-lysine. (Seganov et al. 2008) Although this ligand has a carboxylate functional group within its structure, the saturated aliphatic diamine portion is structurally homologous to cadaverine^{2+} (a by-product of L-lysine metabolism). These structures provide insight into how RNA can specifically bind an ammonium ion/polyamine.

After reviewing the field of polyamine nucleic acid studies the work presented here will focus on and articulate the findings of studies conducted with the following criteria i) data must be generated with a large excess of monovalent ions over polyamines. ii) Solutions must be buffered at a pH that ensures the vast majority of amines are protonated in solution. iii) Polyamine concentrations should be kept low enough to prevent aggregation of RNA. Using these criteria to filter the literature very few articles remain regarding RNA polyamine interactions. One article of exceptional quality is that of Frydman et al. which looks at the interaction of the polyamines spermine^{4+}, spermidine^{3+} and putrescine^{2+} with tRNA. (Frydman et al. 1992) These researchers set out to observe the T_1 relaxation times of ^{15}N labeled polyamines in the absence and presence of tRNA. Their results showed that the T_1 relaxation times for both the primary and secondary amines of spermine^{4+}

and spermidine^{3+} decreased in the presence of tRNA. T_1 times for these amines also showed a temperature dependence where the natural log of T_1 decreased with the inverse of absolute temperature. Contrary to these findings ^{15}N labeled putrescine^{2+} did not have altered tumbling times in the presence of tRNA. From these results Frydman et al. proposed that spermine^{4+} and spermidine^{3+} are hydrogen bonding to the tRNA (in addition to electrostatic interactions) while putrescine^{2+} does not make direct contacts with the RNA surface. The conclusion drawn from this study is that putrescine^{2+} interacts with tRNA primarily through diffuse electrostatic interactions. Since there have not been any reports of specific binding sites on nucleic acids for putrescine^{2+}, we will conclude that interactions involving putrescine^{2+} and RNA are predominantly diffuse and electrostatic in nature.

The osmotic stress response and RNA folding

Although cations balance the charge of anionic components, they are also responsible for providing a quick response to osmotic stress. As the osmolarity of the external environment increases, so does the turgor pressure imposed on the cell membrane. Without any adjustment, the cell will either contract or expand depending on whether the medium is hypertonic or hypotonic respectively. To prevent this, *E. coli* tunes the concentration of solutes in the cytoplasm to an appropriate osmolarity. The initial phase of this adjustment involves the uptake or release of cations. The two main cations implicated in this response are K^+ and putrescine^{2+}. The concentrations of these cations change in an anti-correlated fashion so as to maintain electroneutrality while adjusting turgor pressure

(Spermidine^{3+} concentrations also change during this process but to a much lesser extent.). (Cayley et al. 1989; Capp et al. 1998) After approximately 30 minutes the ion concentrations in the cell return to a normal range due to synthesis or import of neutral Osmolytes. These changes in the cation content of the cell may have a dramatic effect on the stability of RNA *in vivo*.

RNA Folding interpreted through the preferential interaction formalism

The majority of RNA folding studies have been conducted by titrating a salt into an RNA containing solution while monitoring the fraction of folded RNA or the temperature at which a phase transition is 50% complete. Although these studies can be very useful, misinterpretation of these data has lead to a flawed understanding of the mechanism by which counterions stabilize the N-state. The Schimmel lab was one of the first groups to fit Mg^{2+} titration data using the Hill equation. (Lynch et al. 1974; Schreier et al. 1975) Although this group was cautious about the interpretation of the fitted parameters (the Hill coefficient), other groups quickly adopted the Hill equation for similar analyses and interpreted the Hill coefficient as the number of Mg^{2+} ions bound to the native structure. Two important aspects to consider is that i) use of the Hill equation disregards the long range nature of cation-RNA interactions and ii) assumes that cations interact exclusively with the native state (Figure 1-4). Work being conducted concurrently with these folding studies was showing that ions have a strong interaction with the nucleic acids lacking tertiary interactions, supporting the notion that electrostatic

interactions with the I-state are an important consideration. (Manning, 1972; Braunlin et al. 1981, 1982, 1984) This evidence proved that a site binding formalism is not adequate for interpretation of ions interacting with nucleic acids, and that a new approach is needed.

Rather than interpreting ion induced RNA folding as a "binding" event, a more general view can be assembled that does not suffer from false molecular interpretation. The foundation of this scheme can be visualized as a thermodynamic cycle (Figure 1-4). Horizontal arrows represent standard state folding free energies. As shown here, this is the difference in free energy between the N and I-states of an RNA under a given set of conditions. Alternatively this is conceived as the natural log of the ratio of concentrations for the N and I-states. This interpretation defines the conditions of the standard state and allows one to relate the ratio of concentrations to the ratio of the activity coefficients (equation 1-1).

(1-1)

To relate the horizontal arrows in Figure (1-4), the free energies of Mg^{2+} interaction with the N and I-state ($\Delta G_{I\text{-}Mg2+}$ and $\Delta G_{N\text{-}Mg2+}$) must be determined. These elusive values correspond to the vertical arrows in the thermodynamic cycle of Figure 1-4.

It is clear that Mg^{2+} stabilizes the N-state of RNA to a much greater degree than K^{+} does, but a molecular description of the events leading to this increased stability has not yet been provided. Linkage analysis incorporates a general framework upon which both specific and non-specific interactions can be

quantitatively interpreted. Within linkage relations, preferential interaction coefficients (Γ) may be employed to provide a general descriptor for solute interactions. The preferential interaction coefficient is defined as the change in molal concentration of a solute that accompanies the change in molal concentration of another solute in order to maintain constant chemical potential of the first solute (equation 1-2). For the experiments conducted in this thesis, molar and molal concentrations are equivalent. By invoking the chain rule and Euler reciprocity on the first partial derivative in equation 1-2, the change in the activity of a solute (a_1) can be related to the change in the activity coefficient of another solute at constant concentration.

$$\Gamma_1 \equiv \left(\frac{\partial m_1}{\partial m_2}\right)_{\mu_1} = \left(\frac{\partial \ln \gamma_2}{\partial \ln a_1}\right)_{m_2} \qquad 1\text{-}2)$$

For the purposes of the experiments presented in this thesis, it is useful to interpret a_1 as the activity of divalent ion being added to solution and γ_2 as the activity coefficient of RNA at constant concentration of RNA. Through this relation the free energy of solute-solute interaction is attainable without imposing any model of how these solutes interact. Given the spectrum of ways in which cations can interact with RNA (Figure 1-2), this formalism is ideal for describing polyelectrolyte systems.

Figure 1-4

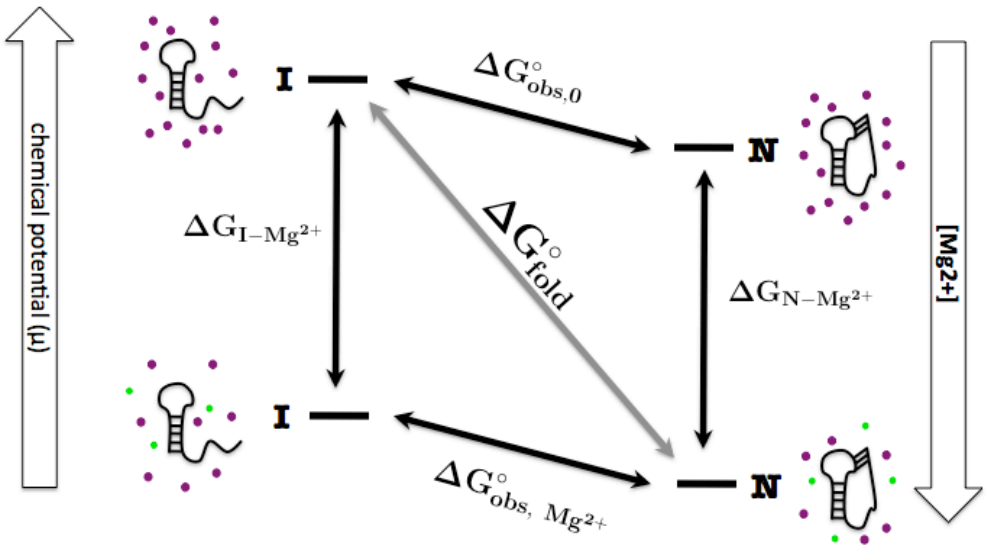

Figure 1-4. Thermodynamic cycle for the folding of an RNA upon addition of Mg^{2+}. RNA folding is depicted with horizontal double arrows while Mg^{2+} interaction is shown with vertical double arrows. Folding scheme corresponding to a binding formalism is shown with the grey diagonal arrow. RNA is represented as a neutral salt with K^{+} ions shown as purple spheres and Mg^{2+} ions represented as green spheres. Chemical potential of the RNA decreases as Mg^{2+} is added to the system.

Visualization of the preferential interaction coefficient can be obtained by conducting a simple thought experiment. In this experiment equilibrium dialysis of a polyelectrolyte is conducted for two sets of conditions. The experiment begins in a beaker containing a large amount of liquid (Figure 1-5). Within this beaker resides a dilute aqueous electrolyte solution of KCl and a dialysis bag. The dialysis bag is semi-permeable, only allowing water and small ions to pass freely from one side to the other. At the initial stage of the experiment, both the chemical potentials and concentrations of H_2O and KCl are equal on both sides of the dialysis bag. A 10mer RNA is then added to the inside of the dialysis bag. It is important to note that the RNA is added into solution as a neutral K^{+} salt. After allowing the system to reach

equilibrium, the chemical potential of each component in solution is the same on both sides of the membrane. The result is an excess of K^+ ions and a deficiency of Cl^- ions inside of the dialysis bag (note that electroneutrality is maintained on both sides of the dialysis membrane). It is the excess and deficiency of ions that provides the conceptual framework of the preferential interaction coefficient. The difference in the concentration of solute particles on the inside vs outside of the dialysis bag relative to the concentration of RNA is equivalent to the preferential interaction coefficient for that solute particle (equation 1-3). In the experiment conceptualized here there is an excess of 9 K^+ ions ($\Gamma_{K+} = 9$) and a depletion of 1 Cl^- ion ($\Gamma_{Cl-} = -1$). Note that the chelated K^+ ion in figure 1-5 is merely one of nine ions in the preferential interaction coefficient. There is no distinction between the types of interactions being made by solutes with this formalism.

In the next phase of the experiment $MgCl_2$ is added to the beaker and the system is allowed to reach equilibrium. The result is a greater concentration of Mg^{2+} inside the dialysis bag relative to the outside of the bag. From this the preferential interaction coefficient of Mg^{2+} can be calculated from equation (1-3).

$$\Gamma \approx \left(\frac{C_{in} - C_{out}}{C_{RNA}} \right) \tag{1-3}$$

As depicted, there is a net release of K^+ from the inside of the dialysis bag upon addition of Mg^{2+}. For each Mg^{2+} ion pair that enters the dialysis bag two K^+ ions move across the membrane thus maintaining electroneutrality. As a result the preferential interaction coefficient profile can be equated to the charge of the nucleic acid through equation (1-4).

$$|\mathbf{Z}| = 2\boldsymbol{\Gamma}_{Mg^{2+}} + \boldsymbol{\Gamma}_{K^+} - \boldsymbol{\Gamma}_{Cl^-} \quad (1\text{-}4)$$

This exchange process is favorable due to the reduced entropic penalty for localizing one (Mg^{2+}) ion in the ion atmosphere as opposed to two (K^+) ions. This is the basis for increased stabilization of RNA by ions of higher valency.

Figure 1-5

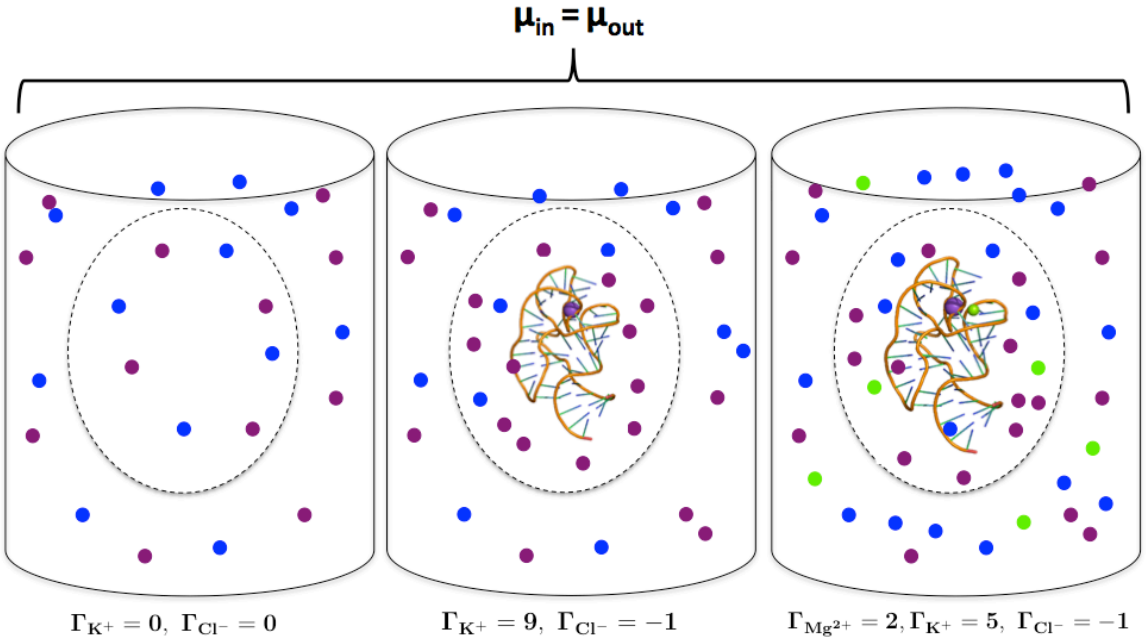

Figure 1-5. Schematic of an equilibrium dialysis experiment. Each beaker represents a different phase of the experiment. The dashed circle inside of the beakers represents a dialysis membrane where ions (K^+ (purple), Cl^- (blue) and Mg^{2+} (green)) and water molecules (not shown) can pass freely. All steps maintain electroneutrality between the inside and outside of the dialysis membrane. The second beaker shows the introduction of a 10mer RNA•K^+ salt. The third beaker shows the introduction of $MgCl_2$ to the system. The preferential interaction coefficients for each ion in solution are shown on the bottom for each phase of the experiment. Note that the chelated ions in the RNA also contribute to the preferential interaction coefficients.

The question still remains of how the excess Mg^{2+} is related to the changes in free energy shown in Figure 1-4. It has previously been shown that integration of the preferential interaction coefficient for Mg^{2+} with respect to bulk Mg^{2+} (C_{Mg2+}) is approximately equal to the free energy of RNA-Mg^{2+} interaction (equation 1-5). (Grilley et al. 2006)

$$\Delta G_{RNA-Mg^{2+}} \approx -RT \int_0^{C_{Mg^{2+}}} \Gamma_{Mg^{2+}} d \ln C_{Mg^{2+}} \tag{1-5}$$

This relation is only valid if the conformation of the macromolecule remains constant over the course of the titration. As mentioned previously, RNA folding is coupled to the addition of Mg^{2+} causing the determination of $\Delta G_{RNA\text{-}Mg2+}$ to be tricky. Yet ways around this issue have previously been undertaken. Leipply et al. have shown that by using a ligand or protein capable of folding RNA in the absence of Mg^{2+} it is possible to lock the RNA of interest into its N-state. (Leipply et al. 2011) Alternatively it possible to mimic the I-state by disrupting tertiary interactions through mutations causing the RNA to stay extended even in the presence of Mg^{2+}. (Grilley et al. 2006)

Outline of the work presented within this dissertation

The work presented here will be focused on understanding how ions impact the folding of RNA *in vivo*. As a first step, RNA stability in the presence of different diamines was probed top determine the importance of putrescine^{2+} to RNA folding. In the next step we sought to understand how RNA stability is affected by the presence of an additional divalent ion. With this mindset, experiments were

conducted in the presence of K^+, Mg^{2+} and putrescine^{2+}, the three most abundant cations in *E. coli*. Further understanding of RNA folding in the presence of these three cations was obtained by monitoring the excess Mg^{2+} for the native and intermediate states of a purine riboswitch as a function of putrescine^{2+} concentration. These studies show that the N-state possesses tightly associated Mg^{2+} ion(s) that do not readily exchange with putrescine^{2+}. To characterize the environment and requirement of this tightly associated Mg^{2+} ion(s) a divalent ion survey was conducted on both the *add* adenine riboswitch as well as three other well-characterized RNAs.

References

1. Adilakshmi, T., Bellur, D. L., and Woodson, S. A. (2008) Concurrent nucleation of 16S folding and induced fit in 30S ribosome assembly, *Nature 455*, 1268-1272.

2. Agrawal, R. K., Penczek, P., Grassucci, R. A., Burkhardt, N., Nierhaus, K. H., and Frank, J. (1999) Effect of buffer conditions on the position of tRNA on the 70 S ribosome as visualized by cryoelectron microscopy, *Journal of Biological Chemistry 274*, 8723-8729.

3. Anderson, C. F., and Record, M. T. (1980) THE RELATIONSHIP BETWEEN THE POISSON-BOLTZMANN MODEL AND THE CONDENSATION HYPOTHESIS - AN ANALYSIS BASED ON THE LOW SALT FORM OF THE DONNAN COEFFICIENT, *Biophysical Chemistry 11*, 353-360.

4. Anderson, C. F., and Record, M. T. (1993) SALT DEPENDENCE OF OLIGOION POLYION BINDING - A THERMODYNAMIC DESCRIPTION BASED ON PREFERENTIAL INTERACTION COEFFICIENTS, *Journal of Physical Chemistry 97*, 7116-7126.

5. Antony, T., Thomas, T., Shirahata, A., and Thomas, T. J. (1999) Selectivity of polyamines on the stability of RNA-DNA hybrids containing phosphodiester and phosphorothioate oligodeoxyribonucleotides, *Biochemistry 38*, 10775-10784.

6. Behrouzi, R., Roh, J. H., Kilburn, D., Briber, R. M., and Woodson, S. A. (2012) Cooperative Tertiary Interaction Network Guides RNA Folding, *Cell 149*, 348-357.

7. Braunlin, W. H., Anderson, C. F., and Record, M. T. (1986) NA-23-NMR INVESTIGATIONS OF COUNTERION EXCHANGE-REACTIONS OF HELICAL DNA, *Biopolymers 25*, 205-214.

8. Braunlin, W. H., Strick, T. J., and Record, M. T. (1981) BINDING OF POLYAMINES TO DNA, *Biophysical Journal 33*, A312-A312.

9. Braunlin, W. H., Strick, T. J., and Record, M. T. (1982) EQUILIBRIUM DIALYSIS STUDIES OF POLYAMINE BINDING TO DNA, *Biopolymers 21*, 1301-1314.

10. Brown, R. S., Dewan, J. C., and Klug, A. (1985) CRYSTALLOGRAPHIC AND BIOCHEMICAL INVESTIGATION OF THE LEAD(II)-CATALYZED HYDROLYSIS OF YEAST PHENYLALANINE TRANSFER-RNA, *Biochemistry 24*, 4785-4801.

11. Bukhman, Y. V., and Draper, D. E. (1997) Affinities and selectivities of divalent cation binding sites within an RNA tertiary structure, *Journal of Molecular Biology 273*, 1020-1031.

12. Castro-Roa, D., and Zenkin, N. (2012) In vitro experimental system for analysis of transcription-translation coupling, *Nucleic Acids Research 40*, 12.

13. Chu, V. B., Bai, Y., Lipfert, J., Herschlag, D., and Doniach, S. (2007) Evaluation of ion binding to DNA duplexes using a size-modified Poisson-Boltzmann theory, *Biophysical Journal 93*, 3202-3209.

14. Draper, D. E. (2004) A guide to ions and RNA structure, *Rna-a Publication of the Rna Society 10*, 335-343.

15. Draper, D. E. (2013) Folding of RNA Tertiary Structure: Linkages Between Backbone Phosphates, Ions, and Water, *Biopolymers 99*, 1105-1113.

16. Draper, D. E. (2008) RNA Folding: Thermodynamic and Molecular Descriptions of the Roles of Ions, *Biophysical Journal 95*, 5489-5495.

17. Fiore, J. L., Holmstrom, E. D., and Nesbitt, D. J. (2012) Entropic origin of Mg2+-facilitated RNA folding, *Proceedings of the National Academy of Sciences of the United States of America 109*, 2902-2907.

18. Frydman, B., Westler, W. M., and Samejima, K. (1996) Spermine binds in solution to the T psi C loop of tRNA(Phe): Evidence from a 750 MHz H-1-NMR analysis, *Journal of Organic Chemistry 61*, 2588-2589.

19. Frydman, L., Rossomando, P. C., Frydman, V., Fernandez, C. O., Frydman, B., and Samejima, K. (1992) INTERACTIONS BETWEEN NATURAL POLYAMINES AND TRANSFER-RNA - AN N-15 NMR ANALYSIS, *Proceedings of the National Academy of Sciences of the United States of America 89*, 9186-9190.

20. Garst, A. D., Heroux, A., Rambo, R. P., and Batey, R. T. (2008) Crystal structure of the lysine riboswitch regulatory mRNA element, *Journal of Biological Chemistry 283*, 22347-22351.

21. Grilley, D., Misra, V., Caliskan, G., and Draper, D. E. (2007) Importance of partially unfolded conformations for Mg2+-lnduced folding of RNA tertiary structure: Structural models and free energies of Mg2+ interactions, *Biochemistry 46*, 10266-10278.

22. Grilley, D., Soto, A. M., and Draper, D. E. (2009) DIRECT QUANTITATION OF MG(2+)-RNA INTERACTIONS BY USE OF A FLUORESCENT DYE, In *Methods in Enzymology: Biothermodynamics,Vol 455, Part A* (Johnson, M. L., Holt, J. M., and Ackers, G. K., Eds.), pp 71-94, Elsevier Academic Press Inc, San Diego.

23. Grohman, J. K., Gorelick, R. J., Lickwar, C. R., Lieb, J. D., Bower, B. D., Znosko, B. M., and Weeks, K. M. (2013) A Guanosine-Centric Mechanism for RNA Chaperone Function, *Science 340*, 190-195.

24. Hayes, R. L., Noel, J. K., Mohanty, U., Whitford, P. C., Hennelly, S. P., Onuchic, J. N., and Sanbonmatsu, K. Y. (2012) Magnesium Fluctuations Modulate RNA Dynamics in the SAM-I Riboswitch, *Journal of the American Chemical Society 134*, 12043-12053.

25. Heerschap, A., Walters, J., and Hilbers, C. W. (1985) INTERACTIONS OF SOME NATURALLY-OCCURRING CATIONS WITH PHENYLALANINE AND INITIATOR TRANSFER-RNA FROM YEAST AS REFLECTED BY THEIR THERMAL-STABILITY, *Biophysical Chemistry 22*, 205-217.

26. Higashi, K., Terui, Y., Suganami, A., Tamura, Y., Nishimura, K., Kashiwagi, K., and Igarashi, K. (2008) Selective Structural Change by Spermidine in the Bulged-out Region of Double-stranded RNA and Its Effect on RNA Function, *Journal of Biological Chemistry 283*, 32989-32994.

27. Kilburn, D., Roh, J. H., Behrouzi, R., Briber, R. M., and Woodson, S. A. (2013) Crowders Perturb the Entropy of RNA Energy Landscapes to Favor Folding, *Journal of the American Chemical Society 135*, 10055-10063.

28. Kwok, L. W., Shcherbakova, I., Lamb, J. S., Park, H. Y., Andresen, K., Smith, H.,

Brenowitz, M., and Pollack, L. (2006) Concordant exploration of the kinetics of RNA folding from global and local perspectives, *Journal of Molecular Biology 355*, 282-293.

29. Lambert, D., and Draper, D. E. (2007) Effects of osmolytes on RNA secondary and tertiary structure stabilities and RNA-Mg2+ interactions, *Journal of Molecular Biology 370*, 993-1005.

30. Lambert, D., Leipply, D., Shiman, R., and Draper, D. E. (2009) The Influence of Monovalent Cation Size on the Stability of RNA Tertiary Structures, *Journal of Molecular Biology 390*, 791-804.

31. Lambert, D., and Draper, D. E. (2012) Denaturation of RNA Secondary and Tertiary Structure by Urea: Simple Unfolded State Models and Free Energy Parameters Account for Measured m-Values, *Biochemistry 51*, 9014-9026.

32. Leipply, D., and Draper, D. E. (2010) Dependence of RNA Tertiary Structural Stability on Mg2+ Concentration: Interpretation of the Hill Equation and Coefficient, *Biochemistry 49*, 1843-1853.

33. Leipply, D., and Draper, D. E. (2011) Effects of Mg(2+) on the Free Energy Landscape for Folding a Purine Riboswitch RNA, *Biochemistry 50*, 2790-2799.

34. Leipply, D., and Draper, D. E. (2011) Evidence for a Thermodynamically Distinct Mg(2+) Ion Associated with Formation of an RNA Tertiary Structure, *Journal of the American Chemical Society 133*, 13397-13405.

35. Manning, G. S. (1969) LIMITING LAWS AND COUNTERION CONDENSATION IN POLYELECTROLYTE SOLUTIONS .I. COLLIGATIVE PROPERTIES, *Journal of Chemical Physics 51*, 924-&.

36. Manning, G. S. (1972) POLYELECTROLYTES, *Annual Review of Physical Chemistry 23*, 117-&.

37. Misra, V. K., and Draper, D. E. (2000) Mg2+ binding to tRNA revisited: The nonlinear Poisson-Boltzmann model, *Journal of Molecular Biology 299*, 813-825.

38. Misra, V. K., and Draper, D. E. (2001) A thermodynamic framework for Mg2+ binding to RNA, *Proceedings of the National Academy of Sciences of the United States of America 98*, 12456-12461.

39. Misra, V. K., and Draper, D. E. (2002) The linkage between magnesium binding and RNA folding, *Journal of Molecular Biology 317*, 507-521.

40. Moghaddam, S., Caliskan, G., Chauhan, S., Hyeon, C., Briber, R. M., Thirumalai, D., and Woodson, S. A. (2009) Metal Ion Dependence of Cooperative Collapse Transitions in RNA, *Journal of Molecular Biology 393*, 753-764.

41. Murthy, V. L., and Rose, G. D. (2000) Is counterion delocalization responsible for collapse in RNA folding?, *Biochemistry 39*, 14365-14370.

42. Pyle, A. M. (2002) Metal ions in the structure and function of RNA, *Journal of Biological Inorganic Chemistry 7*, 679-690.

43. Quigley, G. J., Teeter, M. M., and Rich, A. (1978) STRUCTURAL-ANALYSIS OF SPERMINE AND MAGNESIUM-ION BINDING TO YEAST PHENYLALANINE TRANSFER-RNA, *Proceedings of the National Academy of Sciences of the United States of America 75*, 64-68.

44. Record, M. T. (1975) EFFECTS OF NA+ AND MG++ IONS ON HELIX-COIL TRANSITION OF DNA, *Biopolymers 14*, 2137-2158.

45. Record, M. T., Courtenay, E. S., Cayley, D. S., and Guttman, H. J. (1998) Responses of E-coli to osmotic stress: Large changes in amounts of cytoplasmic solutes and water, *Trends in Biochemical Sciences 23*, 143-148.

46. Rich, A., Crick, F. H. C., Watson, J. D., and Davies, D. R. (1961) MOLECULAR STRUCTURE OF POLYADENYLIC ACID, *Journal of Molecular Biology 3*, 71-&.

47. Roh, J. H., Tyagi, M., Briber, R. M., Woodson, S. A., and Sokolov, A. P. (2011) The Dynamics of Unfolded versus Folded tRNA: The Role of Electrostatic Interactions, *Journal of the American Chemical Society 133*, 16406-16409.

48. Rouzina, I., and Bloomfield, V. A. (1996) Macroion attraction due to electrostatic correlation between screening counterions .1. Mobile surface-adsorbed ions and diffuse ion cloud, *Journal of Physical Chemistry 100*, 9977-9989.

49. Safaee, N., Noronha, A. M., Rodionov, D., Kozlov, G., Wilds, C. J., Sheldrick, G. M., and Gehring, K. (2013) Structure of the parallel duplex of poly(A) RNA: evaluation of a 50 year-old prediction, *Angewandte Chemie (International ed. in English) 52*, 10370-10373.

50. Sakai, T. T., Torget, R., I, J., Freda, C. E., and Cohen, S. S. (1975) BINDING OF POLYAMINES AND OF ETHIDIUM-BROMIDE TO TRANSFER-RNA, *Nucleic Acids Research 2*, 1005-1022.

51. Schreier, A. A., and Schimmel, P. R. (1974) INTERACTION OF MANGANESE WITH FRAGMENTS, COMPLEMENTARY FRAGMENT RECOMBINATIONS,

AND WHOLE MOLECULES OF YEAST PHENYLALANINE SPECIFIC TRANSFER-RNA, *Journal of Molecular Biology 86*, 601-620.

52. Schreier, A. A., and Schimmel, P. R. (1975) INTERACTION OF POLYAMINES WITH FRAGMENTS AND WHOLE MOLECULES OF YEAST PHENYLALANINE-SPECIFIC TRANSFER-RNA, *Journal of Molecular Biology 93*, 323-329.

53. Serganov, A., Huang, L. L., and Patel, D. J. (2008) Structural insights into amino acid binding and gene control by a lysine riboswitch, *Nature 455*, 1263-U1276.

54. Shiman, R., and Draper, D. E. (2000) Stabilization of RNA tertiary structure by monovalent cations, *Journal of Molecular Biology 302*, 79-91.

55. Soto, A. M., Misra, V., and Draper, D. E. (2007) Tertiary structure of an RNA pseudoknot is stabilized by "diffuse" Mg2+ ions, *Biochemistry 46*, 2973-2983.

56. Stein, A., and Crothers, D. M. (1976) CONFORMATIONAL-CHANGES OF TRANSFER-RNA - ROLE OF MAGNESIUM(II), *Biochemistry 15*, 160-168.

57. Strauss, U. P., Helfgott, C., and Pink, H. (1967) INTERACTIONS OF POLYELECTROLYTES WITH SIMPLE ELECTROLYTES .2. DONNAN EQUILIBRIA OBTAINED WITH DNA IN SOLUTIONS OF 1-1 ELECTROLYTES, *Journal of Physical Chemistry 71*, 2550-&.

58. Tabor, C. W., and Tabor, H. (1976) 1,4-DIAMINOBUTANE (PUTRESCINE), SPERMIDINE, AND SPERMINE, *Annual Review of Biochemistry 45*, 285-306.

59. Tabor, C. W., and Tabor, H. (1984) POLYAMINES, *Annual Review of Biochemistry 53*, 749-790.

60. Tang, C. K., and Draper, D. E. (1989) UNUSUAL MESSENGER-RNA PSEUDOKNOT STRUCTURE IS RECOGNIZED BY A PROTEIN TRANSLATIONAL REPRESSOR, *Cell 57*, 531-536.

61. Tyrrell, J., McGinnis, J. L., Weeks, K. M., and Pielak, G. J. (2013) The Cellular Environment Stabilizes Adenine Riboswitch RNA Structure, *Biochemistry 52*, 8777-8785.

62. Wang, Y. X., Lu, M., and Draper, D. E. (1993) SPECIFIC AMMONIUM ION REQUIREMENT FOR FUNCTIONAL RIBOSOMAL-RNA TERTIARY STRUCTURE, *Biochemistry 32*, 12279-12282.

63. Westhof, E., and Sundaralingam, M. (1986) RESTRAINED REFINEMENT OF THE MONOCLINIC FORM OF YEAST PHENYLALANINE TRANSFER-RNA - TEMPERATURE FACTORS AND DYNAMICS, COORDINATED WATERS, AND BASE-PAIR PROPELLER TWIST ANGLES, *Biochemistry 25*, 4868-4878.

64. Winkler, W. C., Cohen-Chalamish, S., and Breaker, R. R. (2002) An mRNA structure that controls gene expression by binding FMN, *Proceedings of the National Academy of Sciences of the United States of America 99*, 15908-15913.

65. Woolridge, D. P., VazquezLaslop, N., Markham, P. N., Chevalier, M. S., Gerner, E. W., and Neyfakh, A. A. (1997) Efflux of the natural polyamine spermidine facilitated by the Bacillus subtilis multidrug transporter Blt, *Journal of Biological Chemistry 272*, 8864-8866.

66. Wu, M., and Tinoco, I. (1998) RNA folding causes secondary structure rearrangement, *Proceedings of the National Academy of Sciences of the United States of America 95*, 11555-11560.

67. Zheng, M. X., Wu, M., and Tinoci, I. (2001) Formation of a GNRA tetraloop in P5abc can disrupt an interdomain interaction in the Tetrahymena group I ribozyme, *Proceedings of the National Academy of Sciences of the United States of America 98*, 3695-3700.

Chapter 2:

Comparison of Interactions of Diamine and Mg2+ with RNA Tertiary Structures: Similar versus Differential Effects on the Stabilities of Diverse RNA Folds.

This work was published in part as:

Trachman R.J., Draper D.E. (2013) Comparison of Interactions of Diamine and Mg2+ with RNA Tertiary Structures: Similar versus Differential Effects on the Stabilities of Diverse RNA Folds. *Biochemistry*, 52(34):5911-9

Abstract

Cations play a large role in stabilizing the native state of RNA *in vivo*. In addition to Mg^{2+}, putrescine^{2+} is an abundant divalent cation in bacterial cells. It is not yet known how RNA responds to the presence of both putrescine^{2+} and Mg^{2+} simultaneously interacting with an RNA. In this study we look at how the stability of four structured RNAs possessing differing interactions with cations are affected by putrescine^{2+} relative to Mg^{2+} and how these two cations together affect the stability of the native state. Through the use of thermal melts we observe that (i) Putrescine^{2+} is much less effective than Mg^{2+} at stabilizing RNA. (ii) The stability imparted by diamines on RNA is a function of charge density as well as flexibility of the counterion. (iii) When magnesium chelation sites are not present in an RNA, the relative change in free energy in the presence of Mg^{2+} upon addition of putrescine^{2+} is negative. The opposite result occurs for RNA containing magnesium chelation sites. This supports the notion that chelation sites are present to expand the structural diversity of RNA, although natural fluctuations in putrescine^{2+} activity may bias gene regulation through altered riboswitch stability.

Introduction

The ionic composition of the cytoplasm plays a large part in dictating the stability of native RNA structure. In addition to the inorganic ions found in cells (predominantly K^+ and Mg^{2+}) organic cations such as putrescine (1,4-diaminobutane) are found in concentrations high enough to warrant attention. In this work putrescine will be referred to as putrescine^{2+} given its charged state inside of the cell. Putrescine^{2+} is the third most abundant cation in vivo with a total concentration that ranges between 10 and 60mM in E coli, depending on the growth medium. (Capp et al. 1996; Cayley et al. 1989) These values are very significant given that the most abundant divalent ion (Mg^{2+}) in the cell has a total concentration of ~100mM. (Record et al. 1998) Despite the clear significance of understanding RNA-putrescine^{2+} interactions, there are relatively few studies focusing on this subject. (Koculi et al. 2004; Heerschap et al. 1985; Braunlin et al. 1982)

The current study seeks to understand the impact of putrescine^{2+} in regards to stabilizing RNA tertiary structure *in vivo*. Comparisons are drawn between the efficacy of putrescine^{2+} and Mg^{2+} at stabilizing the tertiary structure of four different RNAs. These four RNA molecules are intended to be representative of the diverse set of RNA folds found within a bacterial cell. The results are consistent between different RNA structures in that Mg^{2+} stabilizes the native state of all four RNAs to a greater degree than the equivalent concentration of putrescine^{2+}. In the presence of Mg^{2+}, the change in thermal stability upon addition of putrescine^{2+} is found to either

increase or decrease depending on the fold of the RNA. These findings can be attributed to the inability of putrescine^{2+} to occupy Mg^{2+} chelation sites as well as a difference in charge density among different divalent cations.

Results

RNA Selection

To survey the effects of putrescine^{2+} on the stability of RNA tertiary structure, four RNAs that differ in their interactions with inorganic ions were selected for study (Figures 1 and A-1). In this work ions interacting with RNA are categorized as belonging to one of two classes. The first class of ions is referred to as "chelated". (Pyle, 2002) Chelated ions are found in pockets of high negative potential. (Cate et al. 1997; Misra et al. 2001) The hydration of a chelated ion must be altered so that at least two direct contacts are made with the RNA. The second class of ions is much more diverse than chelated ions, and will be referred to as residing in the "ion atmosphere". Due to the nature of electrostatic interactions, ions within the ion atmosphere may stabilize RNA at a distance many Ångstroms from the RNA surface or directly on the surface of the RNA.

The aptamer domain of the *add* adenine riboswitch (A-riboswitch) was chosen as a model system of a structured RNA stabilized by ions residing exclusively in the ion atmosphere. The A-riboswitch folds into its native structure in the absence of divalent ions upon addition of adenine (or adenine derivatives) to the solution. (Lemay et al. 2006; Leipply et al. 2011) Although the RNA shows increased stability in the presence of Mg^{2+} (Lemay et al. 2006; Leipply et al. 2010; Gilbert

2006), crystallographic studies do not resolve any chelated Mg^{2+} or K^{+} ions within the electron density map. (Serganov et al. 2004) In addition, studies on the monovalent ion dependence of A-riboswitch concluded that this RNA shows no monovalent ion selectivity that might suggest K^{+} chelation. (Lambert et al. 2009)

Figure 2-1

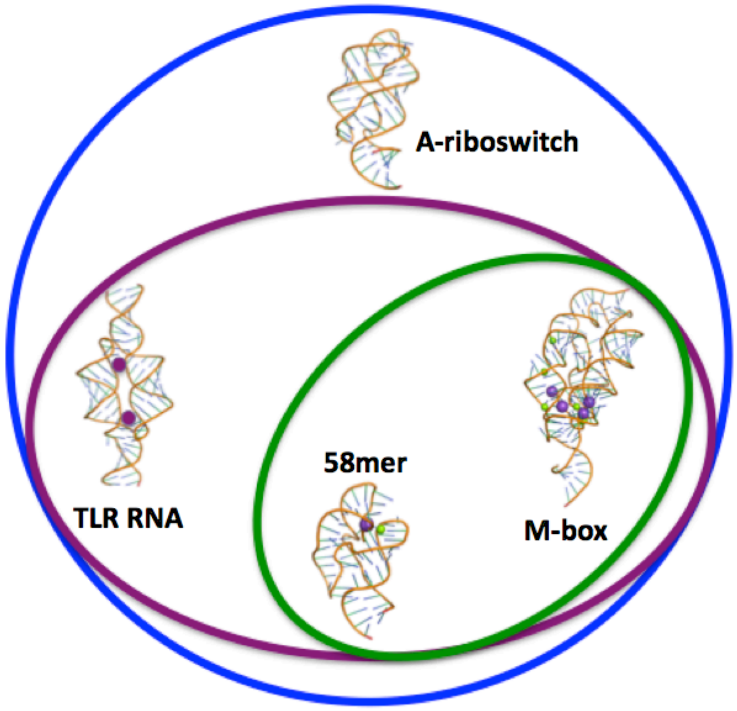

Figure 2-1. Venn diagram of the RNA structures studied. Outer blue circle contains population of RNAs stabilized by electrostatic interactions in the ion atmosphere. Purple ellipsoid contains RNAs with K^{+} chelation sites. Green ellipsoid contains RNAs with Mg^{2+} chelation Northern quadrant (Adenine riboswitch, PDB ID: 1Y26), Western quadrant (tetraloop receptor, PDB ID:2I7E), Southern quadrant (58mer rRNA fragment, PDB ID: 1HC8), Eastern quadrant (M-box riboswitch, PDB ID: 2QBZ).

The homodimeric tetraloop receptor RNA (TLR RNA) was designed as a mimic of one of the tetraloop receptors found in the *Azoarcus* group I intron. (Wang et al. 2010) This RNA is believed to chelate a K^{+} ion at the tetraloop receptor - A-

minor interface. This claim is supported indirectly through resolved electron density of a K^+ ion in the crystal structure of the *Tetrahymena* group I intron at the mimicked site of the TLR RNA. (Basu et al. 1998) As a result there is a total of two chelated K^+ ions in each tetraloop receptor structural unit (one K^+ per tertraloop receptor motif). K^+ chelation is further supported by selective thermal stabilization of the TLR RNA by K^+ relative to other group I ions. (Lambert et al. 2009) These data support the claim that the TLR RNA is stabilized by chelated K^+ in addition to cations within the ion atmosphere.

The aptamer domain of the M-Box riboswitch (M-box) and a 58mer rRNA fragment (58mer) were chosen as examples of RNAs that chelate Mg^{2+}. Structural studies of the 58mer RNA have concluded that both a K^+ and Mg^{2+} are chelated in close proximity within the native fold of the 58mer. (Conn et al. 1999; Conn et al. 2002) This RNA obtains maximum stability in the presence of K^+ relative to other group I monovalent ions. (Shiman et al. 2000) In addition NLPB calculations concluded that a pocket of high negative potential on the RNA is capable of providing enough free energy to partially dehydrate and bind a Mg^{2+} ion. (Misra et al. 2001) The M-box riboswitch is similar to the 58mer in that it too has been shown to chelate both Mg^{2+} and K^+. The high resolution crystal structure of the M-box riboswitch shows a densely packed core containing multiple cation chelation sites. (Dann et al. 2007; Ramesh et al. 2011) Although the M-box has been shown to fold in response to differing divalent ions, Mg^{2+} is most likely the effector molecule given the *in vivo* concentration under which it functions. (Dann et al. 2007; Ramesh et al. 2011

Figure 2-2

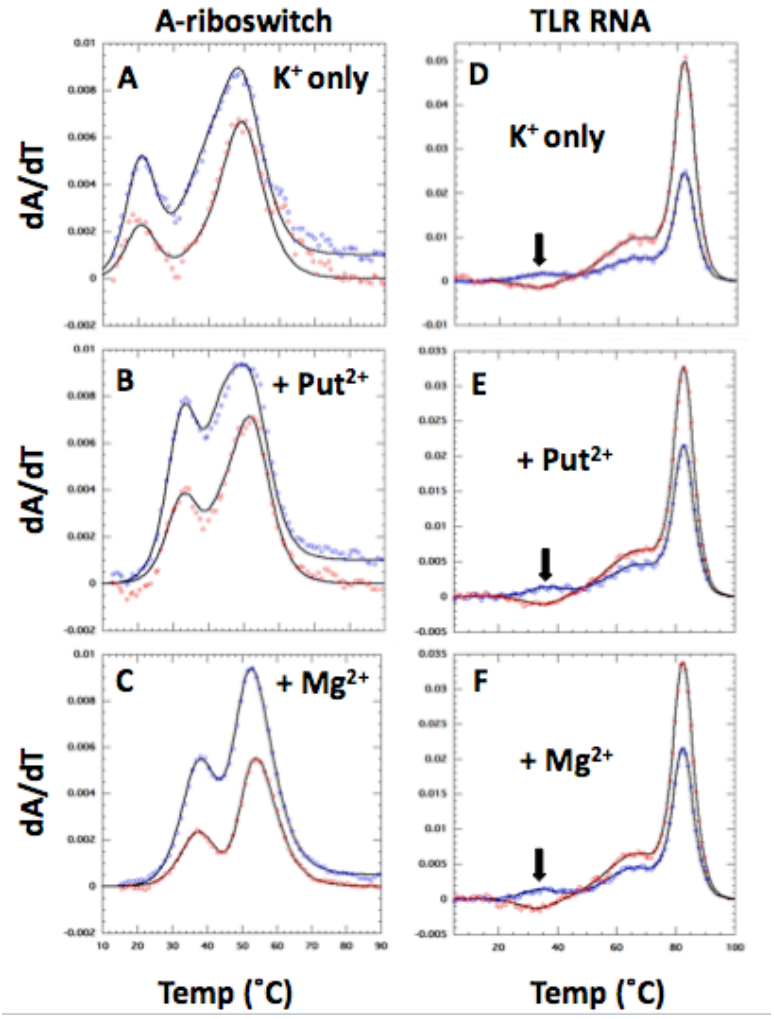

Figure 2-2. Melting profiles of the A-riboswitch (left column) and TLR RNA (right column) at 260 nm (blue) and 280 nm (red). Solid lines are least squares best fits of sequential unfolding transitions using the same T_m and ΔH° parameters for both wavelengths. The T_ms given are for the first unfolding transition. Left column: A-riboswitch under the conditions of 50 mM K+, 40 mM MOPS pH 6.8, 20 μM DAP and 0 mM divalent ion, T_m = 20.7 ˚C (A), 0.05 mM MgCl2, T_m = 32.8 ˚C (B), or 1mM putrescine^{2+}, T_m = 38.6 ˚C (C). Right column: TLR RNA under the conditions of 300 mM K+, 40 mM MOPS pH 6.8, and 0 mM divalent ion, T_m = 33.1˚C (D), 0.1 mM MgCl2, 36.0 ˚C (E), or 0.5 mM putrescine^{2+}, T_m = 35.1 ˚C (F). Arrows indicate the tertiary to secondary structure transition for the TLR.

Thermal Melt Analysis with Putrescine^{2+} and Mg^{2+}

The A-riboswitch and TLR RNA were analyzed using UV absorbance monitored thermal melts. For both the A-riboswitch and TLR RNA, folding/unfolding can be observed in the absence of divalent ions. This is achieved by stabilizing the N-state with either a neutral ligand (2,6-diaminopurine) in the case of the A-riboswitch or high monovalent salt concentration (300 mM KCl) in the case of the TLR RNA. For the A-riboswitch, a distinctive change in the UV signal at 260/280nm is only observed in the presence of ligand (2,6-diaminopurine). The change in absorbance corresponding to loss of tertiary interactions can be shifted to higher T_m upon addition of putrescine^{2+} or Mg^{2+} (Figure 2-2). The TLR RNA is also found to possess a distinct transition in the presence of putrescine or Mg^{2+} and moderate salt conditions. The first transition of the TLR RNA is hyperchromic at 260nm and hypochromic at 280nm (Figure 2-2). (Lambert et al. 2009)

Figure 2-3 shows the change in RNA stability with varying divalent ion concentration for the A-riboswitch and TLR RNA. The data were analyzed by observing the change in T_m of the first melting transition (260nm and 280nm, Figure 2-2A). These transitions are defined here as the native (N) to unfolded (I) transition where "I" represents a partially unfolded structure containing only secondary structure. Through implementation of the Van't Hoff equation (eq 2-3.) and Wyman linkage it is possible to relate the change in T_m to the change in the number of ions taken up in the transition ($\Delta\Gamma$) from the N to I-state (eq. 2-1 and 2-3):

Figure 2-3

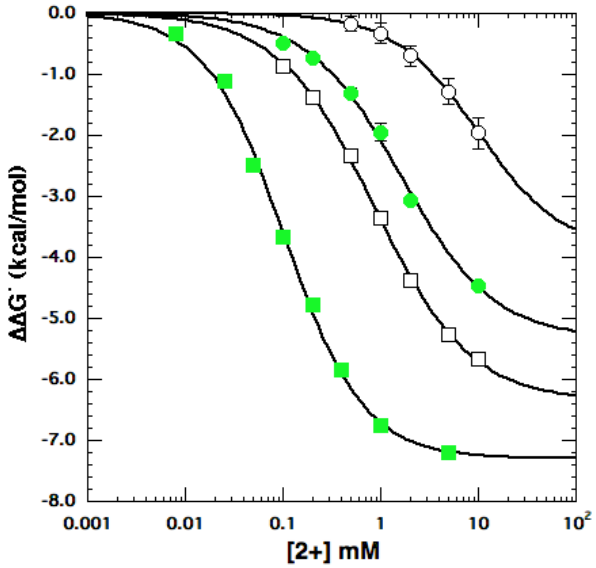

Figure 2-3. Relative stability of the A-riboswitch (squares) and the TLR RNA (circles) with varying concentrations of $MgCl_2$ (green) and putrescine^{2+} (black). TLR RNA data was collected in 300 mM KCl while the A-riboswitch data was collected in 50 mM KCl and 20 μM 2,6-diaminopurine.

$$\Delta\Gamma_{2+} = \left(\Gamma^{N}_{2+} - \Gamma^{I}_{2+}\right) \approx -\frac{1}{RT}\frac{\partial \Delta G^{\circ}_{obs}}{\partial \ln C_{2+}} \qquad 2\text{-}1)$$

where Γ_{2+} is the excess ions interacting with a given state of an RNA, R is a gas constant, T is the temperature and C_{2+} is the concentration of divalent ion under consideration. (Anderson et al. 1993) $\Delta\Gamma_{2+}$ varies over the concentration range of the titration and reaches a maximum at the midpoint of the curve. Figure 3 shows a clear difference in the stability imparted upon the RNAs when comparing putrescine^{2+} and Mg^{2+}. Given that the activities of these two ions are roughly the same at a given concentration (see Materials an Methods), the difference in the ΔΔG°

must be due to factors intrinsic to the counterions. The maximum slope, $\partial\Delta G^{\circ}_{obs,+2}/\partial \ln C_{+2}$ is roughly the same between the A-riboswitch and TLR RNA; both slopes are slightly more negative with Mg^{2+} than with $putrescine^{2+}$. The fact that these slopes are negative show that Mg^{2+} and $putrescine^{2+}$ accumulate in greater excess around the native state (Γ^{N}_{2+}) relative to the I-state (Γ^{I}_{2+}).

Another feature of Figure 2-3 is that the TLR RNA and A-riboswitch do not reach the same maximum stability in $putrescine^{2+}$ as they do in Mg^{2+}. The maximum stability in the presence of $putrescine^{2+}$ is determined from the fit to data preceding 10 mM $putrescine^{2+}$ concentration. Exceeding the $putrescine^{2+}$ concentration used in these experiments lacks physical meaning due to the large excess of chloride. (Grilley et al. 2009) Although, one could argue that the final structures obtained in the presence of $putrescine^{2+}$ may be slightly different from that obtained by Mg^{2+} (see discussion for more details).

Thermal Denaturation with Various Diamines

To better understand how $putrescine^{2+}$ interacts with RNA, several diamines with different carbon linkers (Table 2-1) were used to ask whether RNA stability depends on either the average distance between amines or the rigidity of the linker. It was observed that $\Delta\Gamma_{2+}$ did not vary significantly between different diamines. On the other hand, $\Delta\Delta G^{\circ}_{2+}$ at a particular concentration of diamine did change as a function of both carbon chain length and saturation. We hypothesized that the relative change in free energy for a given diamine was correlated with the average intramolecular distance between amine groups in solution. In order to test this hypothesis the second pKa for each diamine was obtained (Table 2-1.). Based on

Coulomb's law, the second pKa is inversely proportional to the average intramolecular distance between amine groups in solution. A plot of $\Delta\Delta G^{\circ}$ (at a given diamine concentration) vs the 1st acid dissociation constant of the counterion results in an approximately linear trend (Figure 2-4 B).

Figure 2-4

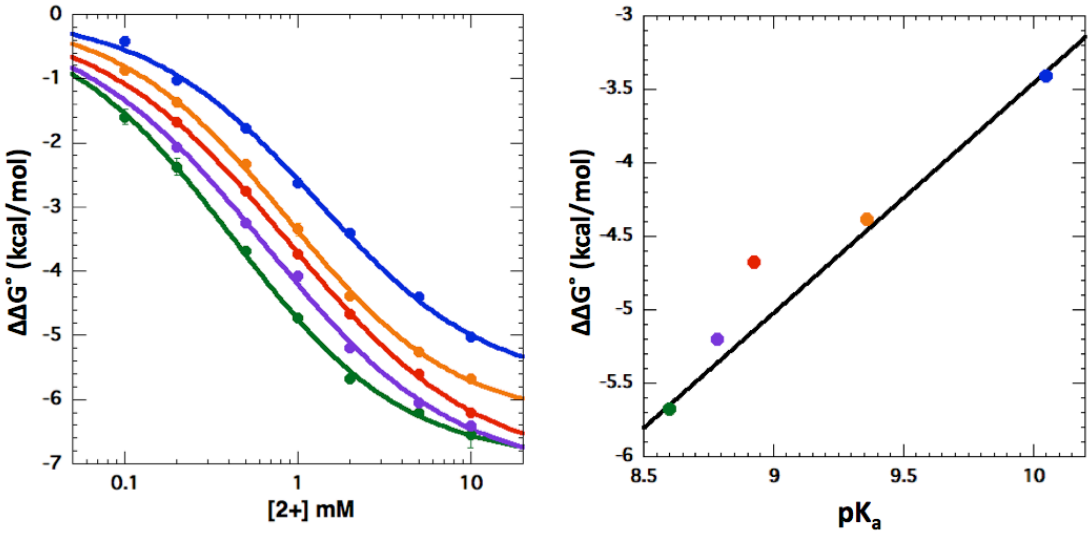

Figure 2-4. Stability of the A-riboswitch in the presence of various diamines, as derived from thermal stability measurements. **A**) $\Delta\Delta G^{\circ}_{obs}$ of the A-riboswitch vs. concentration of cadaverine (blue), putrescine^{2+} (orange), trans-1,4-diaminobutene (red), cis-1,4-diaminobutene (purple) and 1,3-diaminopropane (green). **B**) stability of the A-riboswitch at 2 mM concentration of the diamines listed above vs the first acid dissociation constant (pK_a, Table 1) of the diamine. The slope of the least squares fit to the saturated molecules (black line) is 1.63 kcal/mol (R=0.995).

Table 2-1

RNA	divalent ion	pK_a	$[2+]_0$ (mM)	$\Delta\Delta G^{\circ}_{obs,max}$ (kcal/mol)	$\Delta\Gamma$ (ions/RNA)
A-riboswitch	Mg^{2+}	-	0.104± 0.006	-7.3±0.15	3.31±0.2
TLR RNA	$Putrescine^{2+}$	9.36 (9.35)	0.87± 0.57	-6.36±0.14	2.39±0.11
TLR RNA	Mg^{2+}	-	0.162±0.31	-5.33±0.43	2.06±0.3
A-riboswitch	$Putrescine^{2+}$	9.36 (9.35)	9.80±3.21	-3.88±0.99	1.66±0.47
A-riboswitch	$Cadaverine^{2+}$	(10.05)	1.3±0.15	-5.83±0.26	2.16±0.17
A-riboswitch	1,3-diaminopropane	(8.6)	0.42±0.2	6.99±0.12	2.58±0.13
A-riboswitch	cis-1,4-diaminobutane	8.78	0.65±0.06	-7.19±0.26	2.41±0.21
A-riboswitch	trans-1,4-diaminobutane	8.93	0.89±0.04	-7.09±0.1	2.36±0.07

Table 2-1. Values of parameters from Figure 2-4 determined from fits of the Hill equation along with base titration. pK_a values in parenthesis were gathered from literature sources. (Perrin et al. 1972, 1981; Albert, 1963; Sober, 1968; Serjeant et al. 1979; Dawson et al. 1986)

Thermal stability in the Presence of both Mg^{2+} and Putrescine: A-riboswitch and TLR RNA

As shown in Figure 2-3, Mg^{2+} stabilizes the A-riboswitch and TLR RNA more effectively than $putrescine^{2+}$. Under *in vivo* conditions though, RNA is stabilized by a mixture of several different counter ions. In order to assess how mixtures of $putrescine^{2+}$ and Mg^{2+} influence the stability of RNA we performed thermal denaturation on four RNAs with varying concentrations of $MgCl_2$ and putrescine • $2HCl^-$. As required by charge neutrality, an excess of cations and an exclusion of anions balance the charge of anionic phosphates on the RNA. Thus, any change in $\Delta\Gamma_{put}$ results in a compensatory change in the excess of other ionic species in solution (Equation 2-2).

$$-2\Delta\Gamma_{put} = 2\Delta\Gamma_{Mg^{2+}} + \Delta\Gamma_{K^+} - \Delta\Gamma_{Cl^-} \qquad 2\text{-}2)$$

Figure 2-5

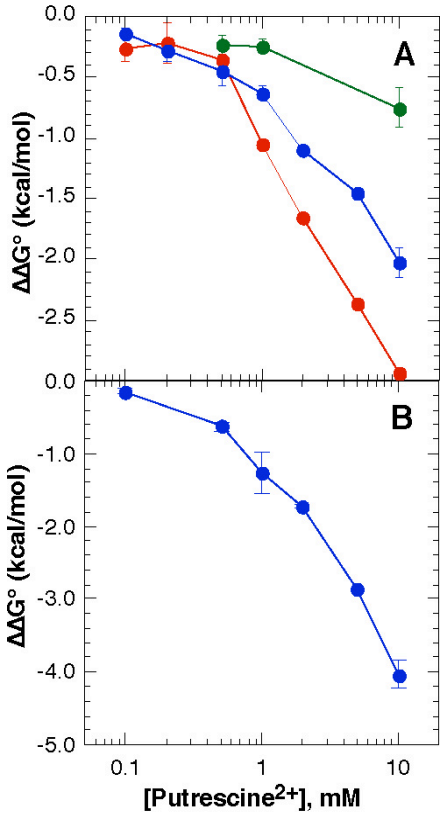

Figure 2-5. Effect of putrescine^{2+} on the stability of RNAs without Mg^{2+} chelation sites. $\Delta\Delta G°_{obs}$ for both RNAs was measured in K•MOPS - EDTA buffer with 50 mM K^{+} and 0.1 mM (red), 0.2 mM (blue) or 0.5 mM (green) $MgCl_2$. 20 μM DAP was included with the A-riboswitch. **A**) A-riboswitch; **B**) TLR RNA.

Figure 2-5A. shows the change in A-riboswitch stability vs. concentration of putrescine^{2+}, with the Mg^{2+} concentration kept constant at the indicated values. The negative slope of this curve indicates that there is a greater accumulation of putrescine^{2+} ions by the N state relative to the I-state. As the Mg^{2+} concentration increases from 0.1mM to 0.5mM the resulting change in free energy upon addition of putrescine^{2+} becomes less negative. From these data we see that uptake of putrescine^{2+} is opposed by increased $MgCl_2$ concentrations as expected on the basis

of equation 2-2. Although there is clearly a net uptake of putrescine^{2+}, the resulting changes in $\Delta\Gamma_{Mg2+}$, $\Delta\Gamma_{K+}$ and $\Delta\Gamma_{Cl-}$ cannot be determined individually. The TLR RNA also shows a net stabilization upon addition of putrescine^{2+} to a $MgCl_2$ containing buffer (Figure 2-5B). The change in ΔG°_{obs} is qualitatively similar to the A-riboswitch although the magnitude of $\Delta\Delta G^{\circ}_{obs}$ is larger for the TLR RNA.

Thermal stability in the Presence of both Mg^{2+} and Putrescine^{2+}: 58mer and M-box

In melting studies of the two Mg^{2+}-chelating RNAs, the 58mer and M-box riboswitch, no transition indicative of tertiary structure (via absorbance at 260, 280 and 295nm) was observed in up to 10 mM putrescine^{2+} in the absence of Mg^{2+}. This is interesting since both of these RNAs show tertiary transitions in submillimolar concentrations of $MgCl_2$ (0.4 mM for 58mer and 0.6 mM for M-box riboswitch). In contrast to the TLR RNA and A-riboswitch, the observed stability for the Mg^{2+}-chelating RNAs in the presence of Mg^{2+} was shown to decrease with increasing concentration of putrescine^{2+} (Figure 2-6, 2-7). The 58mer RNA shows almost no effect of added putrescine^{2+} up to 2 mM, and at higher concentrations is destabilized. Although the increase in ΔG°_{obs} of the 58mer upon addition of putrescine is modest (0.6 kcal/mol in 10mM putrescine^{2+} and 1.0mM or 2.0mM $MgCl_2$) the pattern of destabilization was reproduced over the titration series at varying Mg^{2+} concentrations (Figure 2-7A). In addition the tertiary transition for this RNA was not observed at 10mM putrescine^{2+} and 0.5 mM $MgCl_2$. The requirement for Mg^{2+} in folding emphasizes the role of binding a specific divalent

ion. Thus putrescine presumably weakens this chelation event without being able to compete for direct site binding.

The M-box riboswitch shows a more dramatic pattern of destabilization with increasing putrescine^{2+} concentration (Figure 2-6B). The tertiary transition was destabilized by as much as 1.78 kcal/mol at 1mM $MgCl_2$ (This does not account for the conditions under which there was no observed tertiary transition.). It is also observed that tertiary interactions (as reported by the 260, 280 and 295nm absorbance signals) could be completely disrupted if a sufficient amount of putrescine was added to the system; the concentration of putrescine^{2+} required to disrupt tertiary interactions increased with the concentration of $MgCl_2$ present.

Discussion

In vivo relevance of putrescine to RNA folding

In vivo, the native state of RNA is stabilized by many different solution components. The three most abundant cations in the cell (K^+, Mg^{2+} and putrescine^{2+}) are believed to play a large role in dictating the stability of RNA. It is of great importance to understand how the presence of a particular cation influences both the $\Delta\Gamma_{2+}$ of each species as well as the change in ΔG°_{obs}. This information will allow us to gain insight into the importance of putrescine^{2+} in RNA tertiary structure stability *in vivo*.

Figure 2-6

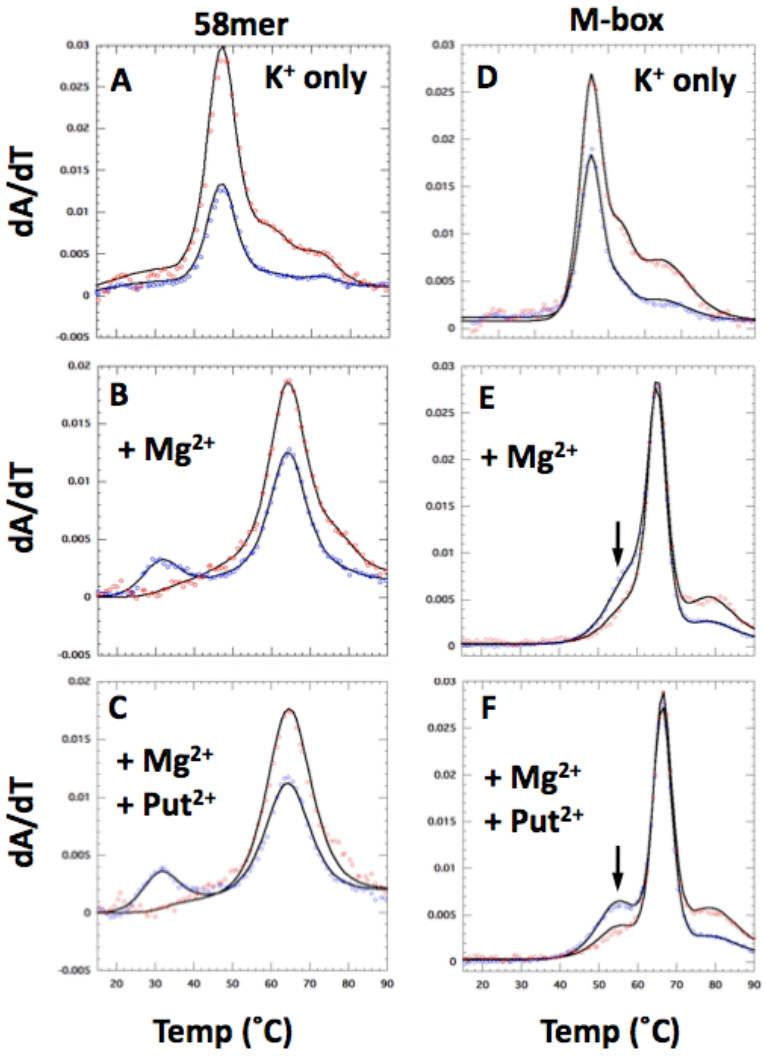

Figure 2-6. Melting profile of the 58mer (left column) and M-box riboswitch (right column) at 260 nm (blue) and 280 nm (red). Solid lines are global least squares fits to the data. Right column: 58mer RNA under the conditions of 50 mM K+, 40 mM MOPS pH 6.8 and no divalent ion (A), 1 mM MgCl2, T_m = 31.1 ˚C (B) or 1 mM MgCl2 and 1 mM putrescine^{2+}, T_m = 31.9 ˚C (C). Right column: M-box riboswitch RNA under the conditions of 50 mM K+, 40 mM MOPS pH 6.8, and no divalent ion (D), 1 mM MgCl2, T_m = 58.7 ˚C (E), or 1 mM MgCl2 and 1 mM putrescine 2+, T_m = 55.7 ˚C (F).

Figure 2-7

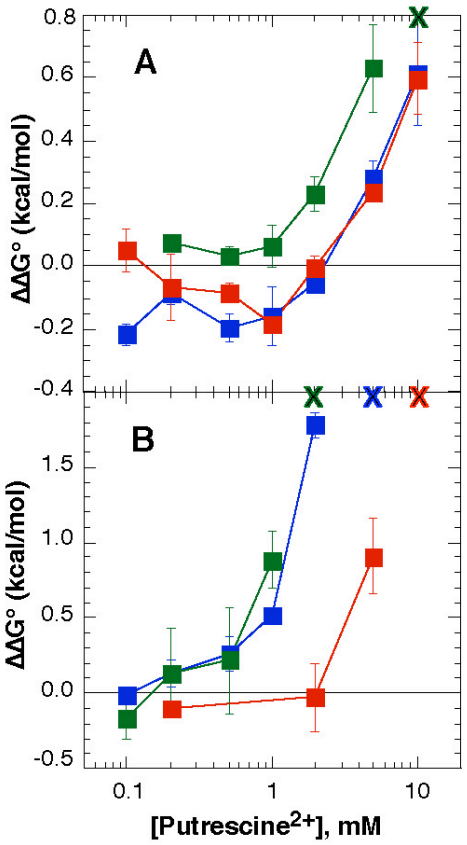

Figure 2-7. Stability of the magnesium-chelating RNAs in varying concentrations of putrescine^{2+}. **A**) stability of the 58mer rRNA fragment relative to stability in buffer with 50 mM K^+ and 0.5 mM (green), 1.0 mM (blue), or 2.0 mM (red) $MgCl_2$. The green "X" at the top of the graph represents the concentration of putrescine^{2+} (with 0.5 mM Mg^{2+}) at which the tertiary structure can no longer be detected in the melting curves. **B**) stability of the M-box RNA relative to buffer with 50 mM K^+ and 0.75 mM (green), 1.0 mM (blue), or 2.0 mM (red) $MgCl_2$. An "X" at the top of graph represents the concentration of putrescine^{2+} where the tertiary structure is no longer observed with 0.75 mM (green), 1 mM (blue), or 2 mM (red) Mg^{2+}.

Given that the data in the present report uses moderate salt conditions, the results can be related to the response of RNA stability *in vivo* with changing concentration of putrescine^{2+}. K^+ activity *in vivo* is ~150 mM. Under these conditions the activity of Mg^{2+} is ~1 mM (1% of the total concentration). If Mg^{2+} and putrescine^{2+} have the same fraction of active molecules *in vivo* then the effects of

putrescine^{2+} on RNA stability would be negligible. Given that the interaction of Mg^{2+} with RNA is very strong relative to putrescine^{2+} it can be anticipated that putrescine^{2+} has a greater fraction of active molecules than Mg^{2+} due to ion exchange. (Braunlin et al. 1982) Putrescine^{2+} activity would thus reside in a concentration range of a couple millimolar. At this activity putrescine^{2+} interactions would be fairly significant and could impose dramatic consequences on the stability of some RNAs. Given the changes in ΔG°_{obs} that have been reported, it is possible that some RNAs may have evolved to exploit fluctuations in putrescine^{2+} concentration in order to regulate cellular events. In particular the M-box riboswitch shows a drastic change in stability upon addition of putrescine^{2+} suggesting that polyamines may play a role in the function of this riboswitch. In order to accurately quantitate RNA stability in response to changing putrescine^{2+} activity, a means of determining the *in vivo* activity of putrescine^{2+} must be worked out.

Mechanisms of stability imparted by divalent ions

Electrostatic interactions have been found to be strong stabilizing factors for RNA tertiary structure. (Leipply et al. 2011) Previous studies have found that the majority of native state stability arises from an entropic contribution from "diffuse" Mg^{2+} interactions in the ion atmosphere. (Misra et al. 2000; Misra et al. 2002) It is likely that putrescine^{2+} interacts with RNA in the same non-bound fashion. (Frydman et al. 1992) However, when comparing thermal stability imparted by putrescine^{2+} or Mg^{2+} for the A-riboswitch and TLR RNA it is clear that Mg^{2+} is always more stabilizing to the native state than putrescine^{2+} (Figure 2-3). In addition the

relative change in ΔG°_{obs} decreases as the amount of Mg^{2+} in the reference state increases (Figure 2-5A). Given that both of these RNA molecules do not chelate Mg^{2+} it is reasonable to conclude that putrescine^{2+} is less efficient at stabilizing the native state for reasons other than competitive binding to chelation sites.

As a means of determining features that are responsible for the discrepancy in tertiary structure stability imparted by Mg^{2+} and putrescine^{2+}, we conducted a series of thermal melts on the A-riboswitch in the presence of a diverse set of diamines (Figure 2-4, Table 2-1). The diamines used in this study vary from 5 - 3 carbons in the alkyl linker and also contain differences in saturation. By introducing these changes into the carbon linker we observe a distinct trend relating stability to the linker length and number of rotatable bonds (Figure 2-4A). A similar study has been conducted on the *Tetrahymena* ribozyme using a series of polyamines with varying charge and volume. (Koculi et al. 2004) Koculi et al. reported that the stability of RNA is dependent upon the charge density of the counterion, where charge density is defined as the charge divided by the Van der Waals molecular volume. The current work has elaborated on this conclusion by observing the stability of RNA in the presence of diamines that vary not only in "charge density" but also carbon linker saturation. In addition, the RNA used in these experiments does not contain chelation sites that can make interpretation of data less straightforward. The current study has observed that at a given concentration of diamine, stability is correlated with the average distance between amine groups (determined by the 2nd pKa of each diamine). As the length of the carbon linker in the diamine increases there is a decrease in the stability imparted upon the RNA

resulting in a relatively linear trend shown in Figure 4B. The most significant outlier from this trend line is the trans-1,4-diaminobutene which has a more positive $\Delta\Delta G^{\circ}_{obs}$ than would be expected from relation to the series. Since the trans alkene linker forces the dimaines to be more separated in solution the divergence from the linearity is due to the inability of the trans butene to compact to a higher charge density in the presence of the RNA. Therefore counterion chain entropy plays a role in the stabilization of RNA by diamines.

Putrescine^{2+} interactions with chelation sites

There is a clear difference in the change in ΔG°_{obs} of Mg^{2+} -chelating RNAs and non-chelators to the presence of putrescine^{2+} (Figures 2-5 and 2-7). Wyman linkage would attribute this phenomenon to putrescine^{2+} having a greater interaction with the I-state of Mg^{2+}-chelators. From our current understanding of electrostatics and RNA folding it is apparent that putrescine^{2+} favors more compact states of RNA in both chelating and non-chelating RNA systems. (Koculi et al. 2004) This shows that the application of mass action principles to these systems are in valid. The difference in the response of these RNAs to putrescine^{2+} is therefore related to electrostatic interactions of putrescine^{2+} with Mg^{2+}-chelation sites.

RNAs that contain Mg^{2+} chelation sites are highly dependent on chelation site occupancy for stability. (Cate et al. 1997; Lambert et al. 2009) These RNAs typically fold only under extreme conditions in the absence of Mg^{2+} (i.e. 8 m TMAO or 1.4 M NH_4^+ for the 58mer) while non-chelators fold under much more moderate conditions (i.e. 2 m TMAO for the A-riboswitch). (Lambert et al. 2010; Bukhman et

al. 1997) Recent work has elaborated on these findings by showing that the change in free energy for chelation site occupancy is a significant fraction of the total Mg^{2+}-RNA interaction free energy. (Leipply et al. 2011) Given that steric constraints prevent putrescine^{2+} from replacing Mg^{2+} in a chelation site it is clear that the positive change in ΔG°_{obs} upon addition of putrescine^{2+} for the Mg^{2+} chelators is due to repulsive electrostatic interactions rather than competitive binding. Therefore we believe the accumulation of putrescine^{2+} in the ion atmosphere increases the screening of the negative potential in the chelation site. This results in a lower propensity for Mg^{2+} chelation. In addition putrescine^{2+} residing in the ion atmosphere has a repulsive interaction with cations. These interactions certainly exist between chelated and non-chelated divalent ions and would ultimately result in Mg^{2+} being expelled from the chelation site. This can be contrasted with the TLR RNA, which also contains chelated K^{+}. Lambert et al. have shown that monovalent ion chelation does provide a significant amount of stability to the N-state. (Lambert et al. 2009) Despite putrescine^{2+} accumulation encouraging dissociation of chelated K^{+}, the stability of the TLR RNA increases upon addition of putrescine^{2+}. This increase in stability is a result of putrescine^{2+} interactions with the RNA that more than compensate for the change in ΔG°_{obs} upon K^{+} dissociation from the chelation site. Ultimately Mg^{2+} chelation sites provide a larger fraction of stability to the native state than K^{+} chelation sites thus resulting in different responses to putrescine^{2+}. Recently, Leipply et al. have shown that a single chelation site in the 58mer rRNA fragment contributes ~10% of the total Mg^{2+}-RNA interaction free energy at 0.1 mM

Mg^{2+}. (Leipply et al. 2011) Given the data presented here this fraction would presumably decrease *in vivo* as chelated Mg^{2+} interacts with diffuse putrescine^{2+}.

In conclusion, Mg^{2+} is much more significant a stabilizer of RNA tertiary structure than putrescine^{2+}. However putrescine^{2+} is capable of biasing the conformational ensemble of an RNA either toward or away from the native state. This is dependent on the architecture of the native state. As a result Mg^{2+} chelation is presumably less stabilizing to the native state *in vivo* than once expected.

Materials and Methods

Chemicals and RNA

All solutions were prepared using distilled deionized water at 18.3 MΩ resistivity. MOPS Buffer was obtained from Sigma and was ≥ 99.5% purity. All buffers where brought to pH 6.8 using Sigma KOH ≥ 99.5% purity. KCl from Fluka ≥ 99.5% purity was then added to a final concentration of 50 mM. All buffers contained 10μM EDTA (Sigma ≥ 99.5% purity) in order to scavenge free transition metals. $MgCl_2$ was purchased from Fluka ≥ 99.5% purity. Solutions of $MgCl_2$ were calibrated against a know standard of EDTA by looking at absorbance at 230nm at pH 8.

Cis-1,4-diaminobutene and trans-1,4-diaminobutene were synthesized using a Staudinger reaction. (Martin et al. 2002) Resulting products were placed through two rounds of recrytaliztion using 1:1 methanol-ether. Products were obtained in 70% and 58% yield respectively. White crystals were analyzed via NMR on a Bruker 400. Residual unassigned peaks accounted for 1.5% of signal. The 2nd pKa of

putrescine, cis-1,4-diaminobutene and trans-1,4-diaminobutene were all determined using a standardized 100mM KOH solution at 25˚C.

All RNAs were transcribed using bacteriophage T7 RNA polymerase. All RNAs were transcribed from plasmid DNA (pLL2) linearized with a SmaI endonuclease. Each RNA sequence was encoded just upstream of a T7 promoter sequence on the plasmid. Resulting transcription products were purified on a 9-12% Poly acrylamide gel (19:1). UV shadowing was used to extract gel slices which then underwent electroelution in an Elutrap Electrophoesis Chamber. Centricon filter units were then used to equilibrate RNA in desired buffer.

Vapor Pressure Osmometry

Vapor Pressure Osmometry measurements were conducted on putrescine using a Wescor VAPRO 5520 (Logan, UT) at ambient temperature. Measurements were done in triplicate and repeated 5 times with fresh stocks. Data was fit to a second order polynomial using Kaliedagraph (Figure A-2).

UV Melting

Thermal denaturation was carried out with a Cary 400 spectrophotometer equipped with a 6x6 thermostatically controlled cuvette holder or an Aviv 14DS 5x1 thermostatically controlled cuvette holder. Each instrument was able to reproduce the results of the other within error. Hysteresis was not observed in any experiments. This was monitored by observing the UV absorbance at 260nm,

280nm and 295nm. The temperature schedule for the experiments was as follows: Heat from room temperature to 65°C, Hold at 65°C for 5 minutes, cool to 10-2°C, followed by heating to 95°C. The rate of change for the temperature varied from 0.5°C/min to 0.66°C/min in the second and third stages. Absorbance data was plotted as the derivative of absorbance with respect to temperature. The program Global Melt Fit was used to fit all resulting data. Simultaneous fitting of 260nm and 280nm were used to extract values for both T_m and $\Delta H°$. All enthalpies reporting on the 3˚ -> 2˚ transition fit within 7% error of one another when allowed to float during boot strap fit. Enthalpies were then fixed at the average value obtained from all floating fits. A sample plot of the M-Box riboswitch is shown in figure 2B. Error in fitted parameters was determined using a boot strap method. Folding free energies at temperature T_0 were calculated from T_m by the formula:

$$\Delta\Delta G° (T_0) = \Delta H° (T_0) (1/T_m - 1/T_0) \qquad 2\text{-}3)$$

Slopes of the $\Delta\Delta G°$ v [+2] were determined using Kaliedagraph.

References

1. Anderson, C. F., and Record, M. T. (1993) SALT DEPENDENCE OF OLIGOION POLYION BINDING - A THERMODYNAMIC DESCRIPTION BASED ON PREFERENTIAL INTERACTION COEFFICIENTS, Journal of Physical Chemistry 97, 7116-7126.

2. Basu, S., Rambo, R. P., Strauss-Soukup, J., Cate, J. H., Ferre-D'Amare, A. R., Strobel, S. A., and Doudna, J. A. (1998) A specific monovalent metal ion integral to the AA platform of the RNA tetraloop receptor, Nature Structural Biology 5, 986-992.

3. Braunlin, W. H., Strick, T. J., and Record, M. T. (1982) EQUILIBRIUM DIALYSIS STUDIES OF POLYAMINE BINDING TO DNA, Biopolymers 21, 1301-1314.

4. Bukhman, Y. V., and Draper, D. E. (1997) Affinities and selectivities of divalent cation binding sites within an RNA tertiary structure, Journal of Molecular Biology 273, 1020-1031.

5. Capp, M. W., Cayley, D. S., Zhang, W. T., Guttman, H. J., Melcher, S. E., Saecker, R. M., Anderson, C. F., and Record, M. T. (1996) Compensating effects of opposing changes in putrescine (2+) and K+ Concentrations on lac repressor-lac operator binding: In vitro thermodynamic analysis and in vivo relevance, Journal of Molecular Biology 258, 25-36.

6. Cate, J. H., Hanna, R. L., and Doudna, J. A. (1997) A magnesium ion core at the heart of a ribozyme domain, Nature Structural Biology 4, 553-558.

7. Cayley, S., Record, M. T., and Lewis, B. A. (1989) ACCUMULATION OF 3-(N-MORPHOLINO)PROPANESULFONATE BY OSMOTICALLY STRESSED ESCHERICHIA-COLI K-12, Journal of Bacteriology 171, 3597-3602.

8. Conn, G. L., Draper, D. E., Lattman, E. E., and Gittis, A. G. (1999) Crystal structure of a conserved ribosomal protein-RNA complex, Science 284, 1171-1174.

9. Conn, G. L., Gittis, A. G., Lattman, E. E., Misra, V. K., and Draper, D. E. (2002) A compact RNA tertiary structure contains a buried Backbone-K+ complex, Journal of Molecular Biology 318, 963-973.

10. Dann, C. E., Wakeman, C. A., Sieling, C. L., Baker, S. C., Irnov, I., and Winkler, W. C. (2007) Structure and mechanism of a metal-sensing regulatory RNA, Cell 130, 878-892.

11. Frydman, L., Rossomando, P. C., Frydman, V., Fernandez, C. O., Frydman, B., and Samejima, K. (1992) INTERACTIONS BETWEEN NATURAL POLYAMINES AND TRANSFER-RNA - AN N-15 NMR ANALYSIS, Proceedings of the National Academy of Sciences of the United States of America 89, 9186-9190.

12. Gilbert, S. D., Stoddard, C. D., Wise, S. J., and Batey, R. T. (2006) Thermodynamic and kinetic characterization of ligand binding to the purine riboswitch aptamer domain, Journal of Molecular Biology 359, 754-768.

13. Grilley, D., Misra, V., Caliskan, G., and Draper, D. E. (2007) Importance of partially unfolded conformations for Mg2+-lnduced folding of RNA tertiary structure: Structural models and free energies of Mg2+ interactions, Biochemistry 46, 10266-10278.

14. Grilley, D., Soto, A. M., and Draper, D. E. (2009) DIRECT QUANTITATION OF MG(2+)-RNA INTERACTIONS BY USE OF A FLUORESCENT DYE, In Methods in

Enzymology: Biothermodynamics,Vol 455, Part A (Johnson, M. L., Holt, J. M., and Ackers, G. K., Eds.), pp 71-94, Elsevier Academic Press Inc, San Diego.

15. Heerschap, A., Walters, J., and Hilbers, C. W. (1985) INTERACTIONS OF SOME NATURALLY-OCCURRING CATIONS WITH PHENYLALANINE AND INITIATOR TRANSFER-RNA FROM YEAST AS REFLECTED BY THEIR THERMAL-STABILITY, Biophysical Chemistry 22, 205-217.

16. Kang, M., Peterson, R., and Feigon, J. (2010) Structural Insights into Riboswitch Control of the Biosynthesis of Queuosine, a Modified Nucleotide Found in the Anticodon of tRNA (vol 33, pg 784, 2009), Molecular Cell 39, 653-655.

17. Koculi, E., Lee, N. K., Thirumalai, D., and Woodson, S. A. (2004) Folding of the Tetrahymena ribozyme by polyamines: Importance of counterion valence and size, Journal of Molecular Biology 341, 27-36.

18. Lambert, D., Leipply, D., and Draper, D. E. (2010) The Osmolyte TMAO Stabilizes Native RNA Tertiary Structures in the Absence of Mg(2+): Evidence for a Large Barrier to Folding from Phosphate Dehydration, Journal of Molecular Biology 404, 138-157.

19. Lambert, D., Leipply, D., Shiman, R., and Draper, D. E. (2009) The Influence of Monovalent Cation Size on the Stability of RNA Tertiary Structures, Journal of Molecular Biology 390, 791-804.

20. Leipply, D., and Draper, D. E. (2010) Dependence of RNA Tertiary Structural Stability on Mg2+ Concentration: Interpretation of the Hill Equation and Coefficient, Biochemistry 49, 1843-1853.

21. Leipply, D., and Draper, D. E. (2011) Effects of Mg(2+) on the Free Energy Landscape for Folding a Purine Riboswitch RNA, Biochemistry 50, 2790-2799.

22. Leipply, D., and Draper, D. E. (2011) Evidence for a Thermodynamically Distinct Mg(2+) Ion Associated with Formation of an RNA Tertiary Structure, Journal of the American Chemical Society 133, 13397-13405.

23. Leipply, D., Lambert, D., and Draper, D. E. (2009) ION-RNA INTERACTIONS: THERMODYNAMIC ANALYSIS OF THE EFFECTS OF MONO- AND DIVALENT IONS ON RNA CONFORMATIONAL EQUILIBRIA, In Methods in Enzymology, Vol 469: Biophysical, Chemical, and Functional Probes of Rna Structure, Interactions and Folding, Pt B (Herschlag, D., Ed.), pp 433-463, Elsevier Academic Press Inc, San Diego.

24. Lemay, J. F., Penedo, J. C., Tremblay, R., Lilley, D. M. J., and Lafontaine, D. A. (2006) Folding of the adenine riboswitch, Chemistry & Biology 13, 857-868.

25. Lorsch, J. R., and Szostak, J. W. (1994) IN-VITRO SELECTION OF RNA APTAMERS SPECIFIC FOR CYANOCOBALAMIN, Biochemistry 33, 973-982.

26. Martin, B., Posseme, F., Le Barbier, C., Carreaux, F., Carboni, B., Seiler, N., Moulinoux, J. P., and Delcros, J. G. (2002) (Z)-1,4-diamino-2-butene as a vector of boron, fluorine, or iodine for cancer therapy and imaging: Synthesis and biological evaluation, Bioorganic & Medicinal Chemistry 10, 2863-2871.

27. Misra, V. K., and Draper, D. E. (2000) Mg2+ binding to tRNA revisited: The nonlinear Poisson-Boltzmann model, Journal of Molecular Biology 299, 813-825.

28. Misra, V. K., and Draper, D. E. (2001) A thermodynamic framework for Mg2+ binding to RNA, Proceedings of the National Academy of Sciences of the United States of America 98, 12456-12461.

29. Misra, V. K., and Draper, D. E. (2002) The linkage between magnesium binding and RNA folding, Journal of Molecular Biology 317, 507-521.

30. Moghaddam, S., Caliskan, G., Chauhan, S., Hyeon, C., Briber, R. M., Thirumalai, D., and Woodson, S. A. (2009) Metal Ion Dependence of Cooperative Collapse Transitions in RNA, Journal of Molecular Biology 393, 753-764.

31. Murphy, K. P., Xie, D., Thompson, K. S., Amzel, L. M., and Freire, E. (1994) ENTROPY IN BIOLOGICAL BINDING PROCESSES - ESTIMATION OF TRANSLATIONAL ENTROPY LOSS, Proteins-Structure Function and Genetics 18, 63-67.

32. Pyle, A. M. (2002) Metal ions in the structure and function of RNA, Journal of Biological Inorganic Chemistry 7, 679-690.

33. Ramesh, A., Wakeman, C. A., and Winkler, W. C. (2011) Insights into Metalloregulation by M-box Riboswitch RNAs via Structural Analysis of Manganese-Bound Complexes, Journal of Molecular Biology 407, 556-570.

34. Record, M. T. (1975) EFFECTS OF NA+ AND MG++ IONS ON HELIX-COIL TRANSITION OF DNA, Biopolymers 14, 2137-2158.

35. Record, M. T., Courtenay, E. S., Cayley, D. S., and Guttman, H. J. (1998) Responses of E-coli to osmotic stress: Large changes in amounts of cytoplasmic solutes and water, Trends in Biochemical Sciences 23, 143-148.

36. Serganov, A., Huang, L. L., and Patel, D. J. (2008) Structural insights into amino acid binding and gene control by a lysine riboswitch, Nature 455, 1263-U1276.

37. Serganov, A., Huang, L. L., and Patel, D. J. (2009) Coenzyme recognition and gene regulation by a flavin mononucleotide riboswitch, Nature 458, 233-U210.

38. Serganov, A., Yuan, Y. R., Pikovskaya, O., Polonskaia, A., Malinina, L., Phan, A. T., Hobartner, C., Micura, R., Breaker, R. R., and Patel, D. J. (2004) Structural basis for discriminative regulation of gene expression by adenine- and guanine-sensing mRNAs, Chemistry & Biology 11, 1729-1741.

39. Shiman, R., and Draper, D. E. (2000) Stabilization of RNA tertiary structure by monovalent cations, Journal of Molecular Biology 302, 79-91.

40. Smith, K. D., Lipchock, S. V., Livinston, A. L., Shanahan, C. A., and Strobel, S. A. (2010) Structural and Biochemical Determinants of Ligand Binding by the c-di-GMP Riboswitch, Biochemistry 49, 7351-7359.

41. Verkhivker, G., Appelt, K., Freer, S. T., and Villafranca, J. E. (1995) EMPIRICAL FREE-ENERGY CALCULATIONS OF LIGAND-PROTEIN CRYSTALLOGRAPHIC COMPLEXES .1. KNOWLEDGE-BASED LIGAND-PROTEIN INTERACTION POTENTIALS APPLIED TO THE PREDICTION OF HUMAN-IMMUNODEFICIENCY-VIRUS-1 PROTEASE BINDING-AFFINITY, Protein Engineering 8, 677-691.

42. Wang, Y. X., Zuo, X. B., Wang, J. B., Yu, P., and Butcher, S. E. (2010) Rapid global structure determination of large RNA and RNA complexes using NMR and small-angle X-ray scattering, Methods 52, 180-191.

43. Winkler, W. C., Cohen-Chalamish, S., and Breaker, R. R. (2002) An mRNA structure that controls gene expression by binding FMN, Proceedings of the National Academy of Sciences of the United States of America 99, 15908-15913.

Chapter 3:

Measurement of ion exchange for three states of a purine riboswitch.

Abstract

Electrostatic compensation of negative charges is essential to both folding and function of RNA. Theory and experiment have been able to describe how monovalent and divalent ions mutually associate with polyelectrolytes. Although this is a great stepping-stone, RNA folding as it occurs *in vivo*, includes the association of numerous types of ions. This requires that different varieties of divalent ions interact with RNA simultaneously. To gain further insight into the electrostatic interactions of cations and RNA, we performed experiments equivalent to equilibrium dialysis on three distinct states of the *add* adenine riboswitch. These experiments contained Mg^{2+} and $putrescine^{2+}$ as well as a large excess of K^{+} (similar to the ionic conditions in *E. coli*). From these experiments we see that the competition between Mg^{2+} and $putrescine^{2+}$ differs between the three states of the A-riboswitch. These results are directly related to the energetics of folding as well as the organization of the ion atmosphere for each state of the RNA.

Introduction

The intracellular environment is in a constant state of flux. During the initial phase of osmotic stress response in *E. coli*, the concentrations of putrescine^{2+} (put^{2+}) and K^+ change in an anticorrelated fashion. (Capp et al. 1996; Cayley et al. 1989) This process allows the cell to maintain turgor pressure and volume while preserving electroneutrality. (Record et al. 1998) During these changes the total concentrations of the first and third most abundant cations (K^+ and put^{2+} respectively) change drastically (~1.0-0.25M and 0.06-0.01M respectively) in an anti-correlated fashion while Mg^{2+} (the second most abundant cation) is believed to remain at a constant concentration of ~0.1M. (Record et al. 1998) These changes can have a significant effect on the stability of RNA due to competition between ions for interaction with RNA. (Trachman et al. 2013)

The mobile network of ions residing around an RNA, known as the ion atmosphere, is a highly dynamic and enigmatic environment. Unlike DNA, RNA possesses complex folds that create a non-uniform electrostatic potential. As a result, cations are distributed in an irregular fashion around RNA. To gain further insight into the relationship between RNA structure and cation accumulation, both theoretical and experimental studies have previously been conducted. (Misra et al. 2001; Soto et al. 2007; Grilley et al. 2007) In one of these studies it has been shown that a theoretical model comes within ~30% agreement of experimental data when considering the interactions of K^+ and Mg^{2+} with both the N and I-state of RNA. (Soto et al. 2007) The 30% discrepancy is due to the simplifying assumptions that are inherent to the NLPB calculations (e.g. implicit solvent, no discrete ions). This is

troubling given that the discrepancies between electrostatic theory and experimental observation will most likely worsen as we try to recapitulate the intercellular environment. In vivo, RNA is capable of interacting with a multitude of diverse cations. (Record et al. 1998) With this in mind, we have sought to gain further insight into how the three most prevalent cations in *E. coli* (K^+, Mg^{2+}, and put^{2+}) mutually interact with RNA.

Using a method analogous to equilibrium dialysis we have quantified the excess Mg^{2+} ions interacting with the native (N), intermediate (I), and partially folded ensemble (En) states of the *add* adenine riboswitch (A-riboswitch) with varying concentrations of put^{2+}. From these experiments we are able to observe the free energy of RNA-Mg^{2+} interaction between the N and I-states. These results show that put^{2+} has a larger impact on the interaction free energy of Mg^{2+} with the I-state than the N-state. This difference is a direct result of how the ion atmosphere of these two states organize to accommodate put^{2+} and Mg^{2+}.

Background

Polyelectrolytes such as RNA maintain charge neutrality through an accumulation of excess cations and a depletion of anions in the vicinity of the macromolecule. These principles are readily captured in an equilibrium dialysis experiment. In such an experiment a polyanionic molecule such as RNA or DNA is localized inside a container with semi-permeable walls (dialysis bag). The polyelectrolyte containing dialysis bag is placed in a solution and allowed to reach equilibrium whereby the chemical potential of the individual components is the

same on both sides of the dialysis membrane. The final result is a greater concentration (excess) of cations and lower concentration (depletion) of anions inside the dialysis bag. The difference in the number ions of a particular species inside the dialysis bag (C^{In}) vs. outside the dialysis bag (C^{Out}) relative to the number of polyanion molecules (C_{RNA}) is approximately equivalent to the preferential interaction coefficient (Γ) for that ion (eq 3-1) (Figure 3-1A). (Leipply et al. 2009) Positive Γ values report on the excess of a particular ion while negative values are characteristic of a deficiency.

$$\Gamma_{Ion} \approx \left(\frac{C_{Ion}^{In} - C_{Ion}^{Out}}{C_{RNA}} \right)_{\mu} \qquad 3\text{-}1)$$

For an RNA system containing the chloride salts K^+, Mg^{2+} and Put^{2+}, the preferential interaction coefficient profile will follow from equation 3-2.

[redacted] 3-2)

Where Z is the number of negative charges of the RNA and each Γ term represents a type of ion denoted by the subscript. If the activity of one of the ionic species in solution changes, the system will equilibrate accordingly. For instance if the activity of Put^{2+} is increased, Γ_{Put2+} will increase while Γ_{Mg2+} , Γ_{K+} and Γ_{Cl-} change in a compensatory fashion (Figure 3-1A). In this paper, we refer to the compensatory changes among the Γs in response to the change in activity of one ionic species as an

"ion exchange" process. By this definition ion exchange is a means by which the system minimizes free energy. Through this concept of ion exchange and use of preferential interaction coefficients it is possible to quantitatively describe RNA folding in a multication system.

Figure 3-1

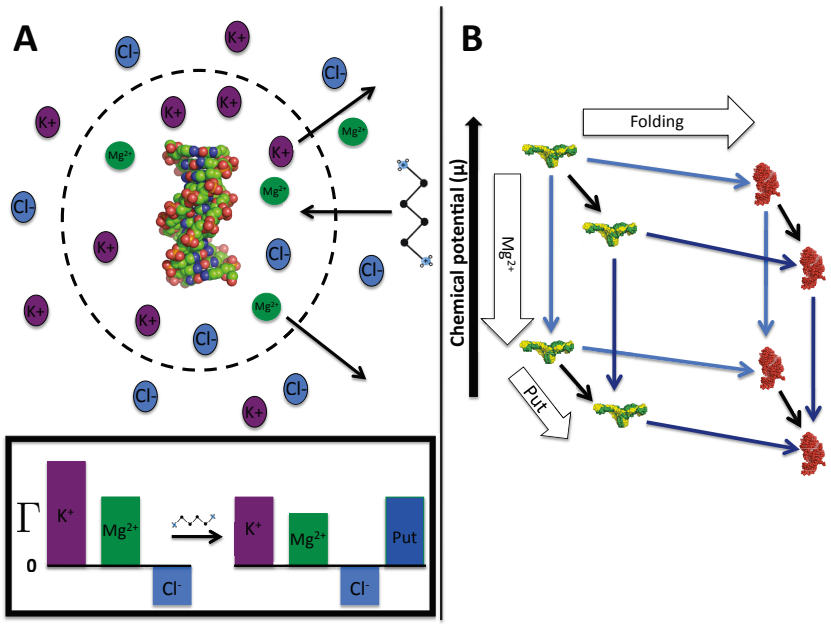

Figure 3-1. The thermodynamics of ion exchange A) Representation of an equilibrium dialysis experiment and how it relates to preferential interaction coefficients (Γ). Top: A polyelectrolyte encased in a semipermiable membrane. An excess of Mg^{2+} (green spheres) and K^{+} ions (purple spheres) are found inside the dialysis bag (dashed circle) while Cl^{-} ions are found in lower concentration inside the bag relative to outside the bag. Upon addition of put^{2+} (ball and sticks) ion exchange occurs between cations interacting with polyelectrolyte on the inside of the dialysis bag resulting in a net decrease in excess Mg^{2+} and K^{+} and a net increase in excess put^{2+}. Bottoms black box shows the hypothetical response of preferential interaction coefficients to the addition of put^{2+}. B) Thermodynamic cube relating the transition from the unfolded state (green and yellow structure) to the folded state (red structure) on the x-axis, with Mg^{2+}-RNA interaction on the y-axis and put^{2+}-RNA interaction on the z-axis. B) Thermodynamic cube relating phase transition from the unfolded state (green and yellow structure) to the folded state (red structure) on the x-axis, with Mg^{2+}-RNA interaction on the y-axis and put^{2+}-RNA interaction on the z-axis.

The linkage between ion exchange and changes in folding free energy is not new to the RNA folding field. One of the main driving forces for RNA folding under physiological conditions is the exchange process by which 1 Mg^{2+} ion replaces ~2 K^{+} ions in the ion atmosphere. (Misra et al. 2000) This results in a net release of ions and increase in entropy, thus decreasing free energy of the system. A greater number of Mg^{2+} ions accumulate in excess around the N-state relative to the I-state. The result is a more negative free energy of RNA- Mg^{2+} interaction for the N-state ($\Delta G^{N}_{RNA\text{-}Mg2+}$) than the I-state ($\Delta G^{I}_{RNA\text{-}Mg2+}$). As shown previously (Grilley et al. 2006), the number of excess Mg^{2+} ions (Γ_{Mg2+}) interacting with a given state of an RNA can be related to the free energy of Mg^{2+}-RNA interaction (eq 3-3) where C_{Mg2+} is the bulk concentration of Mg^{2+}.

$$\Delta G^{N}_{RNA\text{-}Mg2+} - \Delta G^{I}_{RNA\text{-}Mg2+} = -RT \int_{C^{I}_{Mg2+}}^{C^{N}_{Mg2+}} \frac{\Gamma_{Mg2+}}{C_{Mg2+}} \, dC_{Mg2+} \qquad 3\text{-}3)$$

By determining the number of excess ions interacting with each state of an RNA as well as the relative change in folding free energy (ΔG°_{obs}), one can compose a thermodynamic cycle relating Mg^{2+} excess and ion exchange to the observed folding free energies (Figure 1-4).

Combining thermodynamic cycles for both Mg^{2+} and put^{2+} addition generates a thermodynamic cube (Figure 3-1B). The cube can be decomposed into three general processes:

i) the folding free energy (ΔG°_{obs}, represented on the x-axis).

ii) the free energy of Mg^{2+} interacting with the a single state of the RNA ($\Delta G_{Mg2+\text{-}RNA}$, represented on the y-axis).

iii) the free energy of put^{2+} interacting with a single state of the RNA ($\Delta G_{RNA\text{-}Put2+}$, represented on the z-axis).

From these free energy values and thermodynamic linkage, information can be extracted not only on the interactions of ions with the RNA, but also the extent of ion exchange between excess put^{2+} and Mg^{2+}.

Results

Characterization of the folded and extended adenine riboswitch.

The aptamer domain of the *add* adenine riboswitch (A-riboswitch) has been shown to be an exceptional system for the study of RNA folding (Figure A-1). This RNA couples the docking of kissing loops to the binding of adenine or adenine derivatives, and when in conjunction with its expression platform, regulates translation of a gene product responsible for adenine metabolism. (Mandal et al. 2004) Previous reports have shown that when ligand is present in high enough concentrations the N-state dominates the conformational ensemble even in the absence of Mg^{2+}. (Lemay et al. 2009; Leipply et al. 2010) Thus, in the presence of saturating ligand, the free energy of RNA-Mg^{2+} interaction with the N-state may be determined through the application of equation 3-3.

Figure 3-2

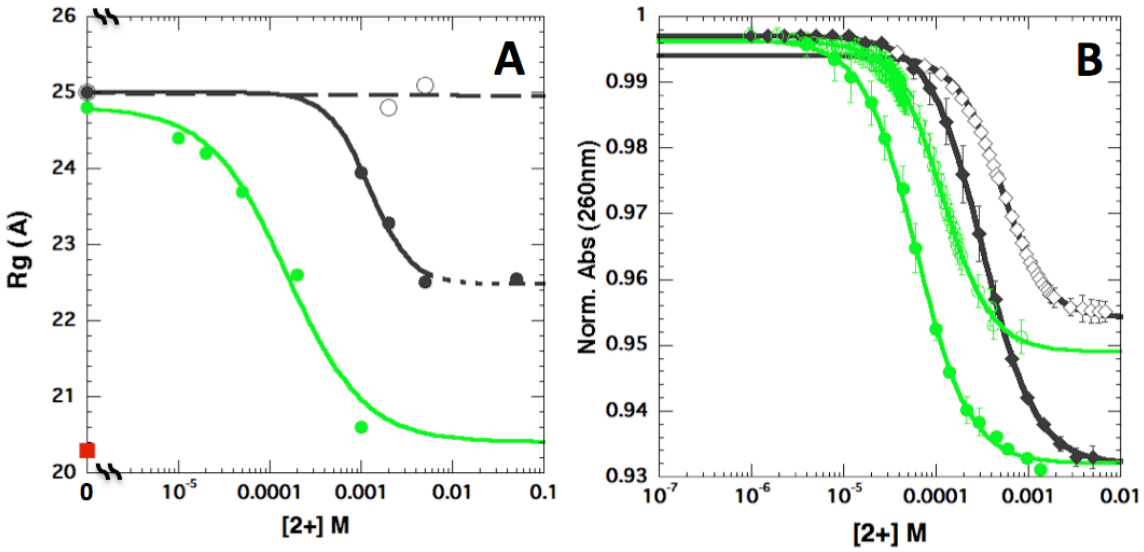

Figure 3-2. Folding of the A-riboswitch. A) Radius of gyration of the A-riboswitch as monitored by small angle x-ray scattering upon addition of divalent ion: closed symbols, wild type sequence in the absence of ligand titrated by either Mg^{2+} (green, data from Leipply et al. 2011) or put^{2+} (black circles). Dashed portion of wt A-riboswitch curve from 5-50 mM put^{2+} represents uncertainty of fit due to high chloride concentrations above 10 mM titrated ion. I-state mimic (C60G mutant) in the presence and absence of put^{2+} is shown in open black circles the R_g for the folded structure is represented by the red square. Double black curves on x-axis represents break point used to show 0 point on log scale. See figure A-3 for P(r) plots. B) Normalized change in absorbance at 260 nm in the presence of 2,6-diaminopurine (closed symbols) and absence of ligand (open symbols) with the same color scheme as shown in panel A.

To impose the I-state conformation, a base involved in a kissing loop interaction can be mutated (C60G) to prevent a long range tertiary interaction. (Lemay et al. 2006) This mutation causes the RNA to maintain an extended structure even in the presence of 1 mM Mg^{2+}. (Leipply et al. 2011) NMR experiments from the Schwalbe lab have shown that mutations disrupting the kissing loop interaction of the pbuX guanine sensing riboswitch (a highly similar riboswitch) impose a requirement for high concentrations of Mg^{2+} in order to fold and bind

ligand. (Buck et al. 2010) To monitor the effect of put^{2+} on the extended structure, SAXS measurements were carried out on the C60G mutant. As expected, addition of put^{2+} caused no change in R_g under the conditions tested (Figure 3-2A). Introduction of the C60G mutation thus prevents coupled folding upon addition of divalent ions.

We have previously shown that both Mg^{2+} and put^{2+} stabilize the folded state of the A-riboswitch. (Trachman et al. 2013) These experiments required the presence of a purine ligand to resolve a sharp melting transition. From this it was determined that organization of the ligand binding pocket is required to resolve a transition from the N to I-state via a UV absorbance signal. To observe the folding of the A-riboswitch in the absence of ligand we employed small angle x-ray scattering (SAXS) and UV absorbance titrations under isothermal conditions (Figure 3-2 A,B). The R_gs determined from the SAXS profiles report mainly on the distance between helices P2 and P3 while the hyperchromic effect observed in the UV absorbance experiments report on base stacking interaction in both the binding pocket and the kissing loop interaction. Upon addition of put^{2+} or Mg^{2+} the wt A-riboswitch decreases its R_g (Figure 3-2 A). While titration of Mg^{2+} in the absence of ligand results in the RNA folding to approximatley the same dimensions as the crystal structure (Leipply et al. 2011), put^{2+} is only observed to reduce the R_g by 2.5 Å. The decreased ability of put^{2+} to promote folding can be ascribed to the high concentrations of chloride at the upper end of the curve (Other factors may be causing this phenomenon as well, see Discussion). Comparison of the wt structure with the C60G mutant upon addition of put^{2+} suggests that put^{2+} folds the RNA to a state that is dependent on the potential for tertiary structure formation.

Isothermal UV titrations of the A-riboswitch monitor the stacking of nucleotide bases upon addition divalent ion. A hyperchromic change is observed upon addition of both put^{2+} and Mg^{2+}. (Trachman et al. 2013) In the presence of ligand both Mg^{2+} and put^{2+} induce the same maximum change in absorbance. This suggests that the two divalent ions promote folding to a highly similair if not identical structure.

Measurement of excess Mg^{2+} upon additon of putrescine^{2+}

It has previously been reported that excess Mg^{2+} ions interacting with an RNA can be quantified using a flourescent reporter 8-hydroxyquinoline sulfonic acid (HQS). (Grilley et al. 2006; Das et al. 2005) In accordance with the thermodynamic cube outlined in Figure 1B and equation 3-3, determining Γ_{Mg2+} is essential in understanding how the free energy of RNA-Mg^{2+} interaction relates to both folding and RNA-Put^{2+} interaction. To gain further insight into how put^{2+} and Mg^{2+} interact in the vicinity of an RNA we conducted HQS titrations in the presence of varying concentrations of put^{2+}. These experiments were performed on the wt A-riboswitch in the presence and absence of ligand (Figure 3-3 A,C respectively) as well as with the C60G I-state mimic (Figure 3-3B).

Figure 3-3

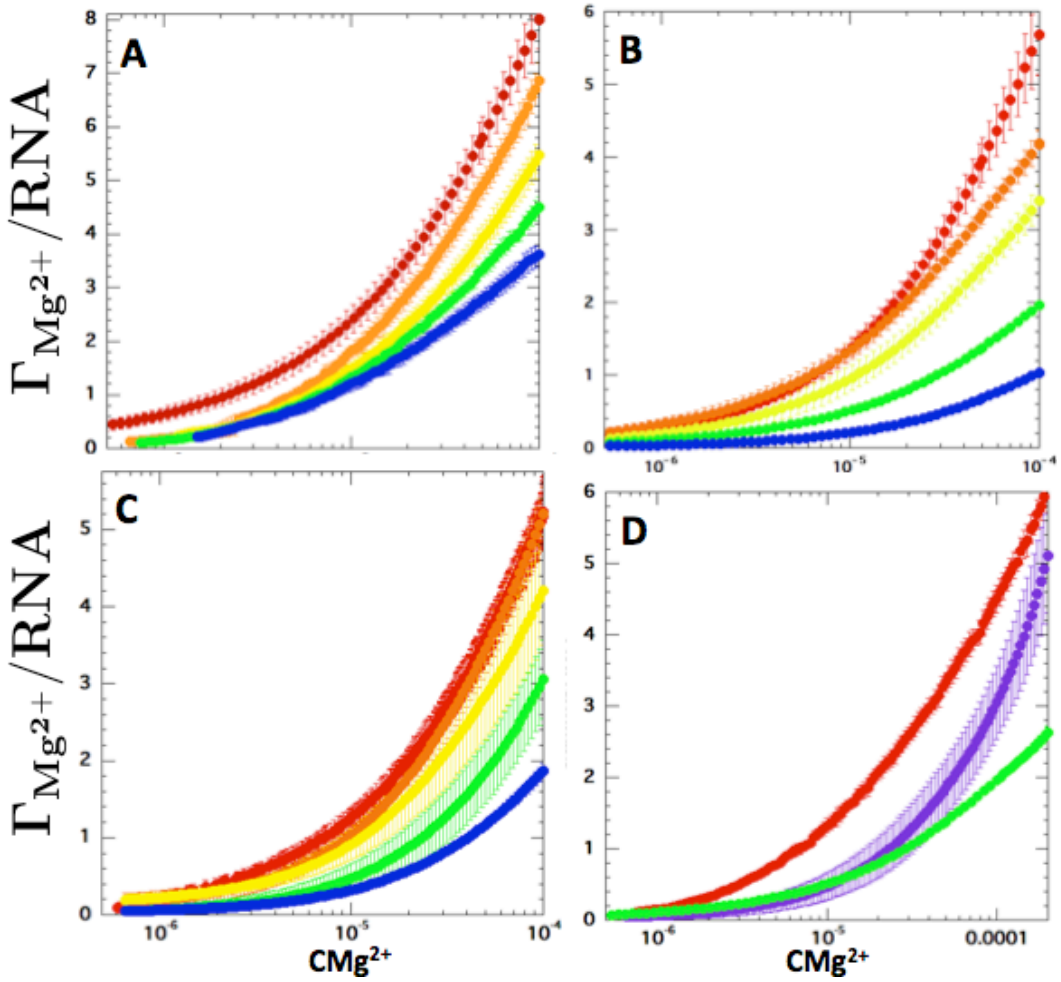

Figure 3-3. HQS Titrations of the A-riboswitch excess Mg^{2+} (Γ_{2+}) as a function of bulk Mg^{2+} concentration (C_{Mg2+}) of the A-riboswitch in 50 mM K^+, pH 6.8 (20°C) and 0 (red), 1 mM (orange), 2mM (yellow), 5 mM (green) and 10 mM (blue) put^{2+}. A) N-state A-riboswitch in 250 μM 2,6-diaminopurine. B) I-state (C60G) mutant. C) wt A-riboswitch in the absence of ligand. D) Curves for the N-state A-riboswitch (red), wt A-riboswitch w/o ligand purple and I-state (C60G) mutant (green) in the presence of 5 mM put^{2+}.

The titration curves show that increasing put^{2+} concentration for any of the three states results in a net decrease in Γ_{Mg2+} over the entire curve. This result is exactly what would be expected on the basis of equation 3-2. Ion exchange by Mg^{2+}

with an ion atmosphere composed of put^{2+}, K^+, and Cl^-, is less favored than it would be in an ion atmosphere composed of K^+ and Cl^- alone.

It is also observed that Γ_{Mg2+} depends on the dimensions of the RNA, with the more compact form (N-state) posessing a larger Γ_{Mg2+} than the less compact I-state and ensemble system, when compared under the same conditions (Figure 3-4,D). This can also be contrasted with Figures A-6,7 which shows variation in excess ions for four different RNAs with different degrees of compaction. Leipply et al. obtained similar results, finding that even a small change in R_g (corresponding to local organization within the RNA) can be associated with a large increase in Γ_{Mg2+}. (Leipply et al. 2011) Figure 3-3 D shows that when compared under the same ionic conditions (50 mM K^+ and 5 mM Put^{2+}), $\Gamma^{N}_{Mg2+} \geq \Gamma^{En}_{Mg2+} \geq \Gamma^{I}_{Mg2+}$ for bulk Mg^{2+} concentrations exceeding 10 μM, (superscripts denote the state of the RNA, folded, ensemble and extended, respectively). The ensemble and intermediate systems possess the same Γ_{Mg2+} at concentrations lower than 10 μM.

Free energies of RNA-Mg^{2+} interaction

By integrating the Γ_{Mg2+} curves in Figure 3-3 (A,B), free energy values that express the RNA-Mg^{2+} interaction are obtained (Figure 3-5). (Grilley et al. 2007) It should be noted that only the curves for the N and I-states provide accurate $\Delta G_{RNA\text{-}Mg2+}$ values since these structures are constant throughout the titration. This analysis shows that the decrease in RNA-Mg^{2+} interaction energy is much more dramatic for the I-state of the A-riboswitch than the N-state. The increased sensitivity to $putrescine^{2+}$ is evident by the larger slope at the titration midpoint of

the I-state (4.5x) than the N-state (2x). This contributes to the increased stability of the N-state in the presence of put^{2+}, Mg^{2+} and K^{+} chloride salts. These results are in agreement with our previous report showing that the A-riboswitch folding free energy becomes more negative upon addition of put^{2+} to a mixed Mg^{2+}, K^{+} system. (Trachman et al. 2013)

Figure 3-4

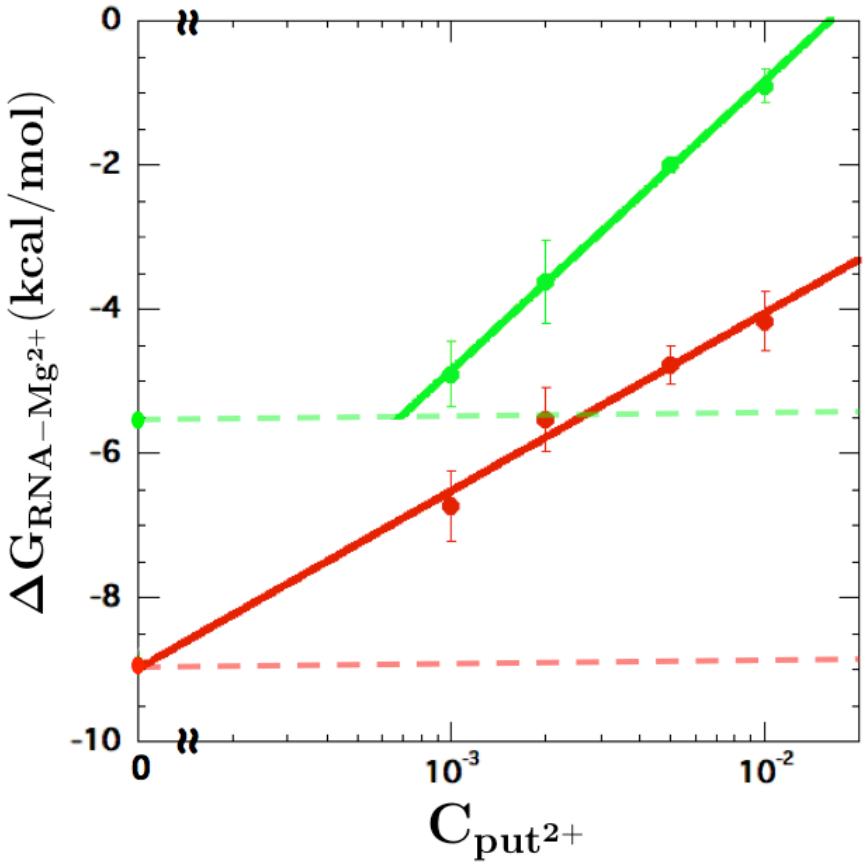

Figure 3-4. The RNA-Mg^{2+} interaction free energy calculated at 0.1 mM Mg^{2+} as a function of bulk put^{2+} concentration for the N-state (red) and I-state (green). Solid trend lines are the linear least square fits of $\Delta G_{RNA\text{-}Mg2+}$ from 1 – 10 mM concentration of $putrescine^{2+}$ for the N-state (red) and I-state (green). Dashed lines indicate the value of $\Delta G_{RNA\text{-}Mg2+}$ at 0 mM $putrescine^{2+}$ (same color scheme) with the free energy value also indicated by a circle on the y-axis.

Comparison of Γ_{Mg2+} for three states upon addition of putrescine^{2+}

It is apparent from the data in Figure 3-3 that the three states of the A-riboswitch differ in the response of Γ_{Mg2+} to the addition of put^{2+}. A scheme that quantifies the exchange of put^{2+} with Mg^{2+} is essential for understanding how these systems differ in their interaction with divalent ions. As one way to quantify the energetics of Mg^{2+}-put^{2+} exchange we looked at the change in excess Mg^{2+} as put^{2+} is titrated under constant bulk concentration of Mg^{2+} (Figure 3-5). So as to make a direct comparison between the different systems of the RNA, titrations starting from the same initial excess Mg^{2+} are compared. Each system contains a different bulk concentration of Mg^{2+} at the same excess of Mg^{2+}. To correct for the difference in bulk Mg^{2+} between the states, the x-axis is plotted as the ratio of the bulk put^{2+} concentration relative to the constant bulk concentration of Mg^{2+}. This is proportional to the change in chemical potential of divalent ions (eq 3-4).

$$\Delta\mu = -\mathbf{RT}\ln\frac{\mathbf{a_{put^{2+}}}}{\mathbf{a_{Mg^{2+}}}} \approx -\mathbf{RT}\ln\frac{\mathbf{C_{put^{2+}}}}{\mathbf{C_{Mg^{2+}}}} \qquad 3\text{-}4)$$

From this analysis we see how Γ_{Mg2+} is affected by the change in chemical potential of the divalent ion, essentially normalizing for the initial bulk Mg^{2+}. **

Figure 3-5

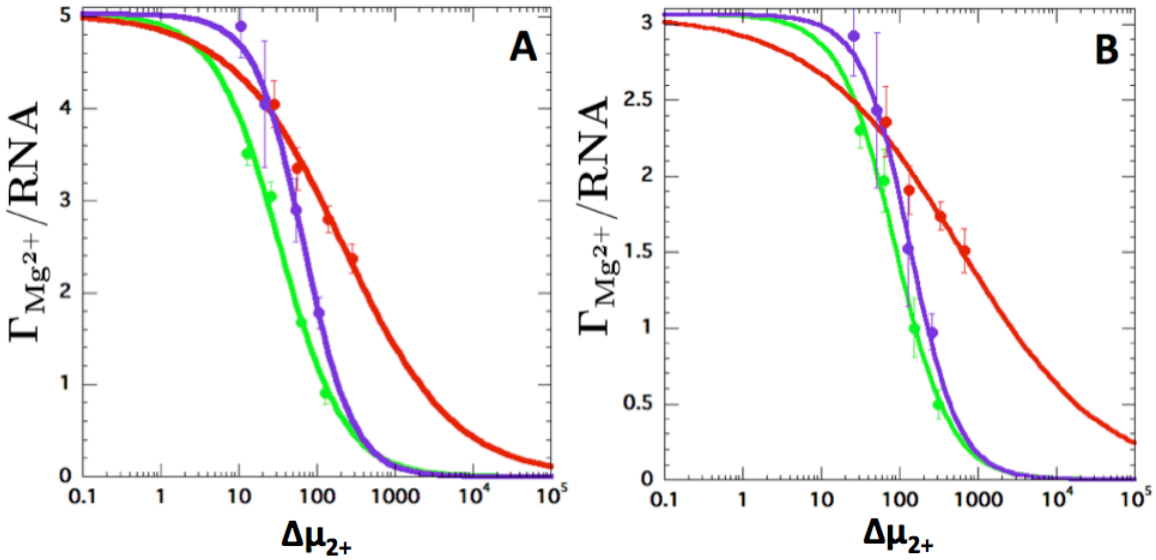

Figure 3-5. Γ_{Mg2+} as a function of the ratio of added put^{2+} to initial Mg^{2+} (held constant) for the native (red), intermediate (green) and ensemble (purple). A) Initial excess Mg^{2+} of five ions per RNA. B) Initial excess Mg^{2+} of three ions per RNA.

By comparing the three states for the A-riboswitch using the method described above we see distinct differences between how Γ_{Mg2+} changes with added put^{2+}. The I-state is much more sensitive to added put^{2+} than the N-state. The N-state requires an order of magnitude larger $\Delta\mu_{2+}$ in order to reach half of the initial Γ_{Mg2+}. This is consistent for all initial Γ_{Mg2+} values tested. From this we conclude that put^{2+} is more effective at replacing Mg^{2+} in the ion atmosphere of lower charge density RNA structures. Further support of this concept is obtained upon comparing the ensemble with the native and intermediate state structures. Measurements of R_g on the wt ensemble show that the RNA reduces in dimensions in the presence of put^{2+}. Despite a moderate reduction in R_g, the midpoint of the Mg^{2+}-put^{2+} exchange resides approximately half way between the native and intermediate curves. The ensemble also has a slope of ~1 at the midpoint of the curve, similar to the I-state

curve. We believe these slopes are related to the exchange between put^{2+} and Mg^{2+}, which is directly correlated with the charge density of the RNA.

The stoichiometry of Mg^{2+}/Putrescine^{2+} exchange

As described previously in this manuscript, electroneutrality must be maintained in solution. For RNA, this means that an excess of cations and depletion of anions neutralize the negative charges that accompany the phosphates on the RNA backbone. In the specific case described here, Mg^{2+} and put^{2+} activities are varied while Γ_{Mg2+} is monitored. An important question to ask from these data is, how many Mg^{2+} ions are displaced for every put^{2+} ion added to the ion atmosphere? Given that both put^{2+} and Mg^{2+} are divalent, one would imagine that one put^{2+} ion would displace exactly one Mg^{2+} (at constant divalent ion activity) thus maintaining electroneutrality. However the ion atmosphere can reorganize in a number of ways. This may involve interactions that are unique for a particular type of ion (e.g. chelation). It is also known that put^{2+} is far less effective at stabilizing RNA native structure therefore, the stoichiometry may diverge from a one to one ratio.

By determining the ratio of the number of put^{2+} ions required to replace a single Mg^{2+} ion, organizational detail of the ion atmosphere may be inferred. This information is readily accessible from the HQS titration data shown in Figure 3-3. This analysis asks the question, if a given amount of put^{2+} is added to a system with an initial Γ_{Mg2+}, how much Mg^{2+} must also be added in order to return to the same value of Γ_{Mg2+}?

The stoichiometry of ion exchange with an RNA is given by the reaction:

$$\mathbf{RNA} \bullet \Gamma_{\mathbf{Mg^{2+}}} = \mathbf{RNA} \bullet (\Gamma_{\mathbf{Mg^{2+}}} - \alpha) + \beta \mathbf{Put^{2+}} + \gamma \mathbf{K^{+}}$$

The left hand side of the reaction defines a state that consists of Mg^{2+} ions neutralizing the negative charges of the RNA. Since each Mg^{2+} ion is capable of neutralizing the charge of two phosphate ions, at the maximum value, Γ_{Mg2+} will equal half the charge of the RNA. Upon addition of putrescine^{2+} and or K^{+}, the cations exchange so as to minimize the free energy of the system. This process occurs in a stoichiometric ratio that maintains electroneutrality making the relation between the stoichiometric coefficients:

$$\beta + 2\gamma = \alpha \qquad 3\text{-}5)$$

Therefore, if Γ_{Mg2+} is to remain constant, the addition of putrescine^{2+} and K^{+} must be exactly compensated for by the addition of Mg^{2+}. Under equilibrium conditions this is equated to:

$$\frac{a_{Put}^{\beta} a_{K+}^{\gamma}}{a_{Mg}^{\alpha}} = 1 \qquad 3\text{-}6)$$

By taking the derivative above with respect to ln a_{Mg2+} we obtain.

$$\beta\left(\frac{d\ln a_{Put}}{d\ln a_{Mg}}\right)_{\Gamma 2+} + \gamma\left(\frac{d\ln a_{K+}}{d\ln a_{Mg}}\right)_{\Gamma 2+} = \alpha \qquad 3\text{-}7)$$

In this chapter, the experiments are performed under constant K^{+} (and approximately constant Cl^{-}) conditions. This makes the second partial derivative in the equation zero. As a result the exchange factor, the ratio of putrescine^{2+} to Mg^{2+}

required to maintain a constant excess of Mg^{2+}, is equated to the coordinated changes in putrescine^{2+} and Mg^{2+} activity.

$$\left(\frac{d\ln a_{Put}}{d\ln a_{Mg}}\right)_{\Gamma 2+} = \frac{\alpha}{\beta} \qquad 3\text{-}8)$$

Figure 3-6

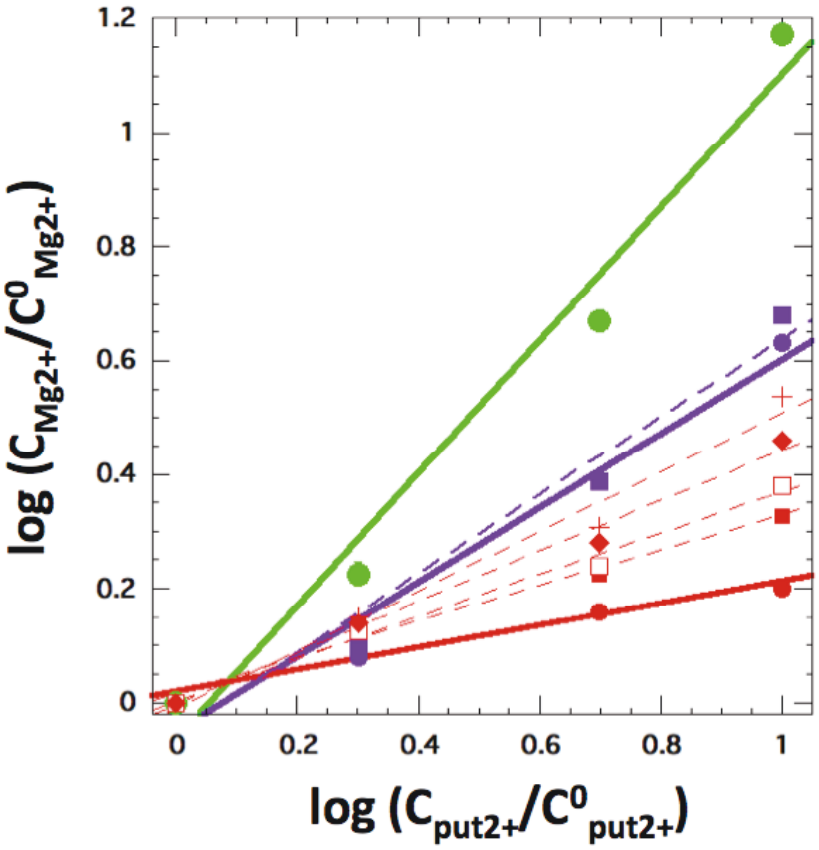

Figure 3-6. Exchange factors of A-riboswitch states. Plots of the relative change in bulk concentration of Mg^{2+} vs the relative change in bulk concentration of put^{2+} needed to maintain a specific value of Γ_{Mg2+}. Solid trend line with slope (s) through filled circles is the linear best fit for the I-state (●, s = 1.16), En-state (●, s = 0.65) and N-state (●, s = 0.19) at Γ_{Mg2+} equal to 1.05. Dashed trend lines show the linear least squares fit for Γ_{Mg2+} = 1.87: En-state (■, s = 0.68), N-state (■, s = 0.31), and also for N-state Γ_{Mg2+} = 2.5: N-state (□, s = 0.37), 3.0 (◆, 0.45) and 3.6 (+, 0.52).

Figure 3-6. provides the slopes described in equation 3-8 for the N, En and I-states at various constant values of Γ_{Mg2+}. The range of Γ_{Mg2+} values over which we can determine a slope is very limited in the case of the I-state, where the maximum Γ_{Mg2+} value that can be compared over the put^{2+} titration is 1.05. This is due to the limited Mg^{2+} range accessible to our experiments. When comparing the three states of the A-riboswitch with the excess of 1.05 Mg^{2+}, ion exchange is correlated with the charge density of the RNA. In the I-state, the Mg^{2+}-put^{2+} exchange factor is approximately a one to one ratio. As helices P2 and P3 move closer in proximity (ensemble state) the exchange decreases to approximately 0.6. The native state, with an organized binding pocket and docked kissing loops has an exchange of approximately 0.2. This single Mg^{2+} ion interacting with the N-state has an interaction energy strong enough to require 5 times as much put^{2+} to displace a single Mg^{2+} ion. This is a result of a difference in the radial distribution of Mg^{2+} and $putrescine^{2+}$ ions in the ion atmosphere.

The ratio of exchange for the N-state is always ≥ 2:1 (put^{2+}: Mg^{2+}) for all Γ_{Mg2+} tested. As the constant Γ_{Mg2+} value increases from 1.05 – 3.6 for the N-state (the accessible range of our experiments) the slope in equation 3-8 also increases from 0.19 to 0.52. This is rationalized by the fact that the free energy required to remove a Mg^{2+} ion from an ion atmosphere decreases as the number of excess Mg^{2+} ions increases. This is due to the Mg^{2+} ion population distributing to regions of lower interaction free energy in the ion atmosphere. As the number of excess Mg^{2+} ions

populating the ion atmosphere increases, the radial distribution of Mg^{2+} will extend to distances further from the RNA surface (Figure 3-7).

Figure 3-7

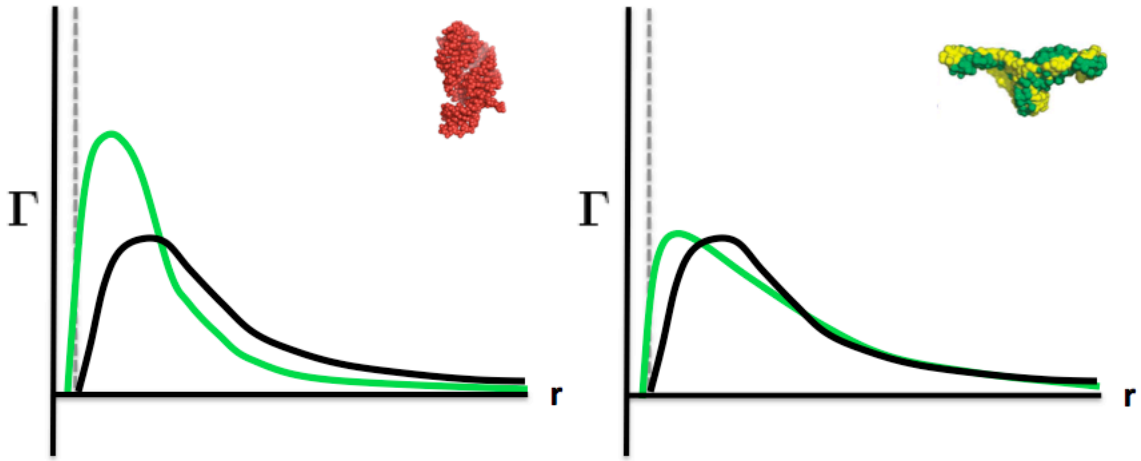

Figure 3-7. Conceptual diagram of the radial distribution of Mg^{2+} (green) and putrescine^{2+} (black) around the native state (left) and intermediate state (right) of the A-riboswitch. The excess of each ion as a function of distance from the surface of the RNA is plotted. Dashed grey line represents the distance from the surface of the RNA where the primary hydration layer of the RNA ends.

Discussion

In vivo there are a multitude of interactions that drive the folding of RNA. (Lambert et al. 2010; Kilburn et al. 2012; Winkler et al. 2004; Draper, 2004) One of the main driving forces of RNA folding is the preferential association of cations with the folded state over the unfolded state. Divalent cations have been shown to be particularly stabilizing to the folded state of RNA. (Draper et al. 2008) In this work, we look at how the two most abundant divalent ions in *E. coli* (Mg^{2+} and put^{2+}) accumulate in excess around three states of the A-riboswitch RNA. This is

accomplished by observing how excess Mg^{2+} changes as a function of bulk put^{2+} concentration.

Ion-RNA interactions

Given that put^{2+} and Mg^{2+} have very different molecular properties, it is important to discuss how these ions interact with the A-riboswitch. Mg^{2+} -RNA interactions have been well documented and fairly well characterized. (Lynch et al. 1974; Stein et al. 1976; Draper, 2008) From previous studies it is clear that Mg^{2+} can stabilize the N-state of RNA through either "chelation" where the ion makes at least two direct contacts with the RNA or through interactions within the ion atmosphere. Ions residing in the ion atmosphere are typically mobile and well hydrated but may reside on the surface of RNA mediated by a single hydration layer. (Draper, 2004) Chelated interactions are fairly rare in RNA structures since high charge density folds are required to form chelation sites. (Misra et al. 2001) Likewise most of the Mg^{2+}-RNA interaction free energy derives from ions within the ion atmosphere. (Leipply et al. 2011) From previous studies it is clear the A-riboswitch is exclusively stabilized by ions residing in the ion atmosphere. (Leipply et al. 2011; Lambert et al. 2009)

Put^{2+}-RNA interactions are far less well characterized than Mg^{2+}-RNA interactions. (Koculi et al. 2004; Heerschap et al. 1985) For the most part, our current knowledge of this subject is extrapolated from studies of polyamines (particularly $spermidine^{3+}$ and $spermine^{4+}$) with DNA. (Braunlin et al. 1982) Both $spermine^{4+}$ and $spermidine^{3+}$ have been shown to directly contact nucleic acids in

solution and can cause DNA to form unusual condensed structures. (Hud et al. 2005) As one would imagine, this is likely due to the ability of the amine groups to hydrogen bond with functional groups of nucleic acids. Furthermore, the hydrocarbon linkers of polyamines have the ability to form van der Waals interactions within the major groove. Despite all of these findings there is little evidence that put^{2+} forms direct contacts with RNA. In fact, Frydman et al. found that put^{2+} did not make direct contacts with tRNA as evidenced by a lack of correlation between the tumbling times of put^{2+} and tRNA. (Frydman et al. 1992) Their work also showed that both $spermine^{4+}$ and $spermidine^{3+}$ posses interactions with RNA (presumably hydrogen bonds) in addition to the expected electrostatic forces. These results are consistent with reports from other groups in the field suggesting direct contact of $spermine^{4+}$ with tRNA. (Jovine et al. 2000; Frydman et al. 1996) From our current and previous work we observe that put^{2+} is capable of folding the A-riboswitch to a compact ligand bound state, in the presence of 2,6-diaminopurine as observed by UV absorbance. (Trachman et al. 2013) From these studies we attribute the increased stability of RNA tertiary structure in the presence of put^{2+} to diffuse electrostatic interactions.

It is no surprise that Mg^{2+} and put^{2+} interact with RNA in different manners. Mg^{2+} is a monatomic divalent ion with high charge density while put^{2+} is an organic divalent ion with low charge density. The presence of a flexible linker adds a significant amount of complexity to put^{2+}. We have previously shown that eliminating the free rotation of a single bond in the carbon linker of put^{2+} increases the stability of the RNA by ~1 kcal/mol at approximately the same activity of

counterion. (Trachman et al. 2013) Thus, linker flexibility is an important factor. Another question is, how does the distance between the amine groups influence the interaction free energy with RNA? Within an electric field, two charges separated by a constant short distance will experience a force that is dependent on their average distance from the source of the field. At a large distance from the source, the two point charges are approximated as a single divalent point charge. As the charges move toward the source of the field the force experienced by each charge resembles that of two monovalent charges separated by a constant distance. In relating this to RNA-put^{2+} interaction, two aspects must be considered: i) as put^{2+} approaches the surface of an RNA it must bring its amine groups into close proximity in order to maximize the interaction energy with the RNA and ii) the "compaction" of put^{2+} results in an entropic penalty which manifests in the free energy. This is a classic case of enthalpy/entropy compensation although hydration of the ion is significant and must be accounted for as well. (Draper et al. 2013)

Characteristics of the ion atmosphere

Both composition and organization are elusive properties of an RNA ion atmosphere. (Bia et al. 2007; Kirmizialtin et al. 2012) In this work, we are able to determine the excess Mg^{2+} for three states of the A-riboswitch under biologically relevant solution conditions. As an unexpected result we found that the exchange between put^{2+} and Mg^{2+} differs between the states of the A-riboswitch. Given that these two divalent ions interact with the A-riboswitch in a diffuse manner, we attribute the difference in exchange between the N and I-state to a discrepancy of

ion atmosphere organization, ultimately manifesting in how each ion radially distributes from the RNA surface.

It has previously been shown that the radial distribution of excess Mg^{2+} ions in the I-state is more dispersed than the N-state. (Draper, 2004) Our findings show that the exchange between put^{2+} and Mg^{2+} is 1:1 for the I-state of the A-riboswitch while the exchange factor is ~5:1 for the N-state. These results can be rationalized by Mg^{2+} having a higher propensity to populate areas close to the surface of the N-state with $putrescine^{2+}$ ions distributing on average at a greater distance from the RNA surface. In contrast, the I-state accumulates excess Mg^{2+} that radially distribute in a manner creating a greater overlap between the populations of Mg^{2+} and $putrescine^{2+}$ in the ion atmosphere. In the I-state both ions are capable of populating the same areas, therefore they may have an equal effect on each other.

The more compact ensemble state of the A-riboswitch shows an exchange that is intermediate between the N and I-state. When taken together with the exchange data for the N and I-state, it is clear that there is a range of ion atmosphere organization that is dependent on the charge density of the RNA. As the helices of the A-riboswitch move closer in proximity, the average distance to the excess ions from the RNA surface decreases more dramatically for Mg^{2+} ions than for $putrescine^{2+}$ ions. This requires, for a given increase in C_{Mg2+}, that a greater amount of put^{2+} be added to solution to maintain constant Γ_{Mg2+}.

The N-state possesses a dense ion atmosphere. Since put^{2+} is large, it is more difficult for this ion to occupy the smaller volume of the N-state ion atmosphere. For the same reason Mg^{2+} is much more likely to occupy areas of high negative potential

found in folded RNA structures. As shown previously, organization of the ligand binding pocket results in a large increase in excess Mg^{2+}. (Leipply, 2011) This region of the RNA creates a large negative potential, therefore creating a strong association with Mg^{2+} ions. In order to replace these Mg^{2+} ions put^{2+} must approach the surface of the folded RNA. In doing so put^{2+} must compact and restrict its conformational landscape. This imposes an energetic penalty on the system for the loss of conformational entropy in the carbon linker. Although this energetic penalty is not extremely large (~1 kcal/mol per bond), it is worth mentioning. (Trachman, 2013) The major component to the deviation from 1:1 exchange between put^{2+} and Mg^{2+} is a difference in organization of the ion atmosphere. Under the conditions tested here there are few Mg^{2+} ions populating the ion atmosphere. These ions will preferentially populate areas of high negative potential close to or on the surface of the RNA. (Leipply et al. 2011) As the number of excess Mg^{2+} ions increases the exchange factor between put^{2+} and Mg^{2+} also increases. This can be attributed to put^{2+} exchanging with Mg^{2+} ions populating the ion atmosphere further from the surface of the RNA. Thus, a visual interpretation of the ion atmosphere organization (Figure 3-7) may arise from the relative differences in ion exchange.

Concluding remarks

Ion exchange is a complex phenomena that is relevant to biological processes. Here we have shown that three distinct states of an RNA differ in the degree to which the two ions compete. This difference in exchange is a contributing factor to the difference in free energy between the native and intermediate states of

the A-riboswitch. In addition, the difference in ion exchange provides insight into the composition and organization of the ion atmosphere. In recent years simulations have been very successful in incorporating preferential interaction coefficients as a means of interpreting the interactions of ions with RNA. (Chen et al. 2009; Hayes et al. 2012) Although simulations have yet to capture the complexities of put^{2+}, the distinct quantitative difference between exchange with the native and intermediate state is a result that simulations should aim to reproduce.

Materials and Method

Solutions and Samples.

All solutions were prepared using water at 18.3 MΩ resistivity. All buffers and salts were ≥ 99.5% purity. MOPS buffer was obtained from Sigma, and brought to pH 6.8 with KOH (K•MOPS). The standard buffer was 40 mM K•MOPS (with 13 mM K^+) and 10 μM EDTA (Sigma). KCl (Fluka) was added to give the indicated total concentrations of K^+, e.g. 37 mM KCl to give 50 mM K^+. $MgCl_2$, and/or diamine were also added as indicated. (At pH 6.8, the diamines used in this study are all greater than 98% of the di-protonated species.) Solutions of $MgCl_2$ (Fluka) were standardized by titration into an EDTA solution (pH 8.0) of known concentration, while monitoring absorbance at 230 nm.

All RNAs were prepared by transcription of linearized plasmid DNA with a histidine-tagged bacteriophage T7 RNA polymerase. Transcription products were purified by preparative electrophoresis on denaturing, 12% polyacrylamide gels. The desired

product band was excised from the gel, from which the RNA was electroeluted in an Elutrap Electrophoresis Chamber (Schleicher & Schuell). Centricon filter units (Millipore) were used to equilibrate an RNA in the desired buffer.

HQS Titrations.

HQS titration experiments were carried out on an Aviv ATF 105 outfitted with a Hamilton automatic titrator. Each experiment contained 20 μM HQS and 2-4 mM of PO_4 from the given RNA. Raw data was analyzed as described previously. (Grilley et al. 2006)

X-ray Scattering.

RNA samples (1-2 mg/ml) were exchanged extensively into buffer containing 40 mM MOPS pH 6.8 with 50 mM K^+ at the final concentration. Buffers contained the appropriate amount of put^{2+} as indicated. The samples were heated to 65˚C for 5 minutes and incubated at RT for at least 30 minutes. SAXS measurements were performed at beamline 12-ID at the Advanced Photon Source (APS) at Argonne National Laboratory. The beam energy was set to 12 keV with an exposure time of 1.5s. Samples were moved through an X-ray flow cell to minimize radiation damage. The ambient temperature was ~29˚C. Thirty data sets were collected for each sample condition in order to obtain good statistics. R_gs were determined from the Guinier fit to averaged data and P(r) plots were generated using GNOM, Figure A-3. (Semenyuk et al. 1991)

References

1. Anderson, C. F., and Record, M. T. (1993) SALT DEPENDENCE OF OLIGOION POLYION BINDING - A THERMODYNAMIC DESCRIPTION BASED ON PREFERENTIAL INTERACTION COEFFICIENTS, Journal of Physical Chemistry 97, 7116-7126.

2. Bai, Y., Greenfeld, M., Travers, K. J., Chu, V. B., Lipfert, J., Doniach, S., and Herschlag, D. (2007) Quantitative and comprehensive decomposition of the ion atmosphere around nucleic acids, Journal of the American Chemical Society 129, 14981-14988.

3. Braunlin, W. H., Strick, T. J., and Record, M. T. (1982) EQUILIBRIUM DIALYSIS STUDIES OF POLYAMINE BINDING TO DNA, Biopolymers 21, 1301-1314.

4. Buck, J., Noeske, J., Wohnert, J., and Schwalbe, H. (2010) Dissecting the influence of Mg2+ on 3D architecture and ligand-binding of the guanine-sensing riboswitch aptamer domain, Nucleic Acids Research 38, 4143-4153.

5. Capp, M. W., Cayley, D. S., Zhang, W. T., Guttman, H. J., Melcher, S. E., Saecker, R. M., Anderson, C. F., and Record, M. T. (1996) Compensating effects of opposing changes in putrescine (2+) and K+ Concentrations on lac repressor-lac operator binding: In vitro thermodynamic analysis and in vivo relevance, Journal of Molecular Biology 258, 25-36.

6. Cayley, S., Record, M. T., and Lewis, B. A. (1989) ACCUMULATION OF 3-(N-MORPHOLINO)PROPANESULFONATE BY OSMOTICALLY STRESSED ESCHERICHIA-COLI K-12, Journal of Bacteriology 171, 3597-3602.

7. Chen, A. A., Draper, D. E., and Pappu, R. V. (2009) Molecular Simulation Studies of Monovalent Counterion-Mediated Interactions in a Model RNA Kissing Loop, Journal of Molecular Biology 390, 805-819.

8. Dann, C. E., Wakeman, C. A., Sieling, C. L., Baker, S. C., Irnov, I., and Winkler, W. C. (2007) Structure and mechanism of a metal-sensing regulatory RNA, Cell 130, 878-892.

9. Das, R., Travers, K. J., Bai, Y., and Herschlag, D. (2005) Determining the Mg2+ stoichiometry for folding an RNA metal ion core, Journal of the American Chemical Society 127, 8272-8273.

10. Draper, D. E. (2004) A guide to ions and RNA structure, Rna-a Publication of the Rna Society 10, 335-343.

11. Draper, D. E. (2008) RNA Folding: Thermodynamic and Molecular Descriptions of the Roles of Ions, Biophysical Journal 95, 5489-5495.

12. Frydman, B., Westler, W. M., and Samejima, K. (1996) Spermine binds in solution to the T psi C loop of tRNA(Phe): Evidence from a 750 MHz H-1-NMR analysis, Journal of Organic Chemistry 61, 2588-2589.

13. Frydman, L., Rossomando, P. C., Frydman, V., Fernandez, C. O., Frydman, B., and Samejima, K. (1992) INTERACTIONS BETWEEN NATURAL POLYAMINES AND TRANSFER-RNA - AN N-15 NMR ANALYSIS, Proceedings of the National Academy of Sciences of the United States of America 89, 9186-9190.

14. Grilley, D., Misra, V., Caliskan, G., and Draper, D. E. (2007) Importance of partially unfolded conformations for Mg2+-lnduced folding of RNA tertiary structure: Structural models and free energies of Mg2+ interactions, Biochemistry 46, 10266-10278.

15. Grilley, D., Soto, A. M., and Draper, D. E. (2006) Mg2+-RNA interaction free energies and their relationship to the folding of RNA tertiary structures, Proceedings of the National Academy of Sciences of the United States of America 103, 14003-14008.

16. Heerschap, A., Walters, J., and Hilbers, C. W. (1985) INTERACTIONS OF SOME NATURALLY-OCCURRING CATIONS WITH PHENYLALANINE AND INITIATOR TRANSFER-RNA FROM YEAST AS REFLECTED BY THEIR THERMAL-STABILITY, Biophysical Chemistry 22, 205-217.

17. Hud, N. V., and Vilfan, I. D. (2005) Toroidal DNA condensates: Unraveling the fine structure and the role of nucleation in determining size, In Annual Review of Biophysics and Biomolecular Structure, pp 295-318, Annual Reviews, Palo Alto.

18. Jovine, L., Djordjevic, S., and Rhodes, D. (2000) The crystal structure of yeast phenylalanine tRNA at 2.0 angstrom resolution: Cleavage by Mg2+ in 15-year old crystals, Journal of Molecular Biology 301, 401-414.

19. Kilburn, D., Roh, J. H., Guo, L., Briber, R. M., and Woodson, S. A. (2010) Molecular Crowding Stabilizes Folded RNA Structure by the Excluded Volume Effect, Journal of the American Chemical Society 132, 8690-8696.

20. Kirmizialtin, S., Pabit, S. A., Meisburger, S. P., Pollack, L., and Elber, R. (2012) RNA and Its Ionic Cloud: Solution Scattering Experiments and Atomically Detailed Simulations, Biophysical Journal 102, 819-828.

21. Koculi, E., Lee, N. K., Thirumalai, D., and Woodson, S. A. (2004) Folding of the Tetrahymena ribozyme by polyamines: Importance of counterion valence and size, Journal of Molecular Biology 341, 27-36.

22. Leipply, D., and Draper, D. E. (2010) Dependence of RNA Tertiary Structural Stability on Mg2+ Concentration: Interpretation of the Hill Equation and Coefficient, Biochemistry 49, 1843-1853.

23. Leipply, D., and Draper, D. E. (2011) Effects of Mg(2+) on the Free Energy Landscape for Folding a Purine Riboswitch RNA, Biochemistry 50, 2790-2799.

24. Leipply, D., and Draper, D. E. (2011) Evidence for a Thermodynamically Distinct Mg(2+) Ion Associated with Formation of an RNA Tertiary Structure, Journal of the American Chemical Society 133, 13397-13405.

25. Lemay, J. F., Penedo, J. C., Tremblay, R., Lilley, D. M. J., and Lafontaine, D. A. (2006) Folding of the adenine riboswitch, Chemistry & Biology 13, 857-868.

26. Lynch, D. C., and Schimmel, P. R. (1974) COOPERATIVE BINDING OF MAGNESIUM TO TRANSFER RIBONUCLEIC-ACID STUDIED BY A FLUORESCENT-PROBE, Biochemistry 13, 1841-1852.

27. Mandal, M., and Breaker, R. R. (2004) Adenine riboswitches and gene activation by disruption of a transcription terminator, Nature Structural & Molecular Biology 11, 29-35.

28. Misra, V. K., and Draper, D. E. (2000) Mg2+ binding to tRNA revisited: The nonlinear Poisson-Boltzmann model, Journal of Molecular Biology 299, 813-825.

29. Misra, V. K., and Draper, D. E. (2001) A thermodynamic framework for Mg2+ binding to RNA, Proceedings of the National Academy of Sciences of the United States of America 98, 12456-12461.

30. Misra, V. K., and Draper, D. E. (2002) The linkage between magnesium binding and RNA folding, Journal of Molecular Biology 317, 507-521.

31. Record, M. T., Courtenay, E. S., Cayley, D. S., and Guttman, H. J. (1998) Responses of E-coli to osmotic stress: Large changes in amounts of cytoplasmic solutes and water, Trends in Biochemical Sciences 23, 143-148.

32. Semenyuk, A. V., and Svergun, D. I. (1991) GNOM - A PROGRAM PACKAGE FOR SMALL-ANGLE SCATTERING DATA-PROCESSING, Journal of Applied Crystallography 24, 537-540.

33. Soto, A. M., Misra, V., and Draper, D. E. (2007) Tertiary structure of an RNA pseudoknot is stabilized by "diffuse" Mg2+ ions, Biochemistry 46, 2973-2983.

34. Stein, A., and Crothers, D. M. (1976) CONFORMATIONAL-CHANGES OF TRANSFER-RNA - ROLE OF MAGNESIUM(II), Biochemistry 15, 160-168.

35. Trachman, R. J., and Draper, D. E. (2013) Comparison of Interactions of Diamine and Mg2+ with RNA Tertiary Structures: Similar versus Differential Effects on the Stabilities of Diverse RNA Folds, Biochemistry 52, 5911-5919.

36. Winkler, W., Nahvi, A., and Breaker, R. R. (2002) Thiamine derivatives bind messenger RNAs directly to regulate bacterial gene expression, Nature 419, 952-956.

37. Woodson, S. A. (2005) Metal ions and RNA folding: a highly charged topic with a dynamic future, Current Opinion in Chemical Biology 9, 104-109.

** Treatment of the data in this manner assumes that the activity coefficients of the divalent ions (put^{2+} and Mg^{2+}) do not change over the course of the titration. This is justified by the large excess of anions present in solution, as reported in the supplemental material of Grilley et al. 2006.

Chapter 4:

Stabilization of Native RNA Structure by Divalent Cations.

Abstract

Cations may populate regions in or near an RNA, requiring different considerations when describing the energetics of association. To gain further insight into how divalent cations interact with RNA, and impart stability to the native state, the folding of four different RNAs and ligand binding to the *add* adenine riboswitch was monitored upon titration with diamines and group II ions. We observe a clear difference in the folding response of RNAs known to chelate Mg^{2+} vs non-chelators upon titration with low charge density cations. RNAs lacking chelation sites show only subtle differences in folding behavior when stabilized by different group II ions. As an unexpected result, putrescine^{2+} was shown to stabilize the native structure of the *add* adenine riboswitch in complex with N6 substituted ligands but not in the apo or N6-unsubstituted ligand bound state. These results show that the difference in folding behavior between group II ions and diamines can be attributed to poor electrostatic compensation by lower charge density cations. Therefore the native fold does not require specific coordination of Mg^{2+}. Yet, Mg^{2+} stabilizes a native-like intermediate while other counterions are unable to drive the RNA into the same intermediate structure. These results support a folding pathway tuned for Mg^{2+} without requiring chelation.

Introduction

The divalent ion magnesium (Mg^{2+}) has been implicated in providing a large fraction of stabilizing energy to the native state of RNA upon folding. (Stein et al. 1974) However, the field of RNA folding is not unified on how magnesium, or other divalent ions, interact with RNA in order to impart stability to the native state. RNA folding studies have used various types of cations to mimic the interactions of biogenic ions and gain insight into how Mg^{2+} and other natural cations stabilize RNA. (Auffinger et al. 2011; Chowrira et al. 1993; Noeske et al. 2007) For the most part, these reports have focused on characterizing RNAs with Mg^{2+} chelation sites. (Koculi et al. 2007; Bukhman et al. 1997) Most studies looking at the divalent ion dependence of RNA folding have sought to find the characteristics that determine chelation specificity. (Travers et al. 2007) Such reports have suggested that the size of the divalent counterion is the main determinant of chelation site occupancy. This can be rationalized by the fact that these chelation sites are buried, requiring cations of specific dimensions and hydration properties in order to occupy chelation sites. What is not evident from these experiments is how the ion atmosphere (all non chelated ions) is organized in the presence of non-biogenic cations and what influence this has on RNA folding. Given the diversity of RNA folds found in nature, we seek to provide a general understanding of how divalent ions interact with RNA by expanding the survey of divalent ions to include a number of RNAs with varying degrees of divalent cation burial.

Various types of interactions between cations and RNA have previously been described (Draper et al. 2004) ranging from chelated (cation is partially dehydrated and makes at least two direct contacts with electronegative groups) to diffuse (cation remains mobile and hydrated in the vicinity of the RNA). Each one of these types of interactions imparts stability to the RNA, with energetic terms from site binding and electrostatic interactions in the ion atmosphere needing to be accounted for separately. (Leipply et al. 2011) To survey the effects of varying divalent cations on the folding of RNA, four RNAs with different degrees of cation burial in their native structures were selected for study (Figure 4-1). The resulting spectrum of RNA-ion interactions afforded by the diversity of these structures allows for a broad study on how divalent ions interact with local environments in an RNA structure.

RNAs that bury or partially bury cations have been shown to have a strong dependence on cation size / charge density for folding. (Moghaddam et al. 2009; Travers et al. 2007) The two left most structures in Figure 4-1 (M-box riboswitch aptamer domain and 58mer rRNA fragment) have been shown to bury and chelate cations upon folding. (Misra et al. 2001; Leipply et al. 2011; Ramesh et al. 2011; Pyle, 2002) The M-box riboswitch regulates the activity of Mg^{2+} *in vivo* by coupling the binding of at least three Mg^{2+} ions to the folding of an aptamer domain and subsequent accessibility of an expression platform. (Dann et al. 2008) The appropriate size and geometry of the counterions in the local environment of the RNA is essential for the folding and ultimately the switching of the regulatory circuit. (Ramesh et al. 2011) Like the M-box RNA, the 58mer rRNA fragment

chelates and partially buries both a Mg^{2+} and K^{+} ion. (Conn et al. 1999; Conn et al. 2002) It has been shown through both theory and experiment that occupancy of these chelation sites provides a significant amount of free energy to the native structure, thus imposing the requirement for Mg^{2+} to fold under physiological conditions. (Misra et al. 2001; Leipply et al. 2011; Lambert et al. 2009)

Not all RNAs have a strict dependence on the types of ions required to fold. The two right most structures in Figure 4-1, the FMN riboswitch and the A-riboswitch, have each been shown to fold upon addition of divalent ions other than Mg^{2+}. (Serganov et al. 2009; Trachman et al. 2013) The A-riboswitch crystal structure does not resolve any buried or partially buried cations. As expected this RNA does not show any selectivity for monovalent ions, thus supporting the notion that the majority of ion induced stability arises from interactions in the ion atmosphere. (Lambert et al. 2009) Like the A-riboswitch, the FMN riboswitch shows no preference for group II ions with respect to binding FMN despite the presence of a partially buried cation adjacent to the phosphate of the ligand in the crystal structure. (Serganov et al. 2009) In the absence of FMN and divalent ions the RNA adopts native-like dimensions in solution. (Baird et al. 2009) In addition, there is no electron density corresponding to a divalent ion in the ligand binding pocket of the apo structure. (Vicens et al. 2011) These data support the idea that this RNA can fold in the absence of ligand to a non-chelating state.

RNA folding can be observed as a divalent ion is titrated into solution while monitoring a spectroscopic signal. Titration curves monitoring a two state RNA folding process have three distinct characteristics, the midpoint of folding, the slope at the

midpoint of folding (the Hill coefficient), and the total change in signal for the folding transition (e.g. Minimum Relative Absorbance). Each one of these parameters is a descriptor of the folding process and when compared with folding curves generated with divalent ions of varying charge density, principles regarding cation induced folding of RNA can be extracted.

When fit to the Hill equation, characteristics of RNA folding reactions can be extracted from the fitted parameters. The midpoint of a transition ($C_{1/2}$) is the concentration of ion at which the free energy to transition between the I to N−state is zero. The slope at $C_{1/2}$ also has physical meaning. Known as the Hill coefficient, this parameter is a measure of the difference in ion excess between the N and I−state ($\Delta\mathbf{\Gamma}_{2+}$). (Leipply, 2010) The native state is more compact than the intermediate state, causing a larger excess of cations to accumulate in the vicinity of the native state. (Grilley et al. 2006) The hyperchromic effect is a result of bases stacking upon folding. The minimum relative absorbance (Rel. $Abs._{Min}$) is related to the fraction of folded RNA by the degree of base stacking occuring. If the same Rel. $Abs._{Min}$ is obtained with different divalent ions, the RNA is believed to fold to the same structure in both counterions. Taken together, these values provide insight into the folding of RNA.

Through the use of UV absorbance spectroscopy we have compared the folding of four RNAs upon titration of both diamines and group II ions. We observe that the burial or partial burial of cations in the native structure imposes a constraint on the size of counterions capable of folding RNA to the native state. RNAs that do not bury cations in the native structure show no dependence on the size of group II ions for folding by UV absorbance. To probe further into this

phenomenon we looked at UV absorbance profile for folding the *add* adenine riboswitch (A-riboswitch) upon titration with Mg^{2+} or putrescine^{2+} and with various purine ligands. We found that for adenine and 2,6-diaminopurine (DAP) both putrescine^{2+} and Mg^{2+} induced the same absolute change in hyperchromicity while the apo and 2-aminopurine bound state did not achieve the same change in hyperchromicity upon titration of putrescine^{2+}. Binding studies of 2-aminopurine showed that these results are possibly due to the requirement of Mg^{2+} for stabilization of the native state in the absence of an N6 substituted ligand. These results show that small perturbations in the RNA can create rather large changes in the ion dependence of folding.

Figure 4-1

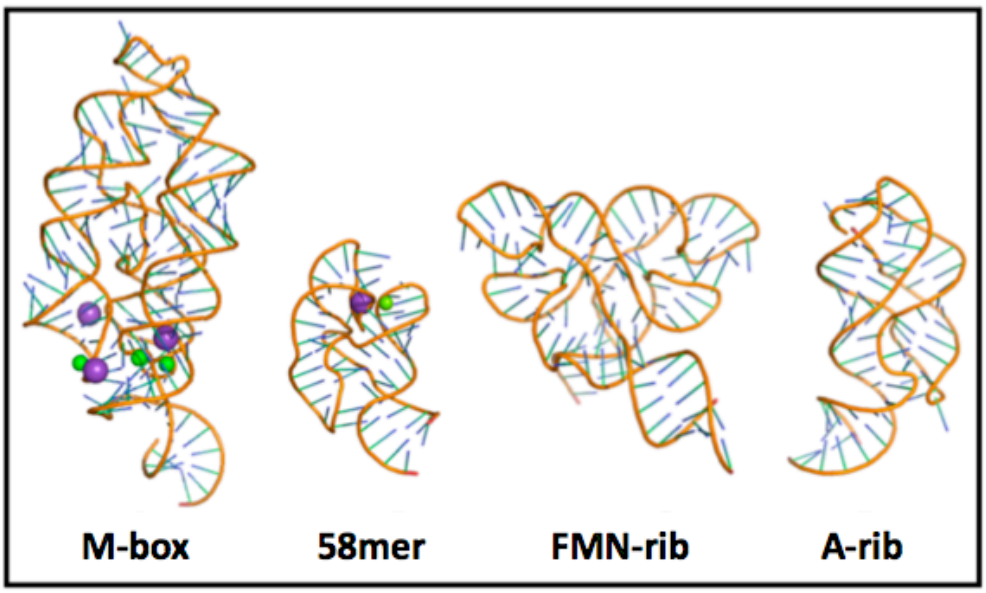

Figure 4-1. Structures of the four RNAs used in this study. M-box riboswitch shows the chelation sites for K^+ (purple spheres) and Mg^{2+} (green spheres) PDB ID: 3PDR. 58mer rRNA fragment showing the chelation sites for K^+ (purple spheres) and Mg^{2+} (green sphere) PDB ID: 1HC8.Crystal structure of the apo FMN riboswitch PDB ID: 2YIF and the *add* adenine riboswitch PDB ID: 1Y26.

Results

Folding of Mg^{2+} Chelators

Figure 4-2 A shows the change in absorbance for the M-box riboswitch aptamer domain upon titration of various divalent ions. Titration of the natural effector molecule for this riboswitch, Mg^{2+}, initially induces a collapse transition to a reduced I-state ensemble followed by a cooperative folding transition to the N-state. Similar three state folding schemes have been observed by multiple methods for other large RNA structures. (Das et al. 2003; Rangan et al. 2003) For the M-box, the initial collapse phase observed here by UV absorbance is correlated with a small decrease in R_g, which is also observed with a mutant of the M-box (M3) incapable of chelating Mg^{2+}. (Dann et al. 2007; Leipply , 2011) The decrease in R_g at 10 mM $MgCl_2$ is 35% of the initial R_g in the absence of Mg^{2+} for the wt M-box while the M3 mutant M-box only decreases its R_g by 6.5% of the initial R_g in 10 mM $MgCl_2$. Therefore, at least partial organization of a chelation site is required for the folding transition to take place. These data show that a collapse transition results in reduced dimensions while the folding transition couples the formation of tertiary interactions with the subsequent organization of chelation sites upon binding divalent ions.

The Ca^{2+} titration of the M-box is similar to the curve generated by Mg^{2+} although the folding transition is induced in half the concentration required for Mg^{2+}. In terms of free energy there is not a significant difference between these two ions. The high concentration of Ca^{2+} required to induce the folding transition (237 μM) is much larger than what would be found under physiological conditions. Other

RNA structures that chelate Mg^{2+} have also displayed a preference for Ca^{2+}, although they do not necessarily bind Mg^{2+} *in vivo*. (Kang et al. 2010; Klein et al. 2009) In some cases selectivity or preference for Ca^{2+} can be selected for by mutations adjacent to Mg^{2+} chelation sites. (Lau et al. 2013; Perrotta et al. 2007) This phenomenon is due to the lower enthalpy of hydration of Ca^{2+} along with its similar ionic radius that allows the cation to be easily accommodated into chelation sites.

In contrast to Mg^{2+}, both Sr^{2+} and Ba^{2+} induce collapse at a lower concentration, although they do not induce a folding transition. These results are not surprising given that even the high charge density trivalent ion, cobalt hexamine, does not induce folding of the M-box riboswitch. (Ramesh et al. 2011) Folding studies of similarly large RNAs (*Azoarcus* and *Tetrahymena* ribozymes) have shown that neither Ba^{2+} nor Sr^{2+} induced the same minimum R_g as Mg^{2+}, although the differences in the minimum R_g are very small. (Moghaddam et al. 2009) Hydroxyl radical footprinting studies of the P4P6 RNA indicate that neither Sr^{2+} nor Ba^{2+} are chelated, though smaller divalent ions are. (Travers et al. 2007) From figure 4-2 A, we believe that folding and local organization of chelation sites is coupled to cation chelation, and sterically excluded cations cannot organize chelation sites through electrostatic interactions in the ion atmosphere.

Figure 4-2

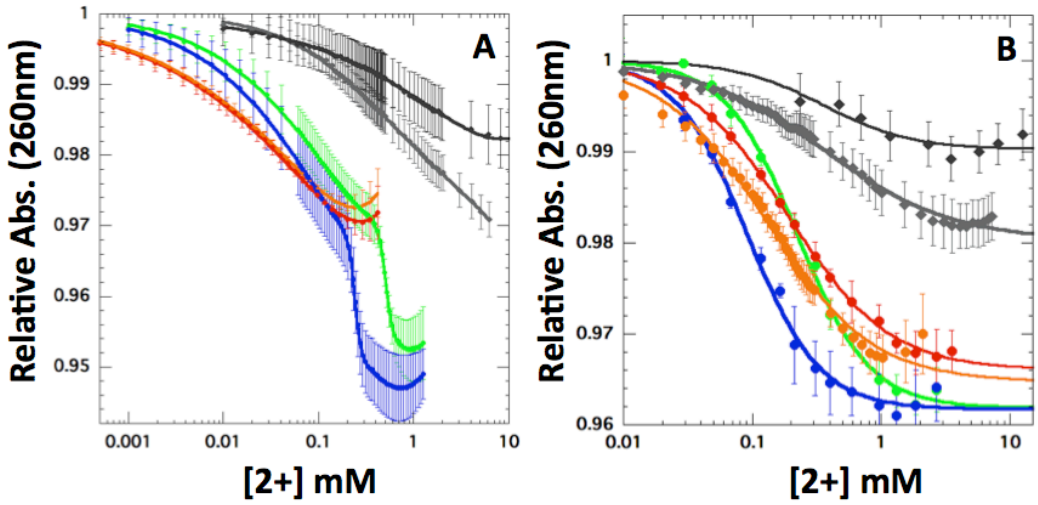

Figure 4-2. Relative UV absorbance of the Mg^{2+} chelators at 260 nm. Mg^{2+} (green), Ca^{2+} (blue), Sr^{2+} (red), Ba^{2+} (orange), 1,3-diaminopropane^{2+} (light grey) or putrescine^{2+} (grey) for the M-box riboswitch (A) and 58mer rRNA fragment (B). Cadaverine^{2+} did not induce a significant change in absorbance over the concentrations tested.

The 58mer rRNA fragment shows only a single transition upon titration of divalent ions. There is a fairly small difference in the Rel. Abs_{Min} between the group II ions for the 58mer rRNA. Both Mg^{2+} and Ca^{2+} obtain the same minimum relative absorbance (0.962). Once again the midpoint of the Ca^{2+} induced transition (92 μM ± 2) occurs at approximately half the concentration required by Mg^{2+} (224 μM ± 1.5) with approximately the same Hill coefficient. The difference in the Rel. Abs_{Min} between the small group II ions (Mg^{2+} and Ca^{2+}) and the large group II ions (Sr^{2+} and Ba^{2+}) is only ~0.02 or (~15% of the total signal). This modest difference between these ions is contrasted by a rather large difference in the Hill coefficients between the small (Mg^{2+} and Ca^{2+}) and large (Sr^{2+} and Ba^{2+}) group II ions. These results may

be due to the presence of a size selective cation binding site in the native state and or alternative cation interactions with the intermediate state.

Table 4-1: UV absorbance titrations of the M-box riboswitch at 260 nm.

M-box	$C_{1/2,\ collapse}$ (μM)	$n_{collapse}$	$C_{1/2,folding}$ (μM)	$n_{folding}$	$Rel.\ Abs_{min}$
Mg^{2+}	45.0 ± 2.1	1.02 ± 0.03	491.6 ± 5.5	8.50 ± 0.72	0.952 ± 0.0003
Ca^{2+}	23.6 ± 6.0	1.09 ± 0.04	237.6 ± 3.5	7.14 ± 0.44	0.945 ± 0.0004
Sr^{2+}	13.0 ± 5.2	0.57 ± 0.03	-	-	0.970 ± 0.0015
Ba^{2+}	14.9 ± 7.2	0.61 ± 0.04	-	-	0.972 ± 0.002
1,3-diamine^{2+}	809 ± 32	0.71 ± 0.01	-	-	0.971 ± 0.0006
Putrescine^{2+}	1044 ± 121	0.57 ± 0.02	-	-	0.982 ± 0.0005

Neither the M-box riboswitch nor the 58mer rRNA obtain the same relative absorbance upon titration with organic divalent ions as with Mg^{2+}. The minimum relative absorbance for the diamines is only a fraction of the change in absorbance obtained by Mg^{2+}. The largest change in absorbance is observed for 1,3-diaminopropane while cadaverine^{2+}, the diamine with the lowest charge density, does not show a significant change in absorbance over the concentration range tested (data not shown). These data suggest that charge density is a significant factor in inducing collapse of RNA while appropriate counterion size is essential for chelation and ultimately folding.

Folding of Non-chelators

Both the FMN riboswitch and A-riboswitch have been shown to fold to compact states in the absence of their respective ligands upon addition of Mg^{2+} and are believed to do so without invoking Mg^{2+} chelation. (Baird et al. 2010; Leipply et

al. 2011; Vicens et al. 2011) As a testament to this, both of these RNAs reach the same relative absorbance in all of the group II ions used in this study (Figure 4-3). In addition the Hill coefficients for the transition from the I to N-state are similar between the different group II ions. These results suggest that all group II ions induce folding to the same state and are thus non-specific in their interaction with these RNAs.

Table 4-2: UV absorbance titrations of the 58mer rRNA at 260 nm.

58mer rRNA	$C_{1/2}$ (μM)	n	ΔAbs_{min}
Mg^{2+}	219.5 ± 12.2	1.61 ± 0.11	0.962 ± 0.001
Ca^{2+}	93.8 ± 6.56	1.50 ± 0.09	0.962 ± 0.0015
Sr^{2+}	193.4 ± 19.4	1.1 ± 0.07	0.966± 0.0015
Ba^{2+}	154.9 ± 21.7	0.95 ± 0.09	0.965 ± 0.0008
1,3-diamine^{2+}	466 ± 99.6	0.75 ± 0.06	0.979 ± 0.0017
Putrescine^{2+}	389.7± 141.5	1.35 ± 1.39	0.99 ± 0.0018

The FMN riboswitch undergoes a single folding transition to its folded apo state (Figure 4-3 A). The group II ions used in this study induce folding to the same relative absorbance for the FMN riboswitch. There is a three-fold difference in the range of the midpoints for these group II ions (Table 4-3). This difference is due to different degrees of interaction with the native and intermediate state of the RNA. Although it is difficult to observe interactions of group II ions with the intermediate state, crystallography can provide insight into the interaction of ions with the native state. Crystal soaks of the FMN riboswitch-Mg^{2+} complex with $BaCl_2$ showed that Ba^{2+} is capable of replacing Mg^{2+} in a buried chelation site along with occupying additional sites on the structure (Figure A-4). (Serganov et al. 2009) The additional

sites occupied by Ba^{2+} were most often found adjacent to N7 atoms of purine bases. These interactions are typical of soft transition metals and highlight the potential soft / polarizable nature of Ba^{2+} and Sr^{2+}. (Bock et al. 1999; Bronnval et al. 2001) These results show that discrepancies between group II ions may arise from factors other than steric exclusion from chelation sites, complicating comparisons between group II ions. What is clear from this and other studies is that ions other than Mg^{2+} are capable of folding the FMN to a native conformation in both the apo and holo state.

Figure 4-3

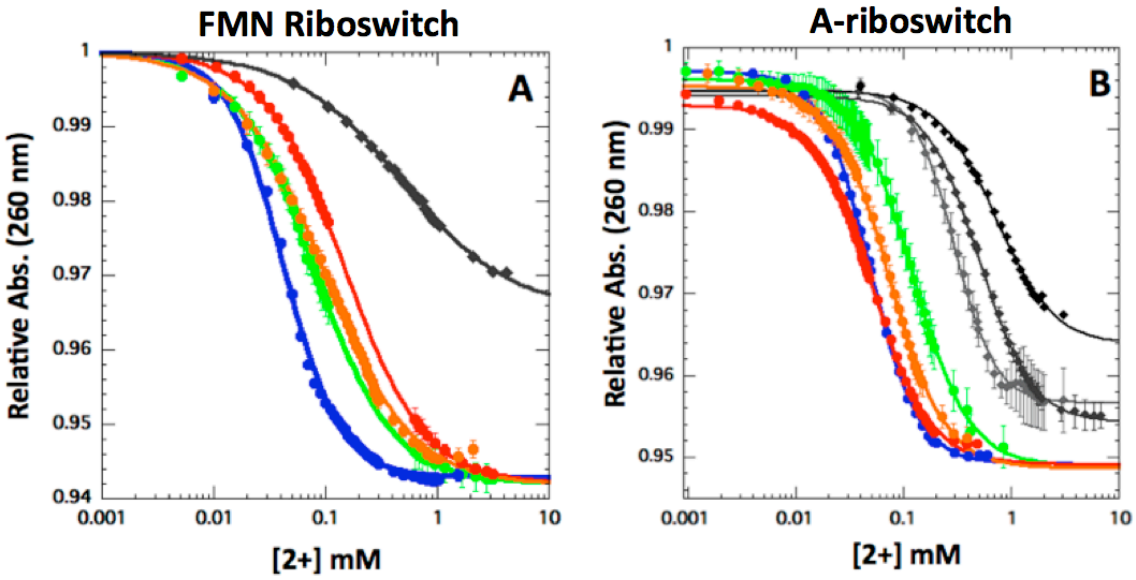

Figure 4-3. Relative UV absorbance at 260 nm of the non-chelators as a function of Mg^{2+} (green), Ca^{2+} (blue), Sr^{2+} (red), Ba^{2+} (orange), 1,3-diaminopropane^{2+} (light grey), putrescine^{2+} (grey) or cadaverine^{2+} (black) concentration for the Apo FMN riboswitch (A) and Apo A-riboswitch (B).

Table 4-3: UV absorbance titrations of the Apo FMN riboswitch and Apo A-riboswitch at 260 nm.

(Apo) FMN riboswitch	$C_{1/2}$ (μM)	n	Rel. Abs_{min}	(Apo) A-riboswitch	$C_{1/2}$ (μM)	n	Rel. Abs_{min}
Mg^{2+}	78.9 ± 5.2	1.22 ± 0.02	0.942	Mg^{2+}	120.5 ± 9.4	1.61 ± 0.12	0.949
Ca^{2+}	42.3 ± 1.5	1.72 ± 0.04	0.943	Ca^{2+}	48.0 ± 0.67	1.93 ± 0.04	0.949
Sr^{2+}	147.8 ± 2.1	1.22 ± 0.01	0.942	Sr^{2+}	50.4 ± 7.5	1.56 ± 0.30	0.949
Ba^{2+}	94.1 ± 3.1	1.09 ± 0.03	0.942	Ba^{2+}	73.1 ± 3.1	1.67 ± 0.09	0.949
1,3-diaminopropane^{2+}	-	-	-	1,3-diaminopropane^{2+}	294.8 ± 15.5	2.06 ± 0.22	0.9566
Putrescine^{2+}	485.4 ± 19.1	0.89 ± 0.02	0.965	Putrescine^{2+}	523.3 ± 12.2	1.66 ± 0.06	0.954
Cadaverine^{2+}	-	-	-	Cadaverine^{2+}	720 ± 20.1	1.52 ± 0.11	0.964

The A-riboswitch is one of the most well-characterized RNAs with regards to folding and structure. The two most prominent characteristics of the A-riboswitch topology are the central ligand binding pocket and the distal kissing loops. These two regions switch from a disordered to an ordered state upon folding in the appropriate solution conditions. The result is a folding scheme that is composed of four distinct states (Figure 4-4). Titration of Mg^{2+} in the absence of ligand produces RNA dimensions similar to the native structure (Leipply et al. 2011). The resulting transition from an extended (E) to an intermediate docked conformation (I_{Dock}) is characterized by docked kissing loops with only partial organization of the ligand binding pocket. It has been shown through HSQC experiments that ligand is required to completely organize the ligand binding pocket although Mg^{2+} can partially organize this region in the absence of ligand. (Noeske et al. 2007) UV

absorbance measurements show that all group II ions induce the same Rel. Abs_{Min} (Figure 4-3 B). This suggests that the group II ions induce folding to the same I_{Dock} state. Despite going through the same transition, the midpoints of each transition differ, with Mg^{2+} requiring the highest concentration to induce folding (Table 4-3). From the current results, we see no obvious trend in terms of counterion characteristics that govern the folding from an E to I_{Dock} conformation.

Figure 4-4

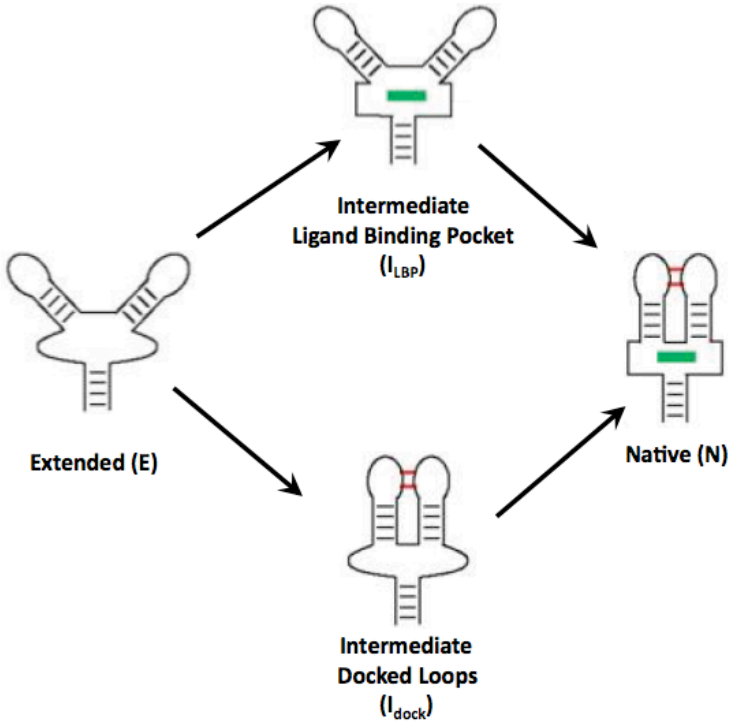

Figure 4-4. Folding pathway for the A-riboswitch. Four states of the A-riboswitch are defined by the organization of the ligand-binding pocket and docked kissing loops. These structures can interconvert during folding and unfolding of the wt A-riboswitch while the E and I_{LBP} structures can be isolated in solution with the use of a C60G mutant. Adapted from Leipply et al. 2011.

Neither the apo-FMN riboswitch nor the apo-A-riboswitch obtain the same relative absorbance upon titration of diamines as found with Mg^{2+} or the other group II ions. These results are consistent with previous reports suggesting that diamines are incapable of folding structured RNAs to their native state. (Koculi et al. 2004) See Discussion for more details.

Folding and ligand binding of the A-riboswitch

The structure of the A-riboswitch ligand binding pocket contains a sharp kink, bringing phosphate oxygens within 3.6 Å of one another. As a result, a large amount of energy (~5 kcal/mol) is required to organize the binding pocket of this RNA. (Leipply et al. 2011) Despite this fact, saturating conditions of 2,6-diaminopurine, in the absence of divalent ions, are capable of providing enough free energy to organize this region and fold the A-riboswitch (Leipply et al 2011). As a means of looking at how organization of the ligand binding pocket influences the ion dependence of folding the A-riboswitch, we monitored UV absorbance in the presence and absence of different purines known to bind the A-riboswitch (Figure 4-5). These experiments observe the hyperchromic response of the RNA as it transitions from an E-state to the N-state, where both docked loops and an organized binding pocket are present. As expected, Mg^{2+} induces folding at significantly lower concentration than putrescine^{2+} in both the presence and absence of ligand. Interestingly, Mg^{2+} and putrescine^{2+} do not obtain the same Rel. Abs_{Min} in the absence of ligand or in the presence of 2-AP. This can be contrasted with the ligands 2,6-diaminopurine and adenine which both obtain the same

relative absorbance upon titration with Mg^{2+} or $putrescine^{2+}$. Comparison of the ligands and UV monitored folding response implicates the N6 position of the ligand in the folding discrepancy between Mg^{2+} and $putrescine^{2+}$. Therefore, N6 substituted purines are capable of organizing the ligand binding pocket in the absence of divalent ions, allowing for low charge density counterions such as diamines to stabilize the native state.

The Rel. Abs_{Min} for the A-riboswitch significantly changes depending on the ligand present in solution (Figure 4-5). The difference between the Rel. Abs_{Min} for the apo and holo forms can be rationalized by a difference in binding pocket organization. However, Mg^{2+} titrations in the presence of 2,6-diaminopurine and 2-aminopurine result in the same Rel. Abs_{Min} while Rel. Abs_{Min} for adenine is 0.04 lower. One possible explanation is that the decrease in Rel. Abs. results from the decrease in absorbance of the free adenine upon binding to the A-riboswitch. Of the three ligands used, adenine is the only one that shows a large absorbance signal at 260 nm under the conditions tested. At a concentration of ~1 μM A-riboswitch, stoichiometric binding of adenine will cause a maximum decrease in Abs of 0.025 for the free ligand (adenine $\varepsilon = 14.4$ / mM). Yet, this does not account for the total difference in signal of 0.04 that we observe. It is possible that there is an additional decrease in absorbance of the RNA upon stacking with adenine that does not occur with the other ligands. Another explanation is that the adenine ligand resides in a different orientation in the binding pocket than 2-aminopurine or 2,6-diaminopurine causing a larger hypochromicity. In the presence of ligand, purine riboswitches have been shown to fold to the same structure regardless of the ligand

occupying the binding site (Gilbert et al. 2006; Serganov et al. 2004) suggesting that orientation is not the cause of the ΔRel Abs_{Min}. Further experiments are required to determine the cause of the difference in absorbance.

Figure 4-5

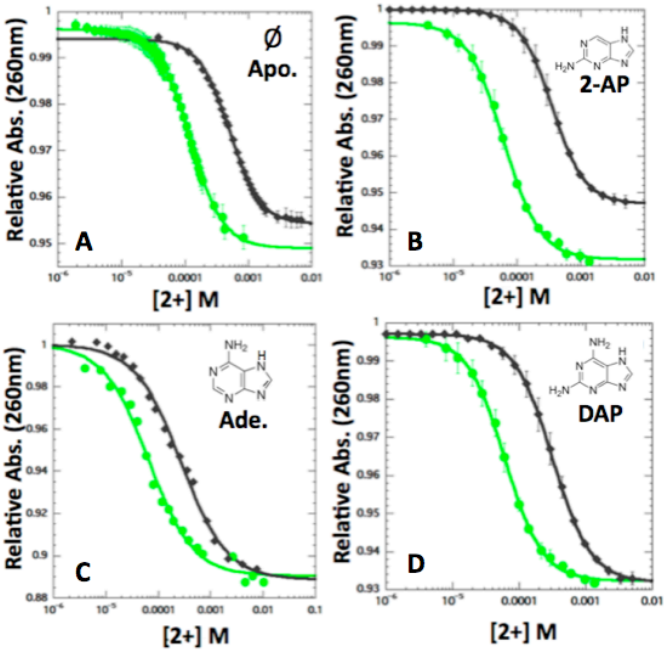

Figure 4-5. Effect of ligand structure on RNA folding. Relative UV absorbance at 260 nm as a function of Mg^{2+} (green) or $putrescine^{2+}$ (grey) for the A-riboswitch in the absence of ligand (A), presence of 16 μM 2-aminopurine (B), 24 μM adenine (C) or 8 μM 2,6-diaminopurine (D).

As a means of looking further into the difference between putrescine and Mg^{2+} in the presence of 2-aminopurine (Figure 4-5), the study was expanded to include the group II ions Ca^{2+}, Sr^{2+} and Ba^{2+} (Figure 4-6 A). All of the group II ions tested obtained approximately the same relative absorbance as that of Mg^{2+} (~0.93). These results show that a high charge density counterion is required in order to transition from an extended state to the native state in the presence of 2-

aminopurine. Therefore a size selective chelation site is not formed upon altering the purine ligand.

Figure 4-6

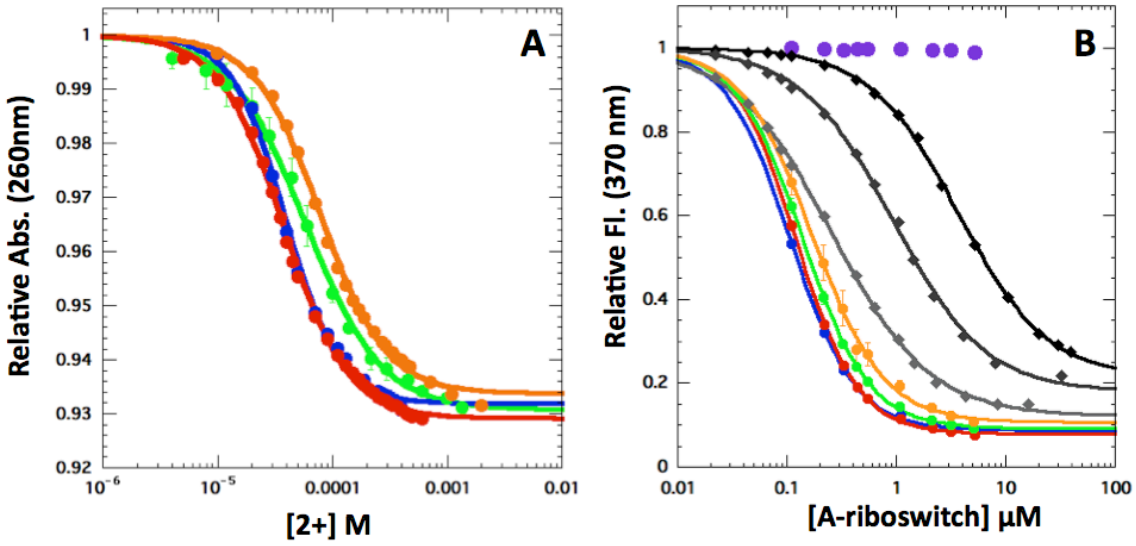

Figure 4-6. RNA folding and ligand binding in 2-aminopurine (A) Relative UV absorbance at 260 nm for the A-riboswitch in the presence of 16 µM 2-aminopurine upon titrating Mg^{2+} (green), Ca^{2+} (blue), Sr^{2+} (red), Ba^{2+} (orange) or putrescine^{2+} (grey). (B) Fluorescence quenching of 2-aminopurine upon titration of A-riboswitch in the presence of 350 µM of group II ions or 5 mM of diamines. Color scheme is identical to (A) with the addition of 50 mM K^{+} only (purple) 1,3-diaminopropane^{2+} (light grey) and cadaverine^{2+} (black).

Table 4-4

260nm Abs.	$C_{1/2}$ (µM)	n	Rel. Abs $_{max}$	370nm Fl.	$C_{1/2}$ (µM)	n	Rel. Fl_{max}
Mg^{2+}	57.7 ± 2.2	1.31 ± 0.057	0.931 ± 0.0006	Mg^{2+}	138.5 ± 1.3	1.43 ± 0.02	0.091 ± 0.003
Ca^{2+}	39.1 ± 1.1	1.86 ± 0.081	0.931 ± 0.0006	Ca^{2+}	106.8 ± 1.0	1.47 ± 0.02	0.088 ± 0.002
Sr^{2+}	37.6 ± 3.7	1.51 ± 0.033	0.930 ± 0.0003	Sr^{2+}	122.1 ± 1.2	1.54 ± 0.02	0.080 ± 0.002
Ba^{2+}	78.3 ± 2.8	1.54 ± 0.048	0.934 ± 0.0006	Ba^{2+}	170.3 ± 5.6	1.32 ± 0.07	0.010 ± 0.001
1,3-diamine^{2+}	-	-	-	1,3-diamine^{2+}	252.7 ± 6.7	0.97 ± 0.02	0.121 ± 0.006
Putrescine^{2+}	356.7 ± 35.4	1.68 ± 0.007	0.947 ± 0.0003	Putrescine^{2+}	925.9 ± 35.3	1.03 ± 0.03	0.180 ± 0.011
Cadaverine^{2+}	-	-	-	Cadaverine^{2+}	3623.2 ± 83.5	1.07 ± 0.02	0.216 ± 0.017

As a complementary experiment to the ion dependence of folding, the fluorescence quenching of 2-aminopurine was monitored upon binding A-riboswitch (Figure 4-6 B). (Lemay et al. 2006) For this study the concentration of group II ions was kept constant at 350 μM while the concentration of diamines was maintained at 5 mM. At these two concentrations, the T_m for the native to intermediate transition is the same for put^{2+} and Mg^{2+}. (Trachman et al. 2013) Upon titration of A-riboswitch, binding of 2-aminopurine occurs in both the diamine and group II ion containing solutions with no binding being observed in the 50 mM K^+ containing solution. From these results it is clear that divalent ions promote binding of ligand.

The 2-aminopurine binding series shows a biased behavior in regards to folding in the presence of group II ions relative to diamines. All of the group II ions promote binding to approximately the same degree as indicated by similar midpoints (~200 pM) and maximum fluorescence quenching (~90.5%). This is contrary to the diamine series, which shows a dramatic difference in binding of 2-aminopurine for each diamine tested. The midpoint and the fractional change in fluorescence are minimized and maximized (respectively) with decreasing linker length (charge density) of the diamine. These results indicate that the quenching of the ligand signal is dependent on charge density of the diamines. The question still remains as to what is the meaning of the maximum fluorescence quenching. Given that each curve contains saturating amounts of A-riboswitch, the fraction of bound ligand should approach 100% at the lower end of each curve. The maximum fluorescence quenching will report on the local environment (binding pocket

organization) of the fluorophore (2-aminopurine) rather than the fraction of bound fluorophore. Therefore, high counterion charge density is capable of compensating for the lack of a N6 substituted ligand and promotes a native-like organization to the ligand-binding pocket.

2-aminopurine binding upon titration with cations

Previous work has looked at both the binding of ligand and folding of the A-riboswitch upon titration with Mg^{2+} and other cations. (Leipply et al. 2011; Noeske et al. 2007) Both reports observed that the folding of this RNA occurs through a cooperative process where the docking of the kissing loops is coupled to organization of the binding pocket upon interaction with ligand. As a means of looking at how cations influence the organization of the ligand binding pocket we observed 2-aminopurine binding in both the cooperative (wild type) and uncoupled (C60G mutant) systems (Figure 4-7). In addition to the group II ions and putrescine^{2+}, cobalt hexamine and $MnCl_2$ were titrated to draw a comparison with NMR experiments designed to observe Mg^{2+} interaction sites on the A-riboswitch. (Noeske et al. 2007; Buck et al. 2010)

A major difference between the 2-aminopurine binding titrations is the maximum fluorescence quenching. Due to the nature of ensemble measurements the difference in fluorescence quenching can be attributed to either the formation of an alternative structure that does not produce the same fluorescence quenching at saturation and / or a lower fraction of bound ligand. We believe that this difference in quenching is due to a slightly different orientation of the ligand in the binding

pocket. If the difference in baseline signal were due to a lower fraction of bound ligand, high concentrations of A-riboswitch would saturate binding. This is not observed in Figure 4-6 B.

For the wt A-riboswitch, all of the ions tested except putrescine^{2+} promote fluorescence quenching to the same degree as Mg^{2+} (Figure 4-7A). This is consistent with the UV absorbance data in the presence of 2-aminopurine, which shows that the RNA does not obtain the same structure in the presence of putrescine^{2+} as in the other divalent ions (Figure 4-6A). Upon uncoupling of binding pocket organization with loop docking through the C60G mutation, the same maximum relative fluorescence obtained by the wild type A-riboswitch with all group II ions and cobalt hexamine (10.0 %) is only achieved in the presence of Mg^{2+} (Figure 4-7 B). The divalent ions Ca^{2+} and Sr^{2+}, and the trivalent ion Cobalt hexamine only quench to 14% of the initial signal while Mn^{2+} can only induce quenching to 18%. The difference in fluorescence quenching between Mg^{2+} and the other cations can be rationalized by Mg^{2+} actively promoting organization of the ligand binding pocket or by the other cations promoting non-native states in the absence of coupled folding.

Titration of the C60G mutant with putrescine^{2+} exhibits a marginal binding of ligand with a midpoint shifted two orders of magnitude higher in concentration than the wild type titrated with putrescine^{2+}. Although this is a drastic change, caution should used when extracting information from these data given the high concentration of Cl^- at the high end of the curve. In addition, the R_g of the C60G A-riboswitch shows no change upon titration of 5 mM putrescine^{2+} while the addition of 1 mM Mg^{2+} is capable of decreasing the dimensions of this RNA (Figure A-3).

(Leipply et al. 2011) Together these results show that organization of the binding pocket and ultimately folding is dependent on a high charge density (charge divided by Van der Waals volume) counterion.

Figure 4-7

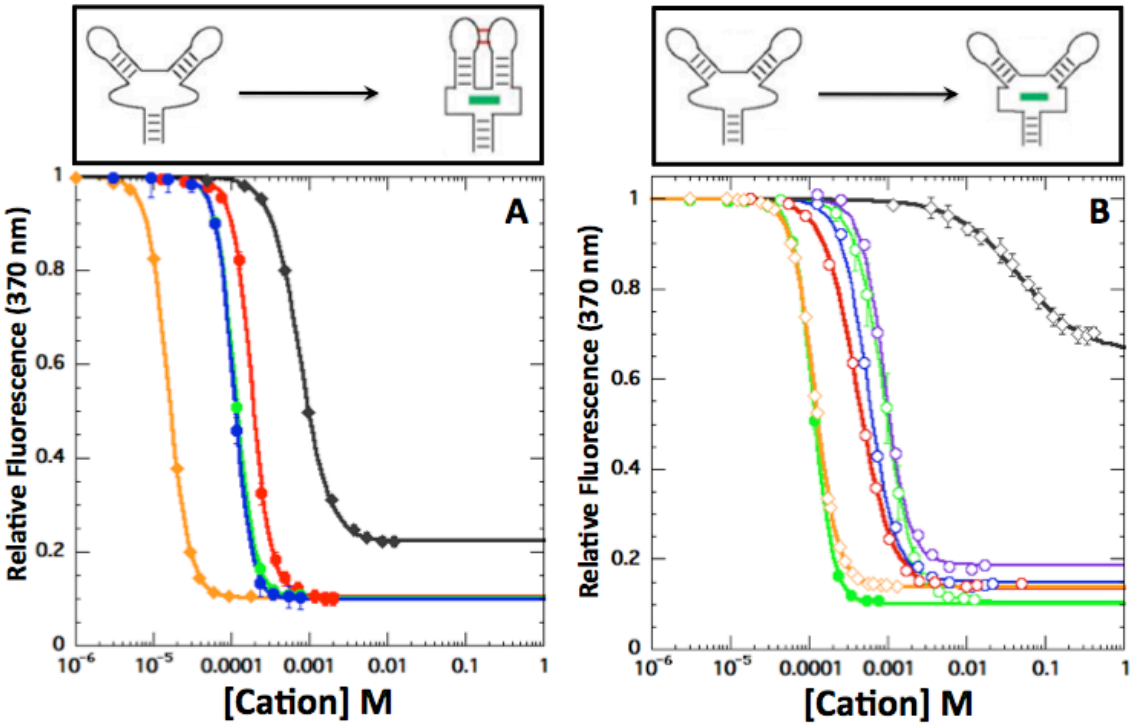

Figure 4-7. 2-aminopurine fluorescence quenching for the extended to native transition (wild type, closed symbols) (A) and the extended to I_{LBP} transition (C60G mutant, open symbols) (B) upon titration of different cations. (A) Wild type A-riboswitch upon titration with cobalt hexamine (orange), $CaCl_2$ (blue), $MgCl_2$ (green), $SrCl_2$ (red) and putrescine^{2+} (grey). (B) C60G mutant upon titration with the ions listed in (A) in addition to $MnCl_2$ (purple). The wild type A-riboswitch upon titration with $MgCl_2$ (green, closed symbols) from panel A is shown as a reference point.

Discussion

RNA folding induced by diamines

RNA folding is highly dependent on the ionic conditions present in solution. In this chapter, we try to gain insight into the principles governing RNA folding by observing the folding of four different RNAs with a series of divalent cations. To our best knowledge the activity coefficients of the cations used in this study are nearly identical to each other over the concentration ranges reported. (Robinson et al. 1948; Trachman et al. 2013) Therefore the differences in RNA folding behavior observed here are due to structural and physical properties of cations rather than differences in effective concentration.

Four RNAs, classified by the degree of interaction they have with divalent ions, were studied in parallel. The M-box riboswitch and 58mer rRNA fragment were chosen to represent "Mg^{2+} chelators" (see Results for description) while the FMN riboswitch and A-riboswitch represent the "non-chelators". There were distinct differences between spectroscopic signals of the Mg^{2+}-chelating RNAs upon titration of low charge density counterions (Sr^{2+}, Ba^{2+}, 1,3-diaminopropane^{2+}, putrescine^{2+} and cadaverine^{2+}) than with the high charge density counterions (Mg^{2+} and Ca^{2+}). These results are consistent with the requirement for a high charge density counterion to occupy and organize a chelation site(s) in order for folding to take place. It should be noted that under extreme conditions (1.6 M NH_4^+ or 8 m TMAO) the 58mer is as able to fold in the absence of Mg^{2+}, showing that alternative folding mechanisms lead to the same native state, showing that the chelated cation

is not an integral part of the native state. (Bukhman et al. 1997; Lambert et al. 2010) The non-chelators (FMN riboswitch and A-riboswitch), in the absence of ligand, fold to the same state in group II ions, but are unable to properly fold upon titration of diamines (Figures 4-3). Comparison of the folding curves of the non-chelators shows no obvious pattern to the stabilization by group II ions. From these results, counterion charge density is not the sole determinant of RNA folding efficiency; factors such as polarizability and hydration potentially contribute.

Despite the varying properties of group II ions, they appear to fold the RNA non-chelators to the same state as assessed by UV absorbance. Although the midpoints of the folding transitions differ between the various cations used in this study, the total change in signal for each of the titrations is consistently the same for the group II ions tested. For the A-riboswitch, both diamines and group II ions promote ligand binding, although only group II ions organize the ligand binding pocket to the same extent as Mg^{2+} for the wt A-riboswitch (Figures 4-6, 4-7). This demonstrates that specific coordination of counterions by electronegative RNA groups is not a requirement to reach the native state.

Consistent with a previous study of diamine effects on RNA folding (Koculi et al. 2004) and results from chapter 2, we find clear differences in RNA folding behavior as the carbon chain length of diamines is altered. For instance, for most of the RNAs examined, the total change in signal (either fluorescence or UV absorbance) was larger for Mg^{2+} than for diamines^{2+}. These results suggest that the final structures stabilized by each ion are different, with the diamines^{2+} stabilizing a less compact, non-native state (Figure 3-2 A). This is consistent with previous

hypotheses that diamines^{2+} can disrupt folding to the native state by interacting with phosphate groups thus preventing efficient packing of helices and tertiary interactions or that the excluded volume of large counterions prevents a sufficient number of counterions from interacting with the RNA. (Koculi et al. 2004) An exception is the A-riboswitch in the presence of N6 substituted purine ligands (2,6-diaminopurine and adenine), where both Mg^{2+} and putrescine^{2+} are shown to fold the A-riboswitch to the same state (Figure 4-5). It is not clear why an N6 substituted purine ligand would relieve a group II ion dependence on RNA folding. The orientation of the ligand and structure of purine riboswitches seem to be invariable, provided that compensatory alterations are made between the two molecules. (Gilbert et al. 2009) The results are rationalized by the inability of 2-aminopurine to organize the ligand binding pocket to the same degree as adenine or 2,6-diaminopurine, requiring greater electrostatic compensation from high charge density counterions to reach the native state (Figure 4-6 B).

Given that the Mg^{2+}-chelators, apo-FMN-riboswitch as well as group I introns are not able to efficiently fold in the presence of diamines the obvious question is: what enables an A-riboswitch-N6 substituted ligand complex to fold in either group II ions or diamines? SAXS studies have reveled that the A-riboswitch can fold to native-like dimensions in the absence of divalent ions in saturating concentrations of 2,6-diaminopurine or in the absence of ligand with Mg^{2+}. (Leipply et al. 2011) This contrasts with folding in the presence of putrescine^{2+} and absence of ligand which only reduces the R_g of the A-riboswitch by 50% of the total change expected (Figure 3-2 A). This shows that there is a large energy barrier to both folding and

organizing the ligand binding pocket that putrescine^{2+} is unable of over come. In sub-saturating concentrations of 2,6-diaminopurine, the free energy required to cooperatively fold the A-riboswitch is relatively low, allowing for putrescine^{2+} to stabilize the native state of the A-riboswitch. Cations induce folding of the A-riboswitch-ligand complex (and other RNAs) by accumulating in sufficiently greater excess in the native state relative to the intermediate state. Since the difference in excess putrescine^{2+} ($\Delta\Gamma_{put}$) is sufficiently large to stabilize the native state, the excluded volume of cations does not seem to be a concern in folding the A-riboswitch. However, $\Delta\Gamma_{put}$ for the A-riboswitch-ligand complex is rather small, 1.54 ± 0.06 and 1.00 ± 0.06 ions for 2,6-diaminopurine and adenine respectively. For RNAs with large free energy barriers to folding, the difference in excess diamine required to induce folding may be much larger, causing excluded volume imposed by excess counterions to become a significant barrier to folding.

It is obvious that the influential factors determining RNA-diamine^{2+} interactions are very different from RNA-group II ion interactions. From the results in this chapter as well as chapter 2 and the literature (Koculi et al. 2004) we conclude that diamines are unable to stabilize some native folds due to i) steric exclusion from chelation sites ii) lower counterion charge density, which prevents efficient electrostatic compensation of local regions with high negative potential and iii) an entropic penalty imposed on counterions with internal degrees of freedom interacting with RNA. From our results with the A-riboswitch we do not see a restriction on folding based on excluded volume, although excluded volume effects may become more significant for larger RNAs. Differences in hydration between

cations may also contribute to altered folding behavior of RNA; the data collected within this chapter are unable to draw conclusions on such matters.

Mg^{2+} promotes native-like interactions

Folding of the A-riboswitch in the presence of ligand occurs through a cooperative process, where the interaction of the kissing loops is coupled to organization of the ligand-binding pocket. (Leipply et al. 2011; Noeske et al. 2007; Lemay et al. 2006) Upon disruption of the kissing loop interaction through the C60G mutation these interactions become decoupled. In this uncoupled system only Mg^{2+} is capable of organizing the ligand binding pocket to the same degree as that found in the wild type structure as indicated by fluorescence quenching of 2-aminopurine. Like the group I intron, the uncoupled A-riboswitch requires Mg^{2+} to organize RNA junctions at the core of the structure. (Rangan et al. 2003) But unlike the group I intron, the A-riboswitch does not show any indication of cation chelation in its core. (Cate et al. 1997) From these results we reach the conclusions that i) Mg^{2+} has unique properties, which stabilize a native-like intermediate in the ligand binding pocket of the A-riboswitch and ii) the kissing loop interaction enables ions other than Mg^{2+} to fold the A-riboswitch to the native state due to the energetic coupling of interactions. It is this coupled interaction network that can mask a non-chelating RNAs preference for Mg^{2+}.

How does Mg^{2+} promote a native-like organization to the ligand binding pocket? One plausible explanation is that Mg^{2+} binds to the RNA surface biasing the conformational landscape. An extensive NMR study using chemical shift

perturbations and line broadening techniques suggested the presence of Mg^{2+} binding sites near the A-riboswitch ligand binding pocket. (Noeske et al. 2007) However, these experiments used cobalt hexamine and Mn^{2+} as Mg^{2+} mimics. Given the results from Figure 4-7, these ions are not necessarily interacting with the A-riboswitch in the same surface locations as Mg^{2+} since they are unable to induce the same degree of fluorescence quenching of ligand in the C60G mutant. Due to a lack of high resolution techniques for observing Mg^{2+}-nucleic acid interactions, rationalizing the unique influence of Mg^{2+} on the ligand binding pocket will probably have to wait for the development of reliable microsecond computer simulations of RNA with hydrated Mg^{2+}.

All of the data collected within this chapter have been under the conditions of thermodynamic equilibrium. The ability of Mg^{2+} to promote native-like intermediates may also play a significant role in the folding landscape and kinetics of this and other RNAs. (Heilman-Miller et al. 2001)

Conclusions

The folding of RNA to compact native structures requires that the large electrostatic potential created by bringing phosphates into close proximity are compensated for by solution components. In this chapter we observed that both size and charge density of divalent ions are important in organizing regions of structured RNAs containing large electrostatic potentials. Although low charge density counterions such as putrescine^{2+} were not capable of stabilizing the native state on their own, increased organization of the RNA by a ligand enabled folding to

the native structure. Therefore, putrescine^{2+} is capable of accumulating in sufficient excess to stabilize the native state. This shows that RNA folding, in the absence of cation chelation sites, can be generally viewed as an issue of electrostatic compensation without requiring specific interactions of cations. The folding of RNA is highly dependent on the sequence of the RNA, with cooperative interactions guiding folding to the native state. These cooperative interactions can mask ion preferences that smooth the folding energy landscape. From our results, it is clear that RNA folding studies must account for Mg^{2+} interactions with both the native and intermediate state and further methods development focusing on RNA-Mg^{2+} interactions is necessary.

Materials and Methods

Chemicals and RNA

All solutions were prepared using distilled deionized water at 18.3 MΩ resistivity. MOPS Buffer was obtained from Sigma and was ≥ 99.5% purity. All buffers where brought to pH 6.8 using Sigma KOH ≥ 99.5% purity. KCl from Fluka ≥ 99.5% purity was then added to a final concentration of 50 mM. All buffers contained 10μM EDTA (Sigma ≥ 99.5% purity) in order to scavenge free transition metals. $MgCl_2$ was purchased from Fluka ≥ 99.5% purity. All goup II ion solutions were calibrated against a know standard of EDTA by looking at absorbance at 230nm at pH 8.

All RNAs were transcribed using bacteriophage T7 RNA polymerase. All RNAs were transcribed from plasmid DNA (pLL2) linearized with a SmaI endonuclease. Each

RNA sequence was encoded just upstream of a T7 promoter sequence on the plasmid. Resulting transcription products were purified on a 9-12% Poly acrylamide gel (19:1). UV shadowing was used to extract gel slices which then underwent electroelution in an Elutrap Electrophoesis Chamber. Centricon filter units were then used to equilibrate RNA in desired buffer.

UV Titrations

UV absorbance titrations were carried out an Aviv 14-DS while observing the 260 and 280 nm wavelengths. Titrations were carried out with either a Hamilton automatic titrator or through manual titrations. Both methods resulted in similar results. Samples contained an appropriate amount of RNA so that the initial absorbance in the absence of divalent ions was approximately 0.6 Abs. at 260nm. The relative absorbance (Rel. Abs.) was determined by dividing the absorbance at a given concentration of divalent ion by the initial absorbance in the absence of divalent ion. Resulting titrations were fit to the Hill equation while allowing the hill coefficient to float.

2-AP Binding Experiments

Florescence measurements were performed on an Aviv ATF 105. 2-aminopurine was excited at 320 nm while emission collection was performed at 370 nm. 2-AP binding studies were carried out in the presence of 100 nM 2-aminopurine. Experiments performed by titrating a solution of RNA were equilibrated with a

given amount of divalent ion (Group II: 350 μM, Organic cations: 5 mM) in order to maintain relatively constant bulk concentration of cation.

Experiments performed through the addition of cation solutions containing 10 μM A-riboswitch in addition to the divalent cation chloride salt being titrated. The relative fluorescence (Rel. Fl.) was determined by dividing all fluorescence intensities at 370 nm by the initial fluorescence signal in the absence of divalent ions.

References

1. Auffinger, P., Grover, N., and Westhof, E. (2011) Metal Ion Binding to RNA, In Structural and Catalytic Roles of Metal Ions in Rna (Sigel, A., Sigel, H., and Sigel, R. K. O., Eds.), pp 1-35, Royal Soc Chemistry, Cambridge.

2. Baird, N. J., and Ferre-D'Amare, A. R. (2010) Idiosyncratically tuned switching behavior of riboswitch aptamer domains revealed by comparative small-angle X-ray scattering analysis (vol 16, pg 598, 2010), Rna-a Publication of the Rna Society 16, 1447-1447.

3. Bock, C. W., Katz, A. K., Markham, G. D., and Glusker, J. P. (1999) Manganese as a replacement for magnesium and zinc: Functional comparison of the divalent ions, Journal of the American Chemical Society 121, 7360-7372.

4. Brannvall, M., and Kirsebom, L. A. (2001) Metal ion cooperativity in ribozyme cleavage of RNA, Proceedings of the National Academy of Sciences of the United States of America 98, 12943-12947.

5. Brannvall, M., Mikkelsen, N. E., and Kirsebom, L. A. (2001) Monitoring the structure of Escherichia coli RNase P RNA in the presence of various divalent metal ions, Nucleic Acids Research 29, 1426-1432.

6. Buck, J., Noeske, J., Woehnert, J., and Schwalbe, H. (2010) Dissecting the influence of Mg2+ on 3D architecture and ligand-binding of the guanine-sensing riboswitch aptamer domain, Nucleic Acids Research 38, 4143-4153.

7. Bukhman, Y. V., and Draper, D. E. (1997) Affinities and selectivities of divalent cation binding sites within an RNA tertiary structure, Journal of Molecular Biology 273, 1020-1031.

8. Cate, J. H., Hanna, R. L., and Doudna, J. A. (1997) A magnesium ion core at the heart of a ribozyme domain, Nature Structural Biology 4, 553-558.

9. Chowrira, B. M., Berzalherranz, A., and Burke, J. M. (1993) IONIC REQUIREMENTS FOR RNA-BINDING, CLEAVAGE, AND LIGATION BY THE HAIRPIN RIBOZYME, Biochemistry 32, 1088-1095.

10. Conn, G. L., Draper, D. E., Lattman, E. E., and Gittis, A. G. (1999) Crystal structure of a conserved ribosomal protein-RNA complex, Science 284, 1171-1174.

11. Conn, G. L., Gittis, A. G., Lattman, E. E., Misra, V. K., and Draper, D. E. (2002) A compact RNA tertiary structure contains a buried Backbone-K+ complex, Journal of Molecular Biology 318, 963-973.

12. Dann, C. E., Wakeman, C. A., Sieling, C. L., Baker, S. C., Irnov, I., and Winkler, W. C. (2007) Structure and mechanism of a metal-sensing regulatory RNA, Cell 130, 878-892.

13. Das, R., Kwok, L. W., Millett, I. S., Bai, Y., Mills, T. T., Jacob, J., Maskel, G. S., Seifert, S., Mochrie, S. G. J., Thiyagarajan, P., Doniach, S., Pollack, L., and Herschlag, D. (2003) The fastest global events in RNA folding: Electrostatic relaxation and tertiary collapse of the tetrahymena ribozyme, Journal of Molecular Biology 332, 311-319.

14. Draper, D. E. (2004) A guide to ions and RNA structure, Rna-a Publication of the Rna Society 10, 335-343.

15. Frydman, B., Westler, W. M., and Samejima, K. (1996) Spermine binds in solution to the T psi C loop of tRNA(Phe): Evidence from a 750 MHz H-1-NMR analysis, Journal of Organic Chemistry 61, 2588-2589.

16. Frydman, L., Rossomando, P. C., Frydman, V., Fernandez, C. O., Frydman, B., and Samejima, K. (1992) INTERACTIONS BETWEEN NATURAL POLYAMINES AND TRANSFER-RNA - AN N-15 NMR ANALYSIS, Proceedings of the National Academy of Sciences of the United States of America 89, 9186-9190.

17. Gilbert, S. D., Stoddard, C. D., Wise, S. J., and Batey, R. T. (2006) Thermodynamic and kinetic characterization of ligand binding to the purine riboswitch aptamer domain, Journal of Molecular Biology 359, 754-768.

18. Grilley, D., Soto, A. M., and Draper, D. E. (2006) Mg2+-RNA interaction free energies and their relationship to the folding of RNA tertiary structures,

Proceedings of the National Academy of Sciences of the United States of America 103, 14003-14008.

19. Heilman-Miller, S. L., Pan, J., Thirumalai, D., and Woodson, S. A. (2001) Role of counterion condensation in folding of the Tetrahymena ribozyme II. Counterion-dependence of folding kinetics, Journal of Molecular Biology 309, 57-68.

20. Heilman-Miller, S. L., Thirumalai, D., and Woodson, S. A. (2001) Role of counterion condensation in folding of the Tetrahymena ribozyme. I. Equilibrium stabilization by cations, Journal of Molecular Biology 306, 1157-1166.

21. Kang, M., Peterson, R., and Feigon, J. (2010) Structural Insights into Riboswitch Control of the Biosynthesis of Queuosine, a Modified Nucleotide Found in the Anticodon of tRNA (vol 33, pg 784, 2009), Molecular Cell 39, 653-655.

22. Kilburn, D., Roh, J. H., Guo, L., Briber, R. M., and Woodson, S. A. (2010) Molecular Crowding Stabilizes Folded RNA Structure by the Excluded Volume Effect, Journal of the American Chemical Society 132, 8690-8696.

23. Klein, D. J., Edwards, T. E., and Ferre-D'Amare, A. R. (2009) Cocrystal structure of a class I preQ(1) riboswitch reveals a pseudoknot recognizing an essential hypermodified nucleobase, Nature Structural & Molecular Biology 16, 343-344.

24. Koculi, E., Lee, N. K., Thirumalai, D., and Woodson, S. A. (2004) Folding of the Tetrahymena ribozyme by polyamines: Importance of counterion valence and size, Journal of Molecular Biology 341, 27-36.

25. Koculi, E., Hyeon, C., Thirumalai, D., and Woodson, S. A. (2007) Charge density of divalent metal cations determines RNA stability, Journal of the American Chemical Society 129, 2676-2682.

26. Lambert, D., and Draper, D. E. (2007) Effects of osmolytes on RNA secondary and tertiary structure stabilities and RNA-Mg2+ interactions, Journal of Molecular Biology 370, 993-1005.

27. Lambert, D., Leipply, D., and Draper, D. E. (2010) The Osmolyte TMAO Stabilizes Native RNA Tertiary Structures in the Absence of Mg(2+): Evidence for a Large Barrier to Folding from Phosphate Dehydration, Journal of Molecular Biology 404, 138-157.

28. Lambert, D., Leipply, D., Shiman, R., and Draper, D. E. (2009) The Influence of Monovalent Cation Size on the Stability of RNA Tertiary Structures, Journal of Molecular Biology 390, 791-804.

29. Lau, M. W. L., and Ferre-D'Amare, A. R. (2013) An in vitro evolved glmS ribozyme has the wild-type fold but loses coenzyme dependence, Nature Chemical Biology 9, 805-+.

30. Leipply, D., and Draper, D. E. (2010) Dependence of RNA Tertiary Structural Stability on Mg2+ Concentration: Interpretation of the Hill Equation and Coefficient, Biochemistry 49, 1843-1853.

31. Leipply, D., and Draper, D. E. (2011) Effects of Mg(2+) on the Free Energy Landscape for Folding a Purine Riboswitch RNA, Biochemistry 50, 2790-2799.

32. Leipply, D., and Draper, D. E. (2011) Evidence for a Thermodynamically Distinct Mg(2+) Ion Associated with Formation of an RNA Tertiary Structure, Journal of the American Chemical Society 133, 13397-13405.

33. Lemay, J. F., Penedo, J. C., Tremblay, R., Lilley, D. M. J., and Lafontaine, D. A. (2006) Folding of the adenine riboswitch, Chemistry & Biology 13, 857-868.

34. Misra, V. K., and Draper, D. E. (2000) Mg2+ binding to tRNA revisited: The nonlinear Poisson-Boltzmann model, Journal of Molecular Biology 299, 813-825.

35. Misra, V. K., and Draper, D. E. (2002) The linkage between magnesium binding and RNA folding, Journal of Molecular Biology 317, 507-521.

36. Moghaddam, S., Caliskan, G., Chauhan, S., Hyeon, C., Briber, R. M., Thirumalai, D., and Woodson, S. A. (2009) Metal Ion Dependence of Cooperative Collapse Transitions in RNA, Journal of Molecular Biology 393, 753-764.

37. Noeske, J., Schwalbe, H., and Wohnert, J. (2007) Metal-ion binding and metal-ion induced folding of the adenine-sensing riboswitch aptamer domain, Nucleic Acids Research 35, 5262-5273.

38. Perrotta, A. T., and Been, M. D. (2007) A single nucleotide linked to a switch in metal ion reactivity preference in the HDV ribozymes, Biochemistry 46, 5124-5130.

39. Pyle, A. M. (2002) Metal ions in the structure and function of RNA, Journal of Biological Inorganic Chemistry 7, 679-690.

40. Ramesh, A., Wakeman, C. A., and Winkler, W. C. (2011) Insights into Metalloregulation by M-box Riboswitch RNAs via Structural Analysis of Manganese-Bound Complexes, Journal of Molecular Biology 407, 556-570.

41. Rangan, P., and Woodson, S. A. (2003) Structural requirement for Mg2+ binding in the group I intron core, Journal of Molecular Biology 329, 229-238.

42. Schreier, A. A., and Schimmel, P. R. (1975) INTERACTION OF POLYAMINES WITH FRAGMENTS AND WHOLE MOLECULES OF YEAST PHENYLALANINE-SPECIFIC TRANSFER-RNA, Journal of Molecular Biology 93, 323-329.

43. Serganov, A., Huang, L. L., and Patel, D. J. (2009) Coenzyme recognition and gene regulation by a flavin mononucleotide riboswitch, Nature 458, 233-U210.

44. Serganov, A., Yuan, Y. R., Pikovskaya, O., Polonskaia, A., Malinina, L., Phan, A. T., Hobartner, C., Micura, R., Breaker, R. R., and Patel, D. J. (2004) Structural basis for discriminative regulation of gene expression by adenine- and guanine-sensing mRNAs, Chemistry & Biology 11, 1729-1741.

45. Stein, A., and Crothers, D. M. (1976) CONFORMATIONAL-CHANGES OF TRANSFER-RNA - ROLE OF MAGNESIUM(II), Biochemistry 15, 160-168.

46. Stokes, R. H., and Robinson, R. A. (1948) IONIC HYDRATION AND ACTIVITY IN ELECTROLYTE SOLUTIONS, Journal of the American Chemical Society 70, 1870-1878.

47. Trachman, R. J., III, and Draper, D. E. (2013) Comparison of Interactions of Diamine and Mg2+ with RNA Tertiary Structures: Similar versus Differential Effects on the Stabilities of Diverse RNA Folds, Biochemistry 52, 5911-5919.

48. Travers, K. J., Boyd, N., and Herschlag, D. (2007) Low specificity of metal ion binding in the metal ion core of a folded RNA, Rna-a Publication of the Rna Society 13, 1205-1213.

49. Vicens, Q., Mondragon, E., and Batey, R. T. (2011) CRYSTAL STRUCTURE OF A F. NUCLEATUM FMN RIBOSWITCH - FREE STATE, Nucleic Acid Database.

50. Winkler, W. C., Cohen-Chalamish, S., and Breaker, R. R. (2002) An mRNA structure that controls gene expression by binding FMN, Proceedings of the National Academy of Sciences of the United States of America 99, 15908-15913.

51. Woodson, S. A. (2005) Metal ions and RNA folding: a highly charged topic with a dynamic future, Current Opinion in Chemical Biology 9, 104-109.

Chapter 5:

Conclusions

The diversity of RNA structures allows for a broad range of functional roles for this biomolecule. In order to expand functional diversity, RNA has evolved to exploit interactions with cations. In doing so, cation-RNA interactions range from being long range and diffuse to buried and chelated. What is not so well understood is how the stability of differing RNA folds, which range in the extent to which cations are excluded from solvent, are coupled to solution conditions.

In the first part of this thesis we looked at how four different RNAs respond to the presence of putrescine^{2+}, a biologically relevant organic cation. In solutions containing a single monovalent counterion only the non-Mg^{2+} chelating RNAs showed increased stability in the presence of putrescne^{2+}. The stability imparted by diamines was shown to be a function of charge density as related to the distance between the amine groups in solution. In addition, RNAs that were found not to chelate Mg^{2+} obtained increased stability upon addition of putrescine^{2+} to solutions containing both magnesium and potassium chloride. On the other hand RNAs shown to chelate Mg^{2+} were destabilized by the presence of putrescine^{2+}. The discrepancy between these two genres of RNA is attributed to the repulsive electrostatic interactions between diffuse putrescine^{2+} cations and the chelated Mg^{2+} ions.

Next, we used the *add* adenine riboswitch as a model system to look at how excess Mg^{2+} is altered by the presence of putrescine^{2+}. The system was presented as

a polyelectrolyte that is allowed to undergo ion exchange with its environment in order to maintain electroneutrality. Ion exchange was measured for both the folded and unfolded state providing information on the folding free energy landscape. Putrescine^{2+} was shown to have a greater exchange with Mg^{2+} in the vicinity of the intermediate state of the A-riboswitch than for the native state. This was suggested to be due to the difference in how these two ions populate the ion atmosphere of this RNA.

In order to probe deeper into the organization and specificity of cations interacting with RNA, a divalent ion survey consisting of diamines and group II ions was conducted on four characterized RNAs. The RNAs used in this study ranged in the extent to which they bury Mg^{2+} ions within their native structures. There were clear differences in the spectroscopic signals observed upon folding Mg^{2+} chelating RNAs as apposed to non-chelating RNAs. As indicated by the slopes of the folding curves, $\Delta\Gamma$ differs between the divalent ions for a given RNA. This was attributed to the soft nature of the Sr^{2+} and Ba^{2+}. Almost universally, the organic ions were unable to induce the same change UV absorbance as found with Mg^{2+}. This was not the case for the A-riboswitch in the presence of adenine or 2,6-diaminopurine. This phenomena was attributed to the N6 position of the purine ligand compensating for a divalent cation binding interaction. Further investigation by fluorescence binding assay showed that this cation binding site is selective for Mg^{2+} despite not showing characteristic signs of being a true chelation site.

Appendix

Figure A-1

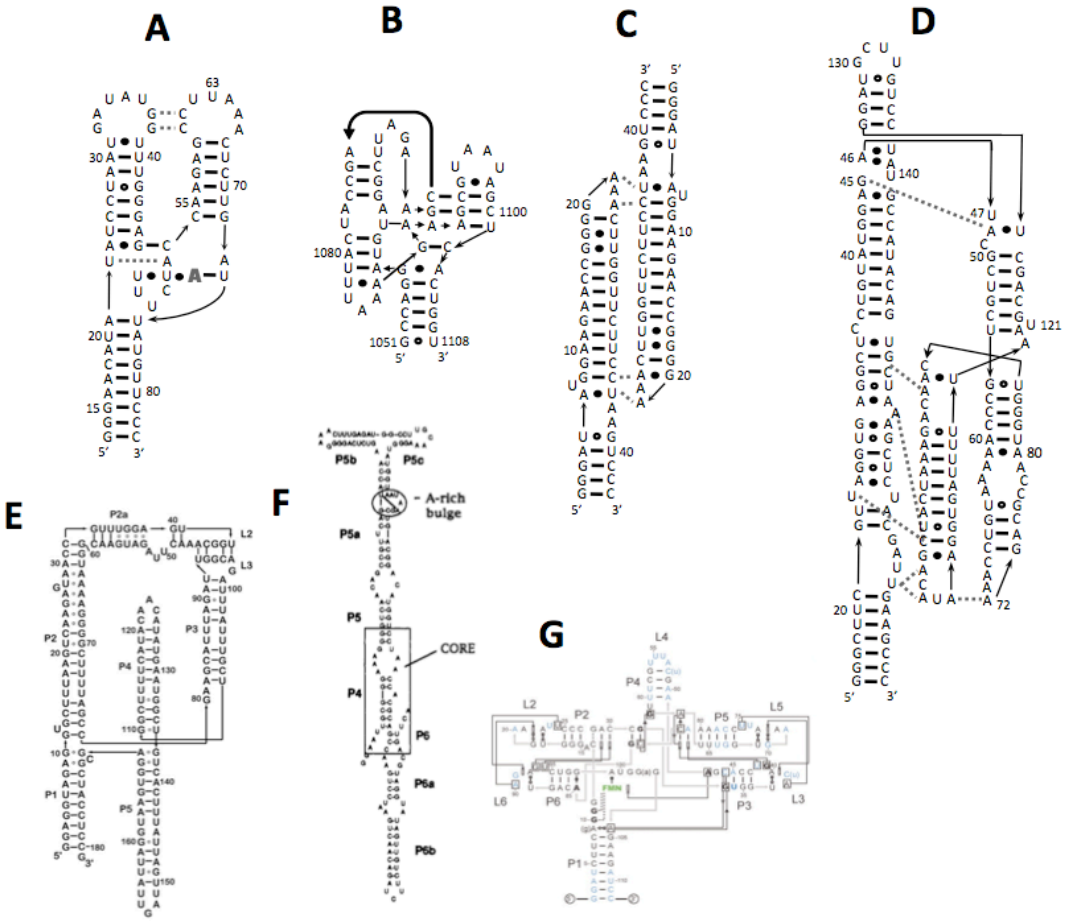

Figure A-1. The secondary structure map of all the RNAs used throughout this thesis. *add* adenine riboswitch (A), 58mer rRNA fragment (B), homodymeric tetraloop receptor (C), mgtE M-box riboswitch (D), L-box lysine riboswitch (E), P4P6 *Tetrahymina* ribozyme fragment (F) and the FMN riboswitch. Figure adapted from Trachman et al. 2013, Baird et al 2009, Murphy et al. 1993 and Vicens et al 2011

Figure A-2

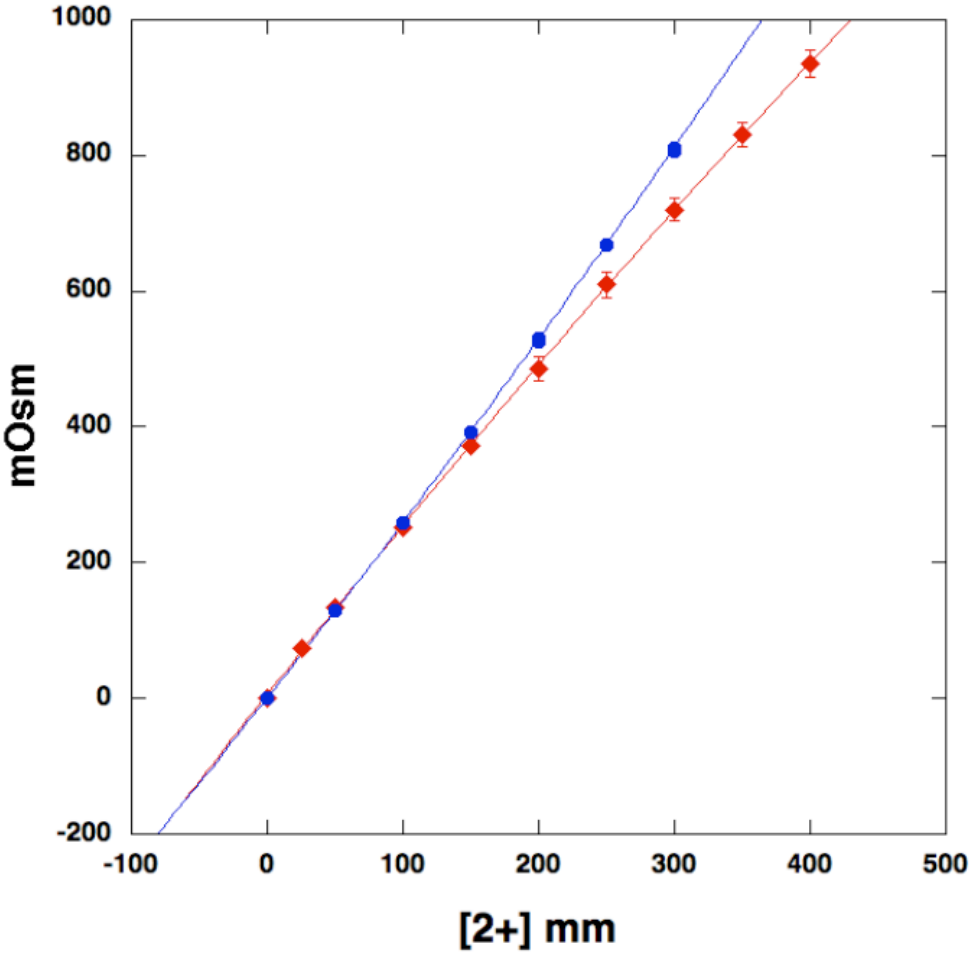

Figure A-2. Vapor pressure osmometry measurements of MgCl2 (blue) (*Kumbhar et al. 2007*) or putrescine • 2HCl (red). Data have been fit to second order polynomials through the origin.

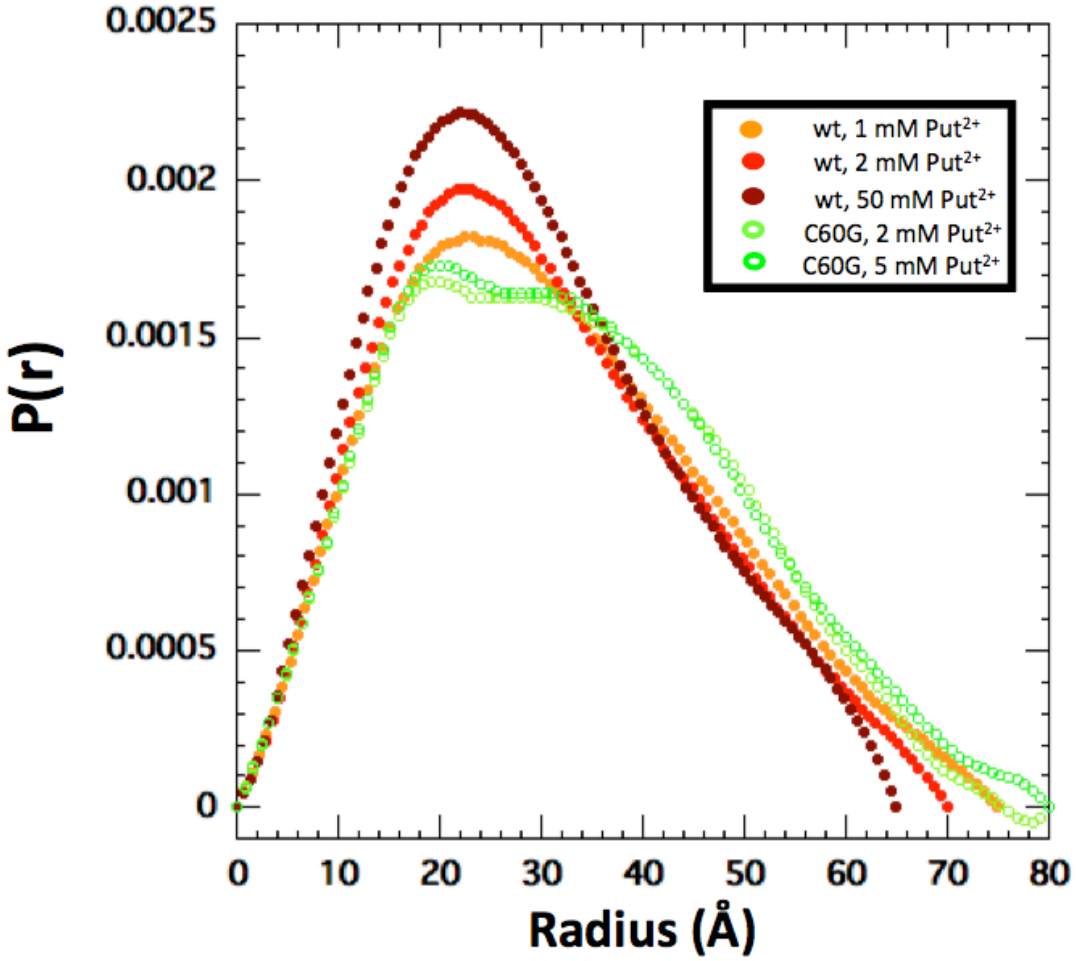

Figure A-3. P(r) plots for the A-riboswitch. wild type (reds) and C60G mutant (greens) SAXS data were collected in KMOPS buffer at pH 6.8 with 50 mM K^+ and 20 μM EDTA. 30 shots with an exposure time of 1.6s at 1 keV were averaged with subtraction of buffer. All data were collected at APS beamline 12-ID.

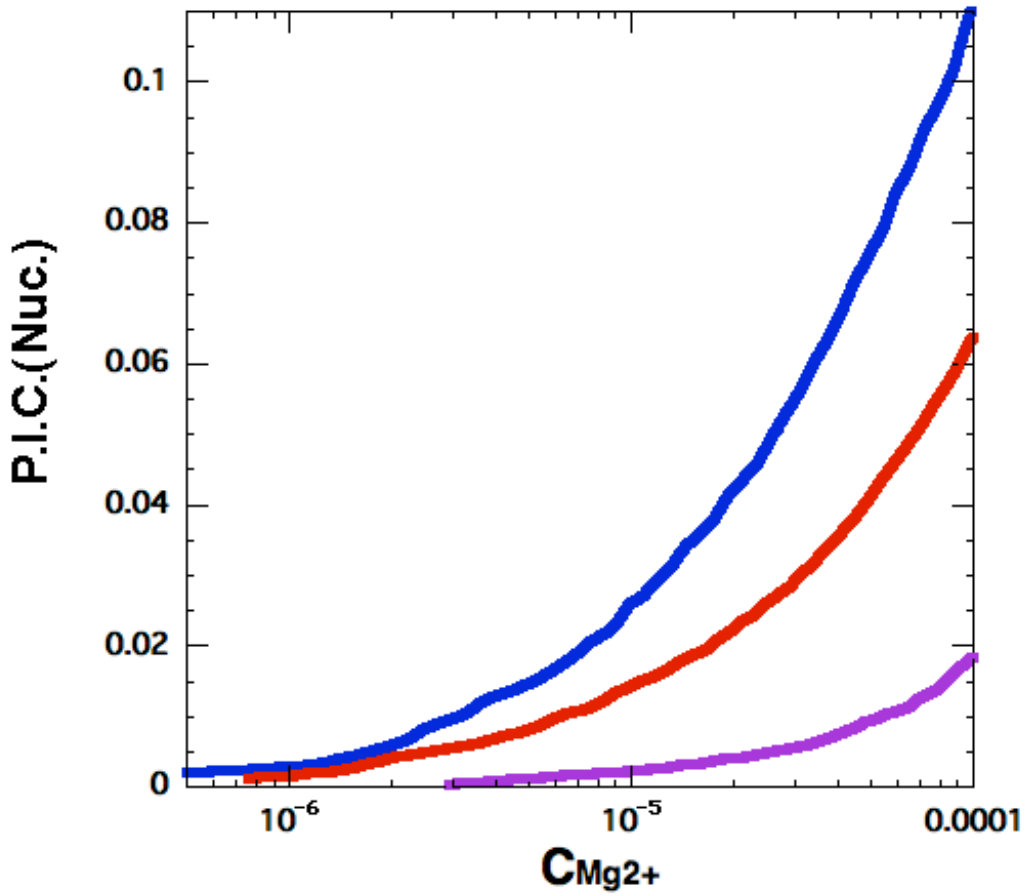

Figure A-4. Excess Mg^{2+} per nucleotide as a function of bulk Mg^{2+} for the M-box riboswitch in the presence of 0 (blue), 1 mM (red) and 2 mM (purple) bulk putrescine^{2+}. Data shows the best fit of three independent runs.

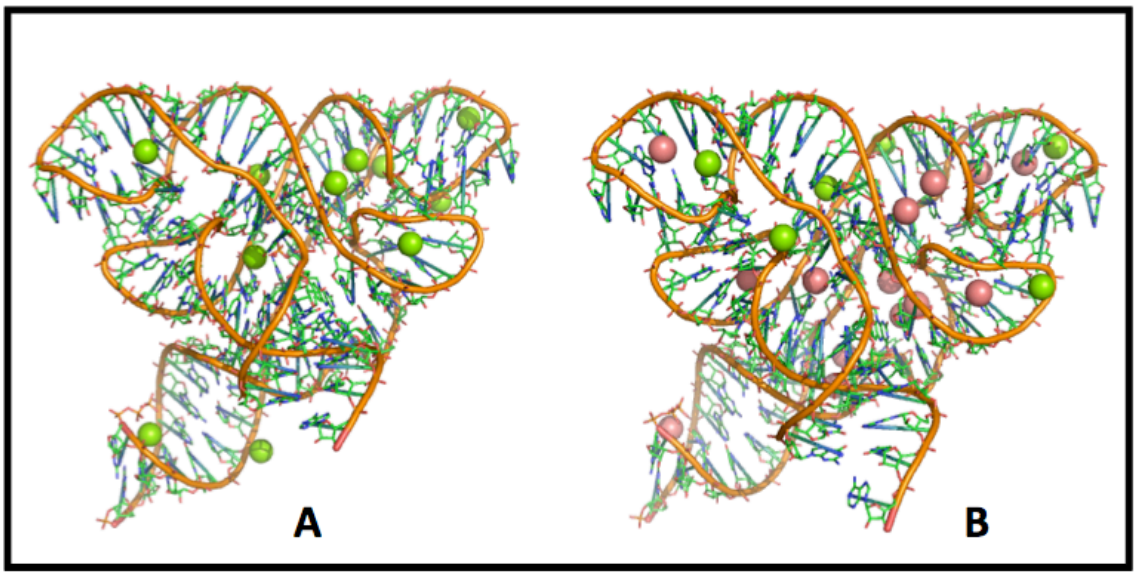

Figure A-5. Structures of the FMN riboswitch (A) Structure of the FMN bound FMN riboswitch crystalized in the presence of Mg^{2+} (green spheres) and with $BaCl_2$ (orange spheres) soak (B). Ions making crystal contacts were removed from both structures. PDB ID: 3F2W and 3F2Q respectively.

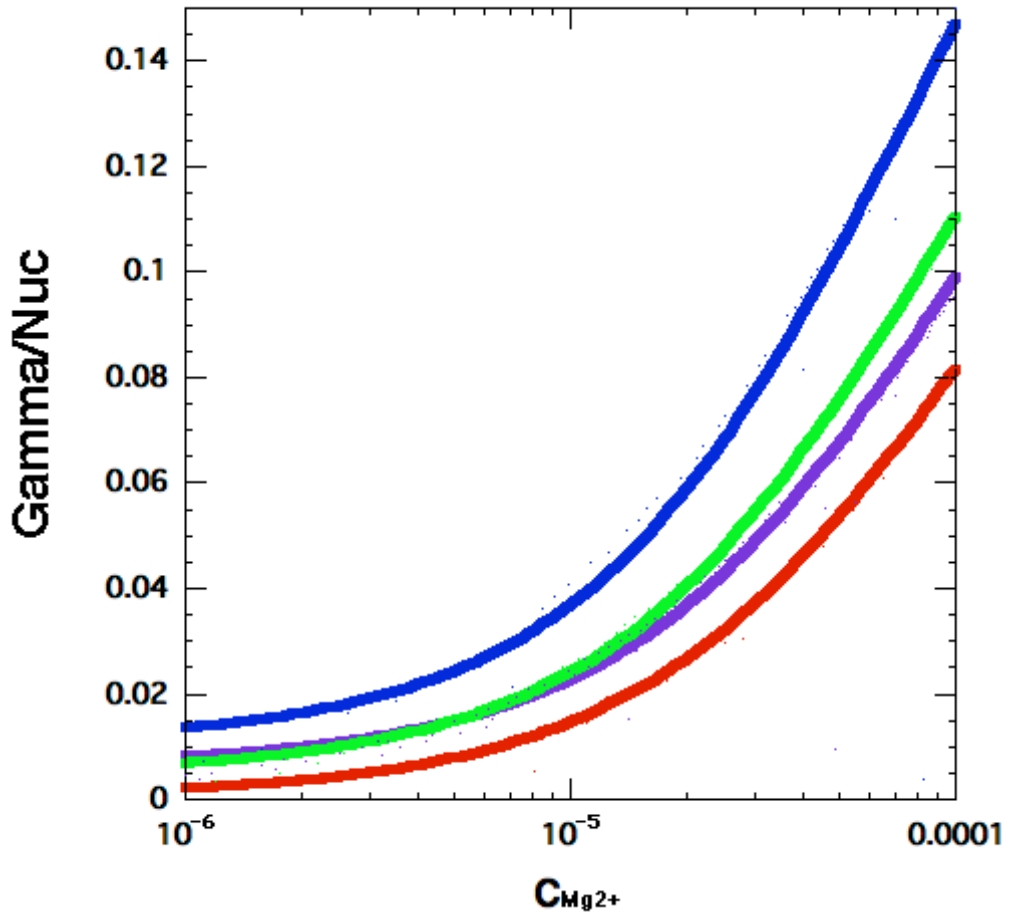

Figure A-6. HQS titrations of the 160 nt RNAs. Excess Mg^{2+} per nucleotide as a function of bulk Mg^{2+} for the L-box riboswitch (blue), M-box riboswitch (green) P4P6 extended state mutant pB55a (purple) and P4P6 RNA (red). Data is plotted as the best fit of three independent runs.

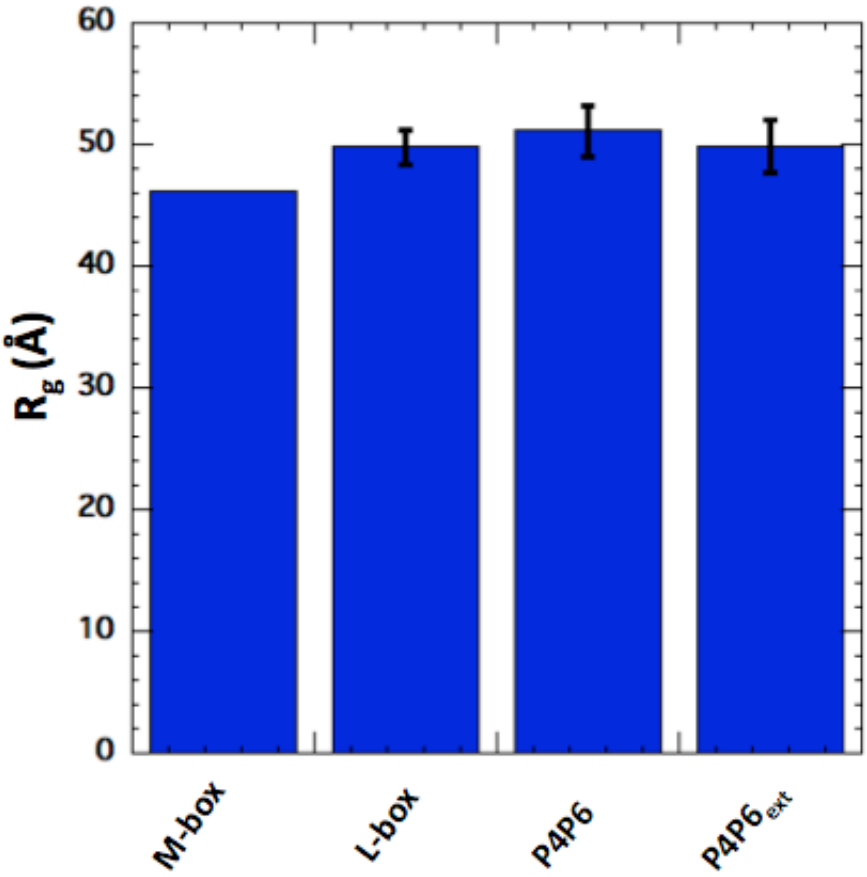

Figure A-7. Radius of gyration for the 160 nt RNAs determined from fit of Guinier approximation. SAXS experiments were conducted at pH 6.8 (20 mM MOPS) with 50 mM K^+ and 10 μM EDTA. Data for the M-box riboswitch was collected by Desirae Leipply. All data were collected at APS beamline 12-ID.

Vita

Robert J. Trachman III was born and grew up in Toms River N.J. Upon graduating from Toms River High School East he entered The University of the Sciences in Philadelphia as both a biochemistry and pharmacy major. After his first year he switched his pharmacy major to bioinformatics. This switch was due to a new found interest in modeling three dimensional biomolecules. He eventually graduated with two B.S. degrees in biochemistry and bioninformatics and a M.S. degree in bioinformatics. After graduation, he began part time work as a lab assistant and also installed private docks. He began his Ph.D. training in 2008, upon acceptance in the program in molecular biophysics at Johns Hopkins University. Upon graduation he will be taking a position at the (N.I.H.) National Heart Lung and Blood Institute in Bethesda, Maryland.